# STEM Diffraction Contrast of Crystalline Defects: Advantages and Opportunities


Center for Electron Microscopy and Analysis

Matthew Bowers, Tim Smith, Michael Mills

*Department of Materials Science and Engineering*

*Center for Electron Microscopy and Analysis (CEMAS)*

Patrick Phillips

*Department of Physics*

*University of Illinois-Chicago*

Marc DeGraef

*Department of Materials Science and Engineering*

*Carnegie Mellon University*

# *Go Bucks!!*


Tecnai F-20 STEM
PHILIPS
TECNAI
Center for Electron
Microscopy and Analysis

# *Outline*

- Brief Motivation for "Micro/Mesoscale" structure studies

- Conventional Diffraction Contrast Imaging

- STEM-based Diffraction Contrast Imaging:
  - Experimental considerations
  - Advantages over conventional CTEM

- Simulation of Diffraction Contrast of Defects

- 3D and Other Possibilities
  - Tilt series reconstructions
  - High order g imaging
  - Zone axis imaging

# Integrated Computational Materials Engineering

*Micro and Mechanism Characterization*

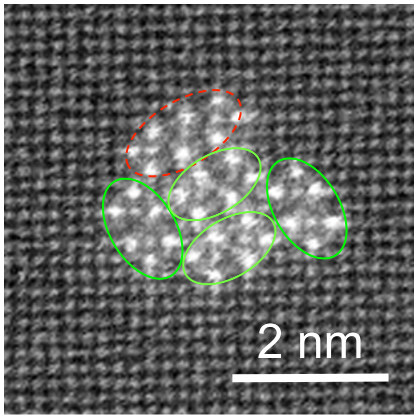


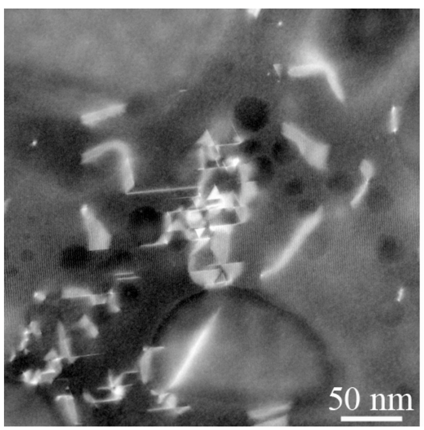


*Meso-scale Mechanism Modeling*

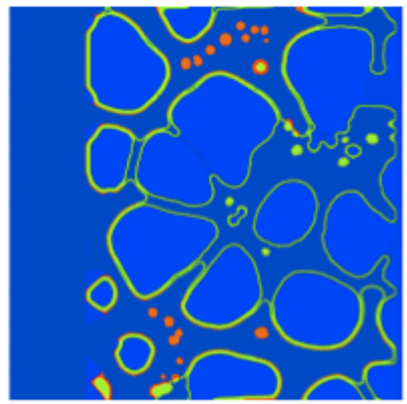

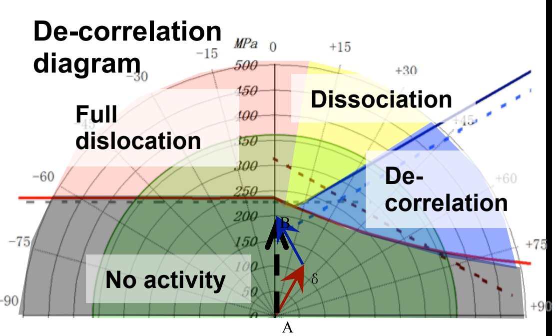


*Microstructure-Based FEA Modeling*

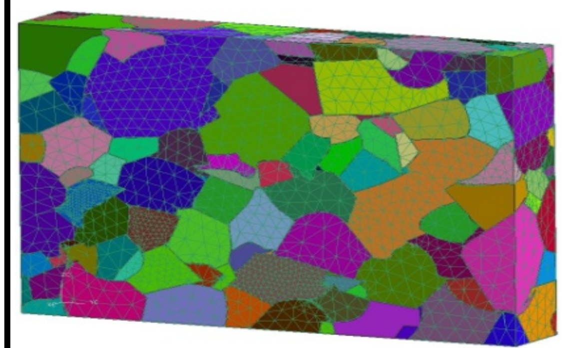

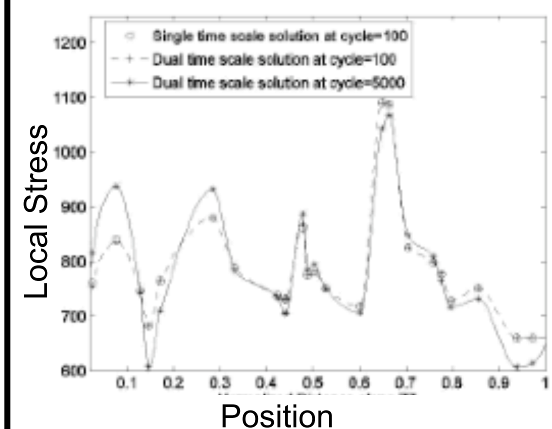


*Characterization underpins ICME for structural/functional materials*

# Characterizing Dislocation Structures

- Dislocation density
- Morphology – preferential line directions
- Dislocation reactions
- Interaction with precipitates
- Dislocation dissociation for fault energies
- Core structure for mobility
- Segregation to defects

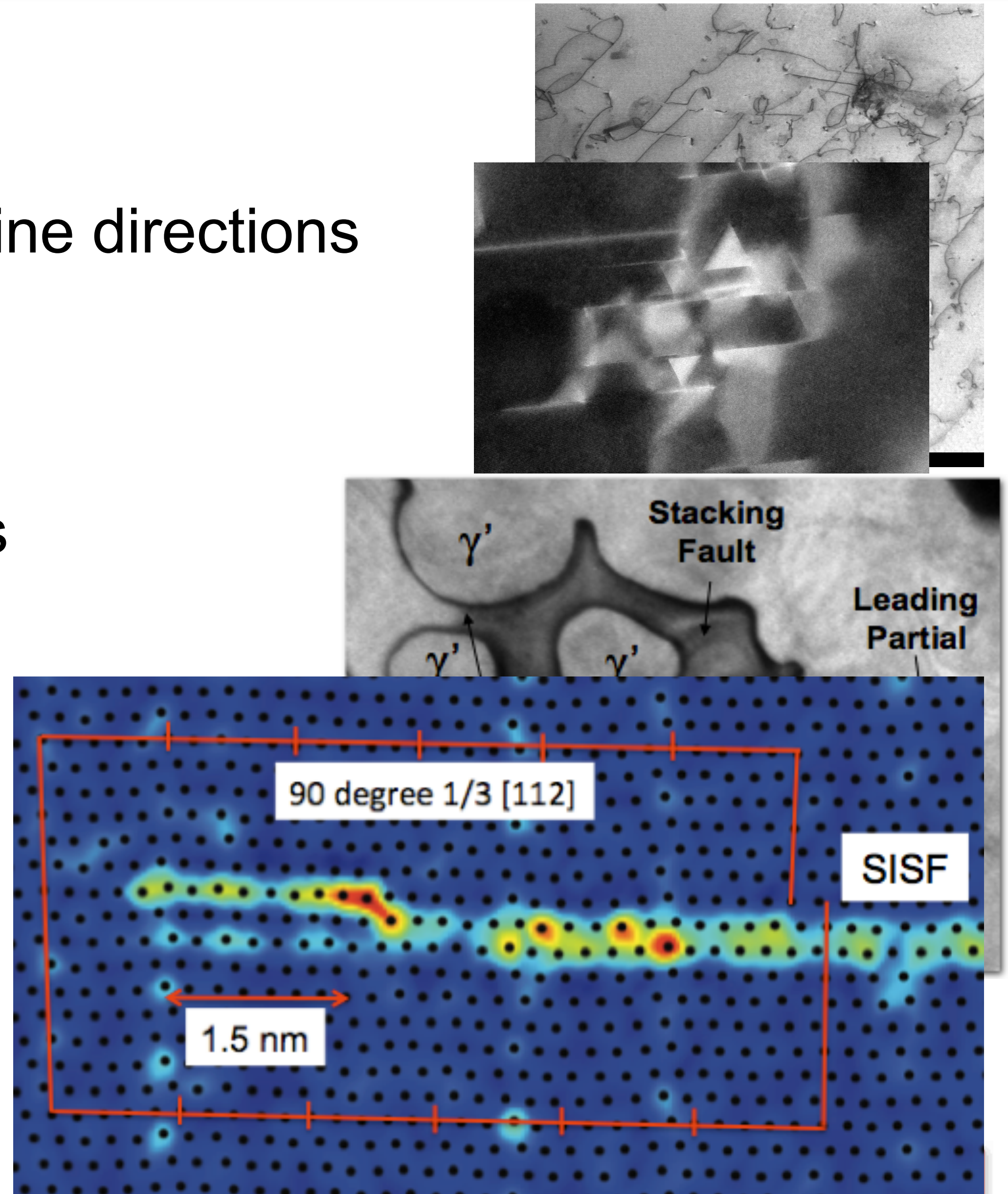

# Microstructure Can Alter Deformation Mechanisms

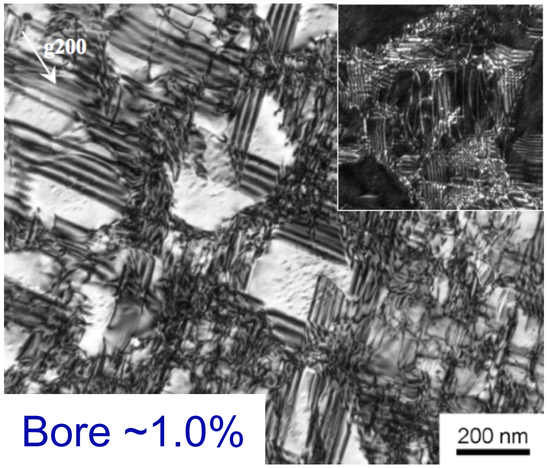


Bore ~1.0%

Increased a/2<110> matrix dislocation activity and SISF shearing of secondary γ/γ'

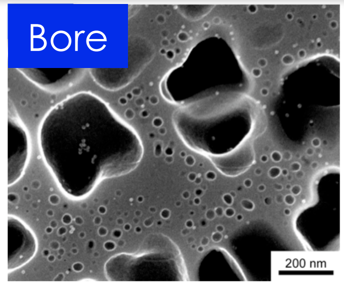


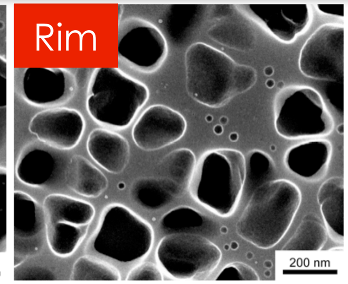


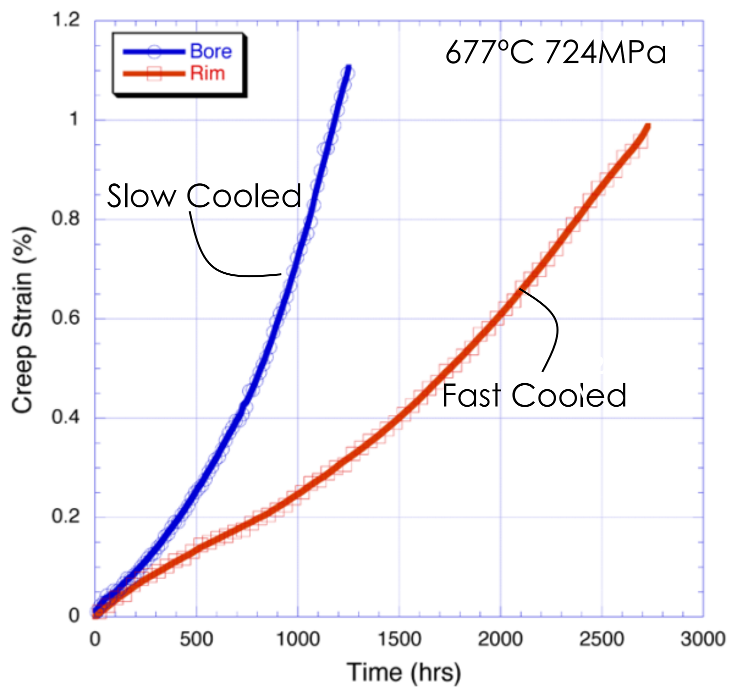


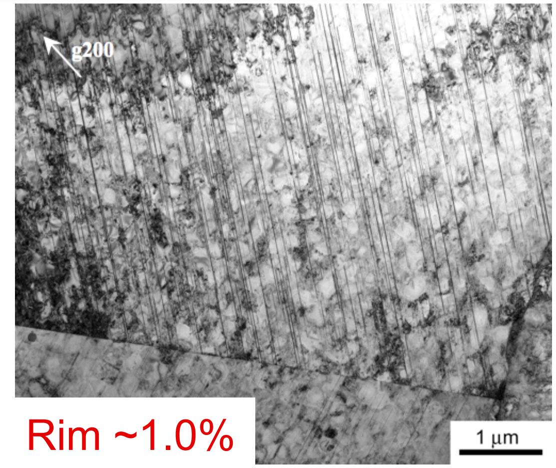


Rim ~1.0%

Microtwinning is the dominant creep deformation mechanism

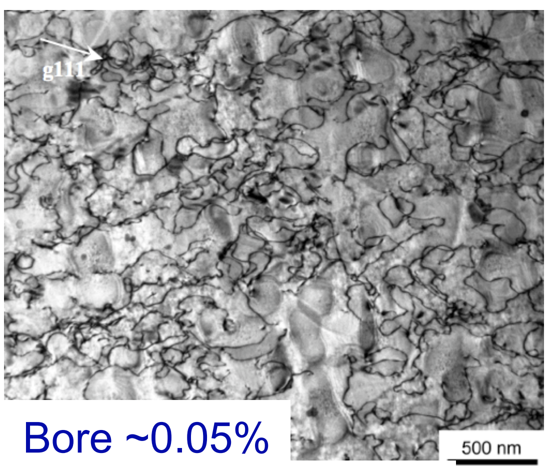


Bore ~0.05%

a/2<110> matrix dislocation activity

*Microstructure scale can alter creep mechanisms*

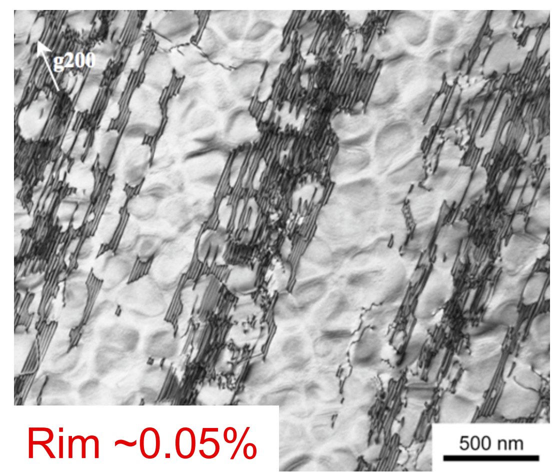


Rim ~0.05%

Matrix intrinsic stacking faults

Unocic et al, Superalloys (2008)

# Intragranular Mechanisms in ME3 as Function of Deformation Conditions at 1300°F

Low Stress Creep: *Microtwins*

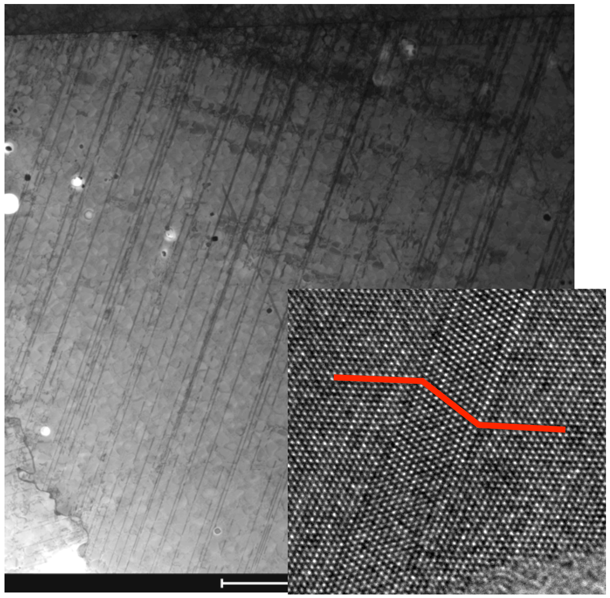

Dwell Fatigue: *SF ribbons*

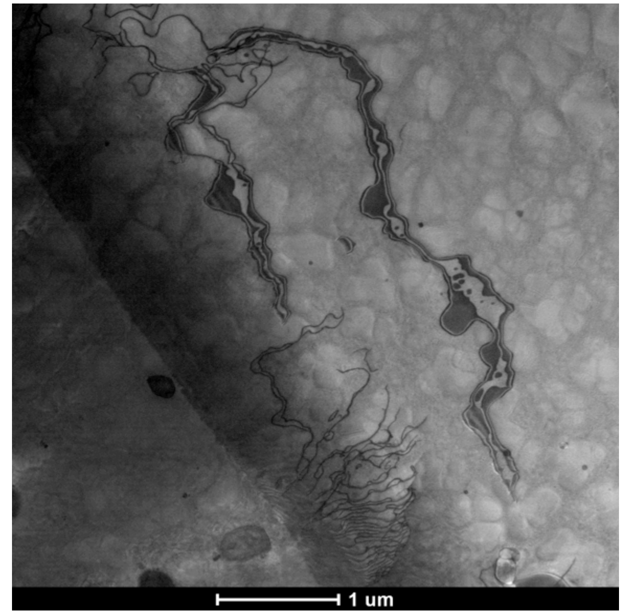


High Stress Creep/ Constant Strain Rate/ Low Cycle Fatigue

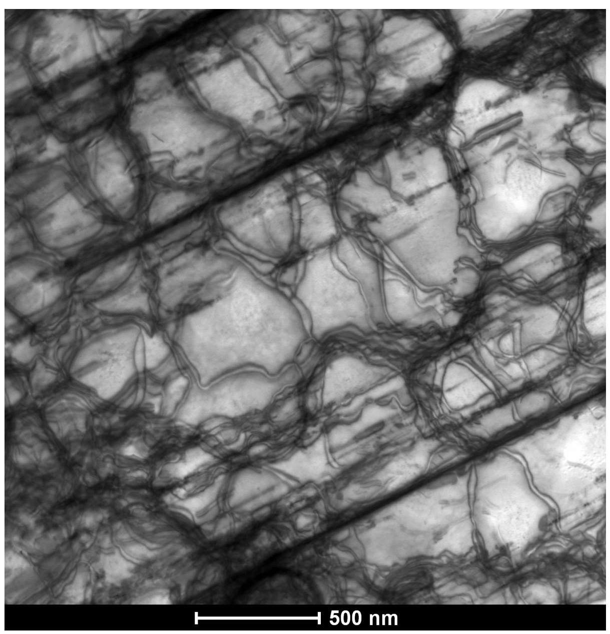


*Planar slip by paired dislocations*

*Wavy slip*

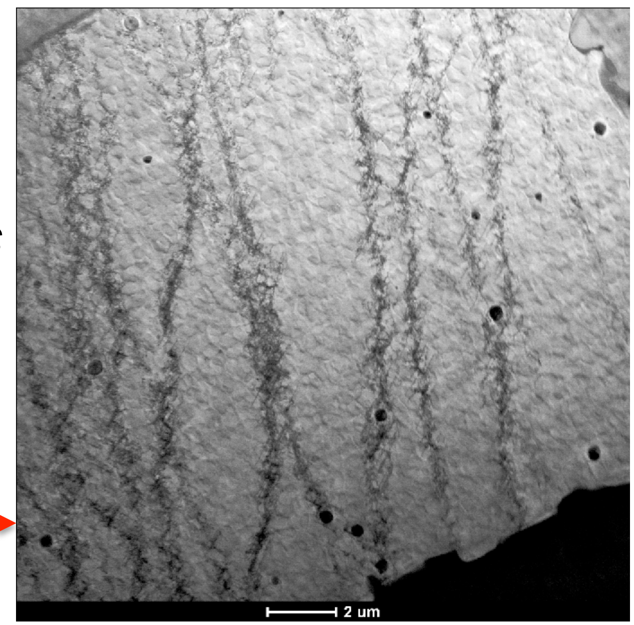

# Dynamic In-Situ Loading

- Continuous ω scanning
- Dynamic Loading
  - Constant ε-rate ($10^{-8} – 10^{-2}\ s^{-1}$)
  - Creep & Fatigue loading possible
- COM and strain measurements
- ~1 $mm^3$ volume
- ~700 grains

*Lienert, Bernier, Barton, Brandes, Mills, Miller, JOM (2011)*

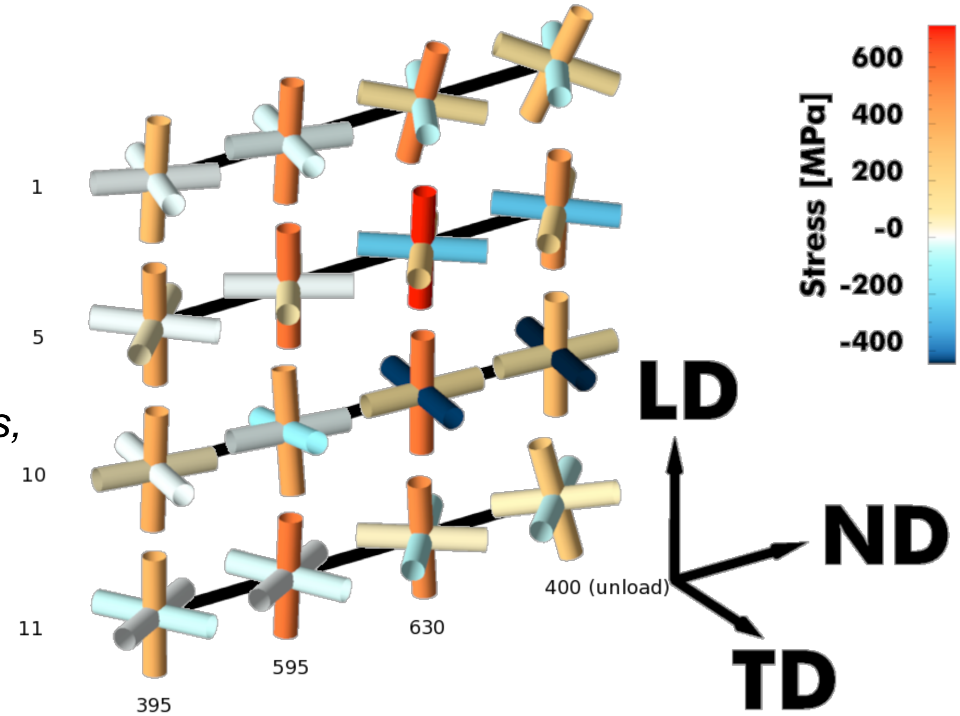


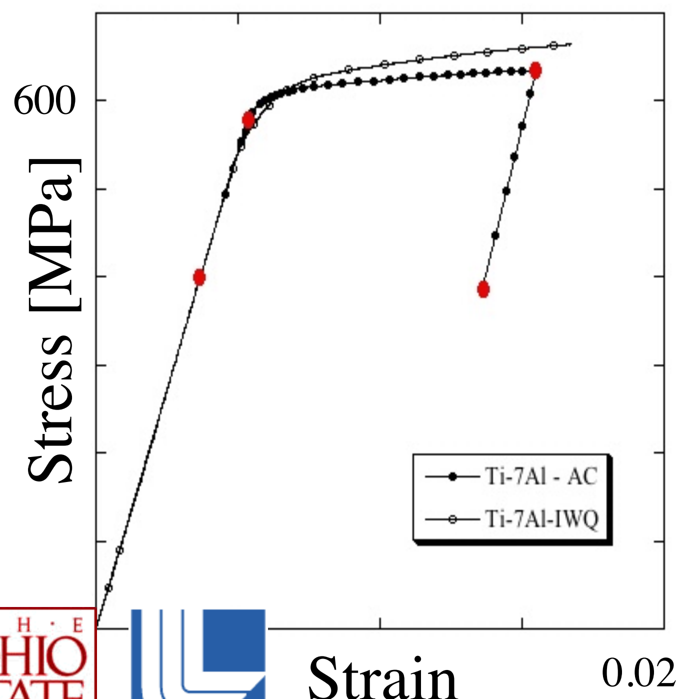


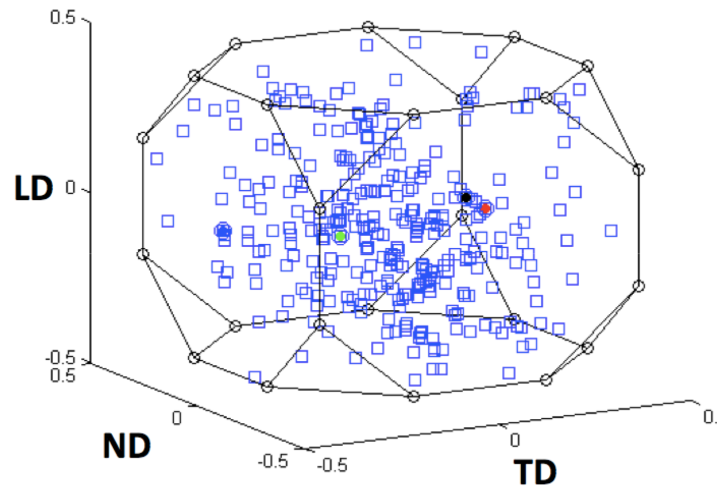


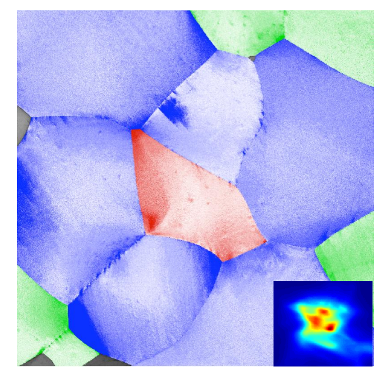

# Correlating Dislocation Structure with “X-ray Signatures”

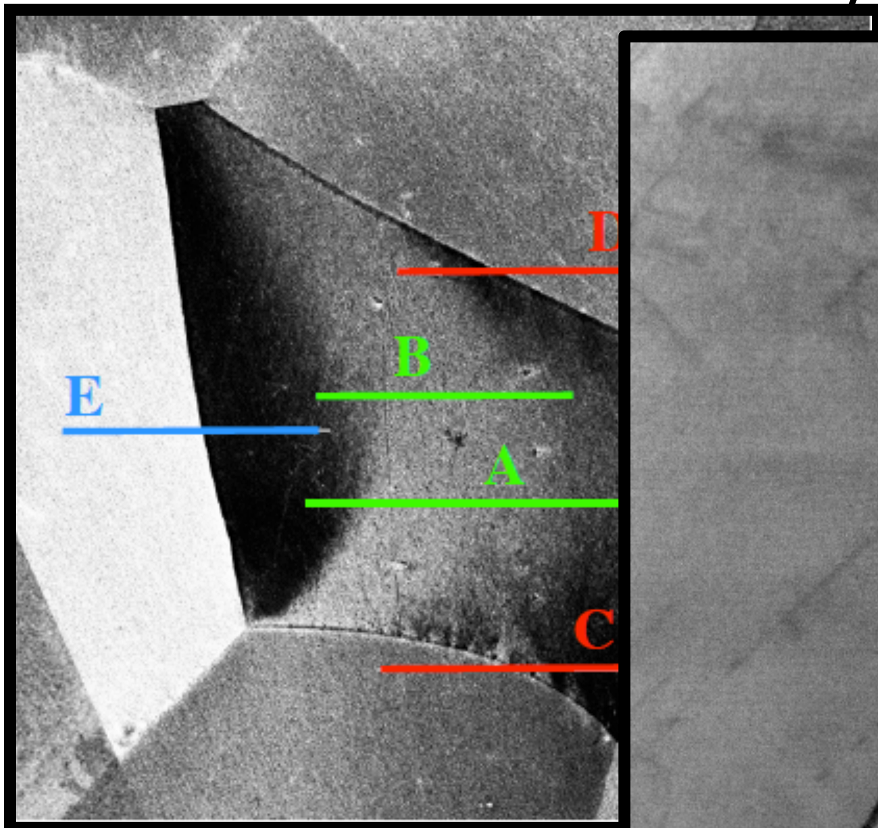


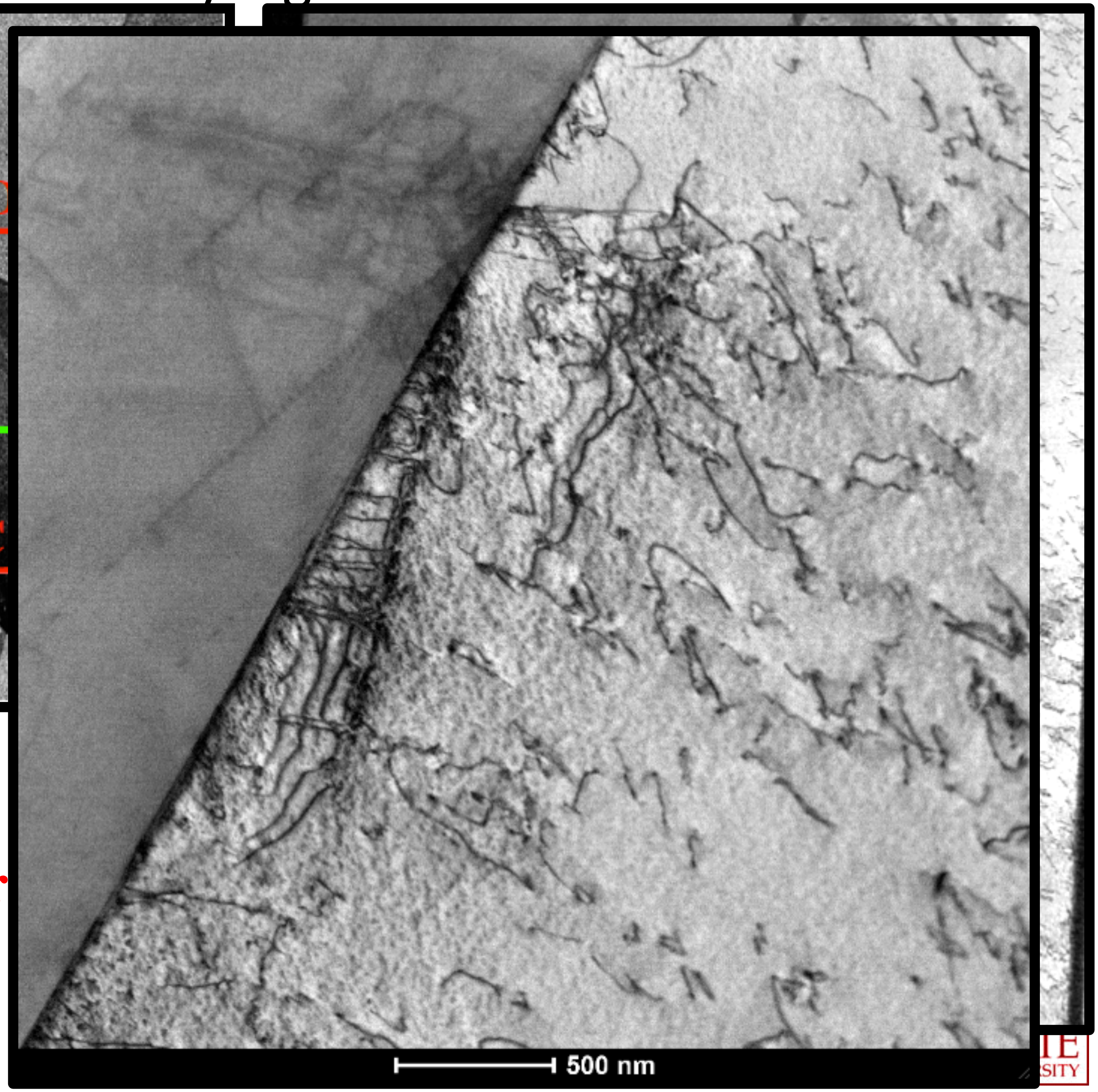


- **FIB Foil Extraction**
- **Dislocation structur**

# Spiral History of TEM

*A. Howie, M&M Proceedings, 2012*

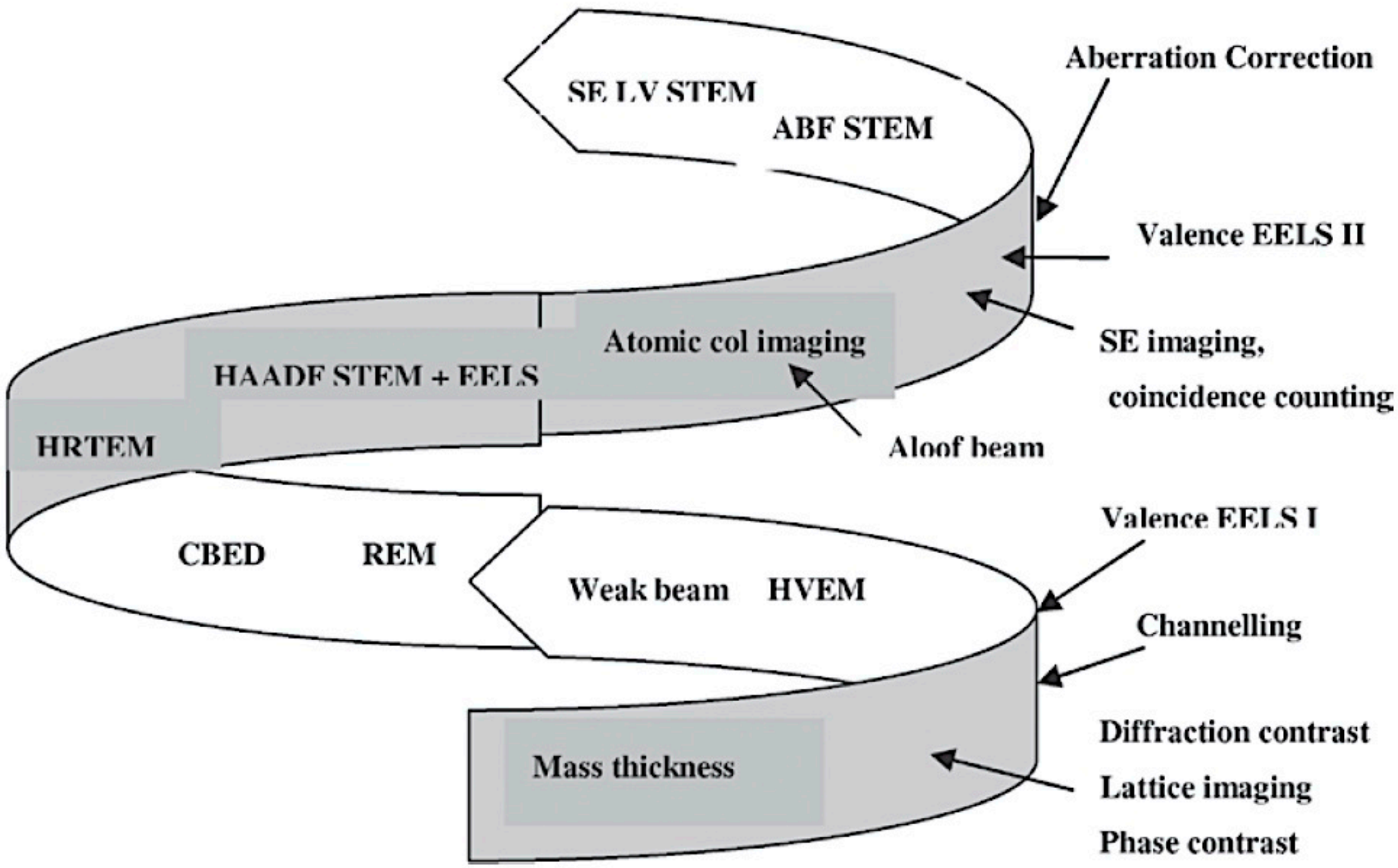

# Spiral History of TEM

*A. Howie, M&M Proceedings, 2012*

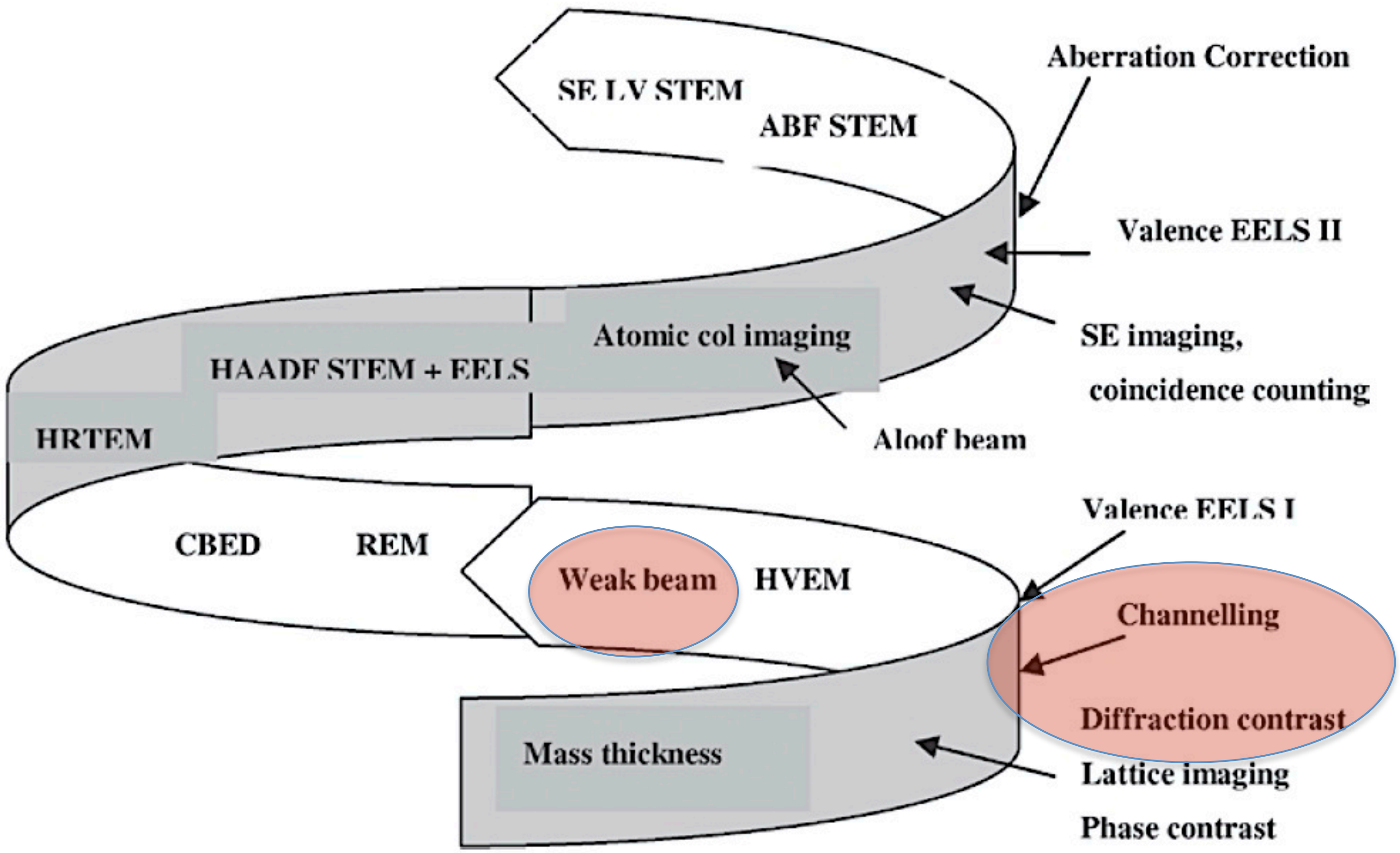

# "Conventional" Diffraction Contrast

Basic Imaging Concepts: *Difference in Crystal Orientation*

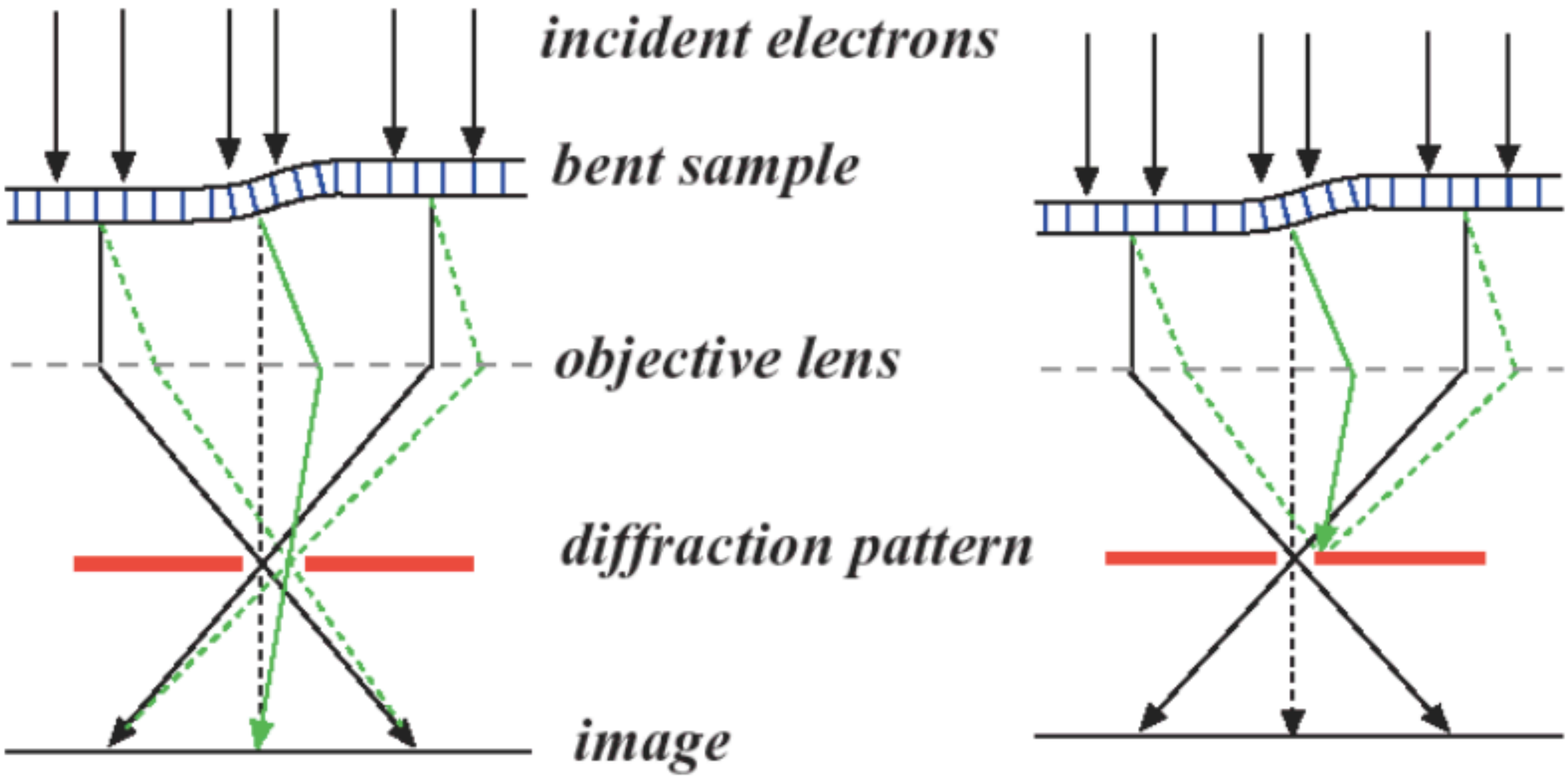


*Basis of bend contour and dislocation contrast*

# “Conventional” Diffraction Contrast

- Dislocation Contrast:

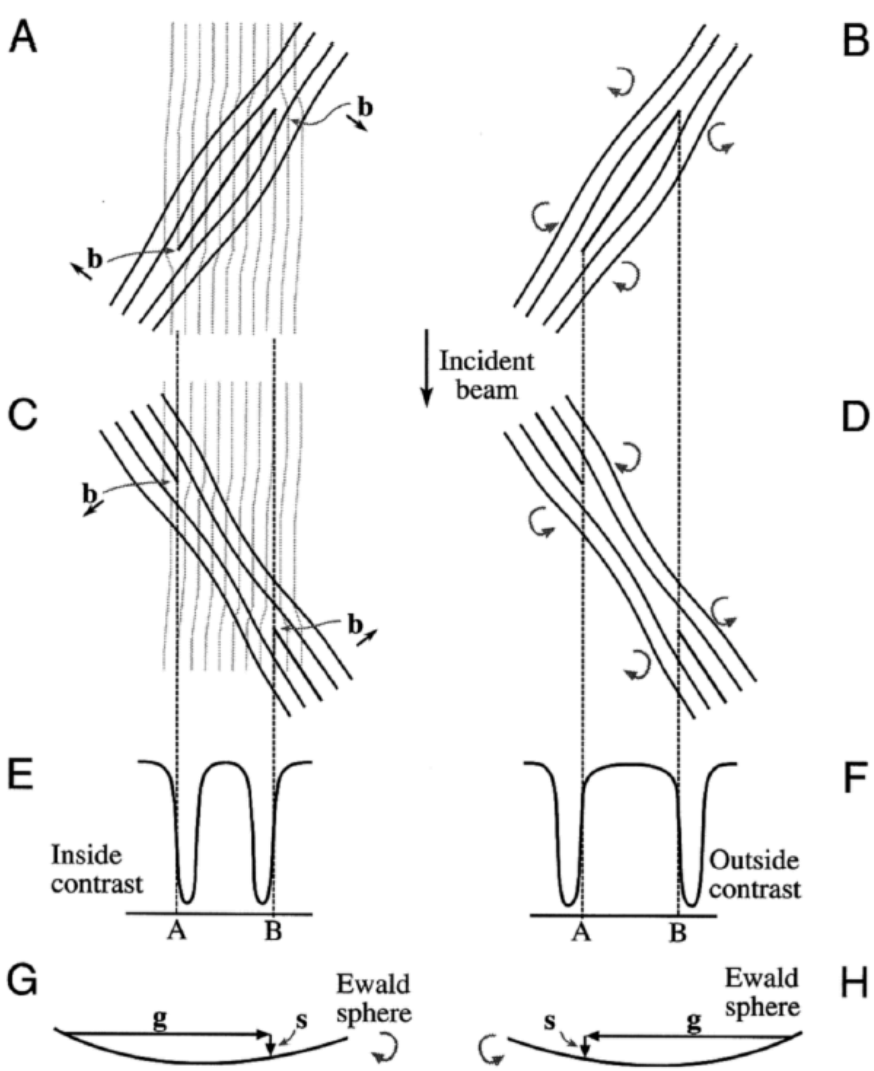


*Williams and Carter*

*Viswanathan (2006)*

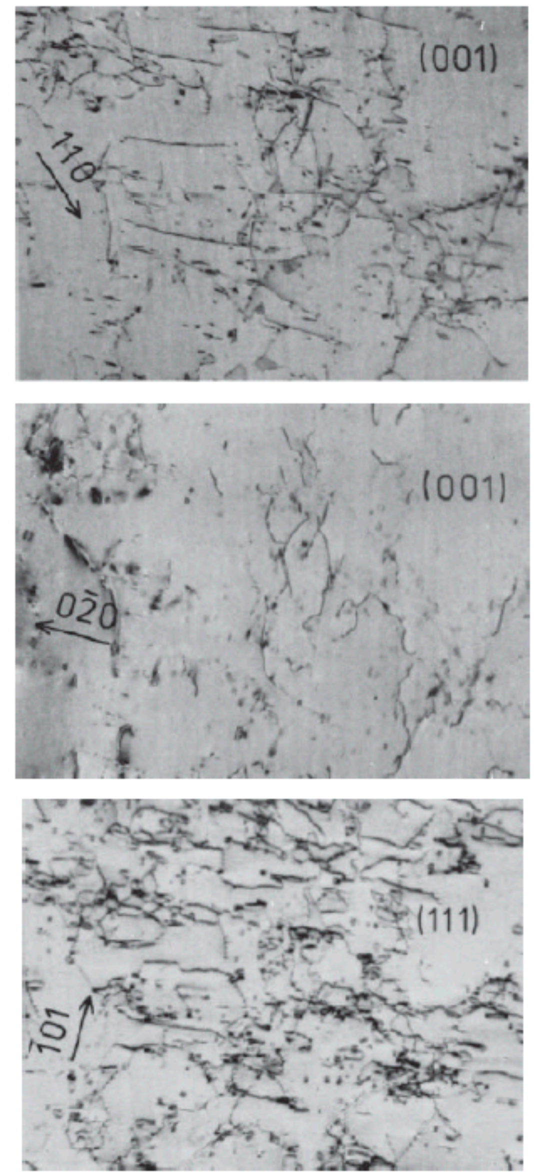

# "Conventional" Diffraction Contrast

- Weak beam imaging

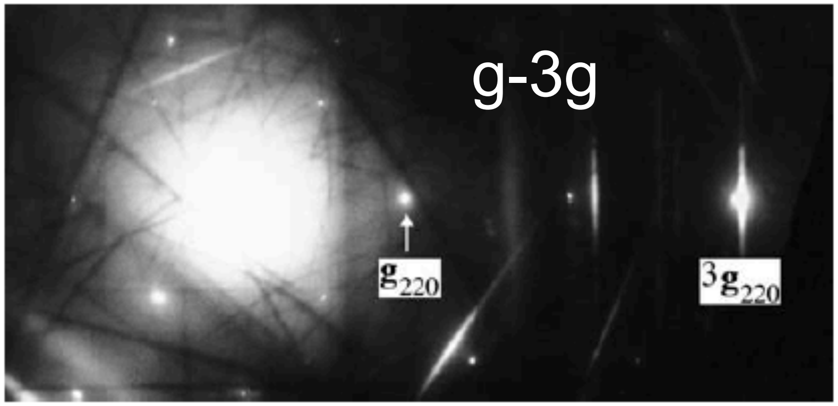


***Rule of thumb*** – Image width proportional to:

$$\xi_g^{eff} = \frac{\xi_g}{\left(1 + s^2 \xi_g^2\right)^{\frac{1}{2}}}$$

So enhance resolution by increasing deviation parameter

*Williams and Carter*

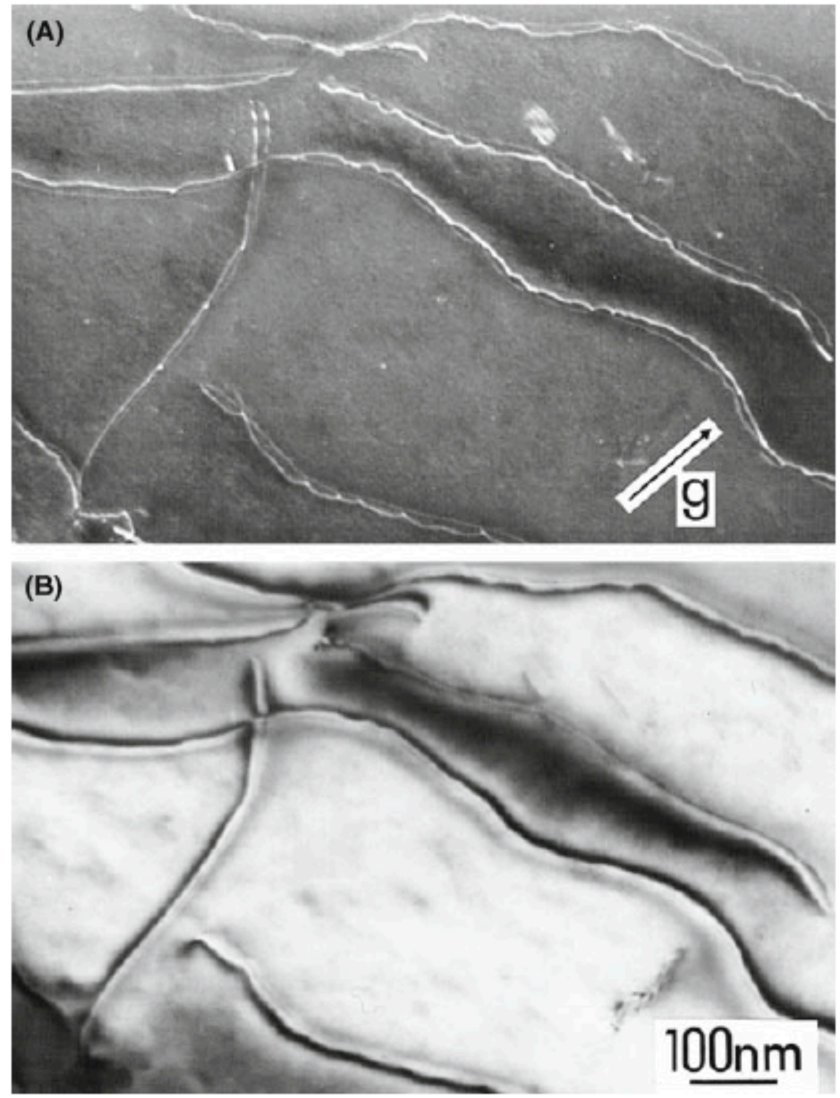


FIGURE 27.8. A comparison of dislocation images in a Cu alloy formed using (A) WB and (B) strong-beam ($s_g > 0$) conditions.

# Weak Beam Imaging

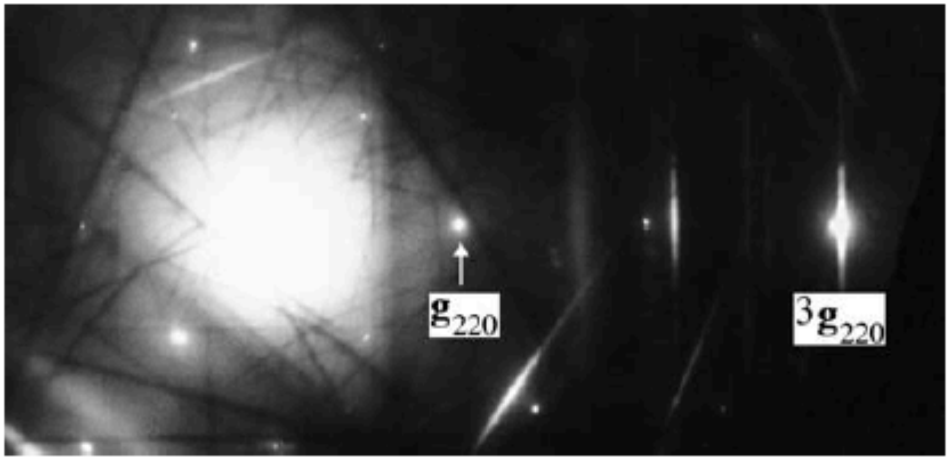


- Large deviation parameters reveal fine details associated with defect strain fields
- Large contrast but weak intensities
- Long exposure times
- Drift, sample stability and contamination
- Very thin and flat foils required

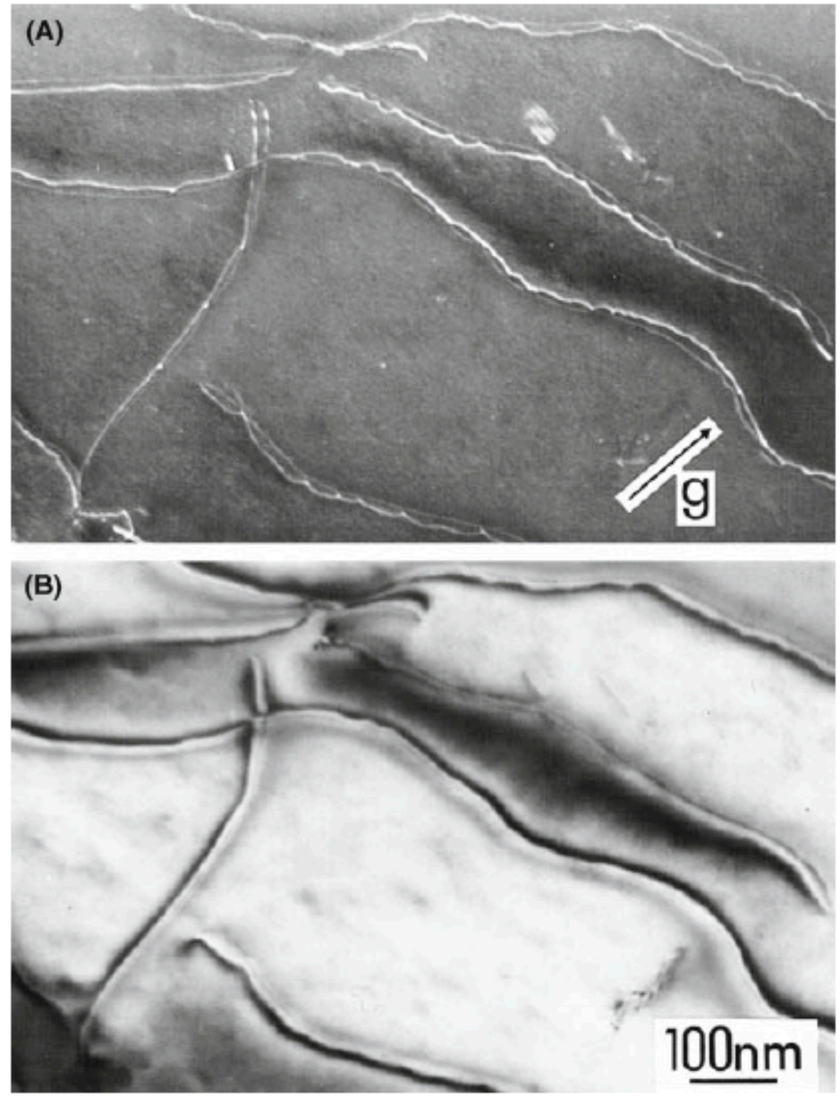


FIGURE 27.8. A comparison of dislocation images in a Cu alloy formed using (A) WB and (B) strong-beam ($s_g > 0$) conditions.

# “Conventional” Diffraction Contrast

- Weak beam imaging
  - APB coupled a<101> dislocations in $Ni_3Al$

*Baluc, et al, Phil Mag 64 (1991)*

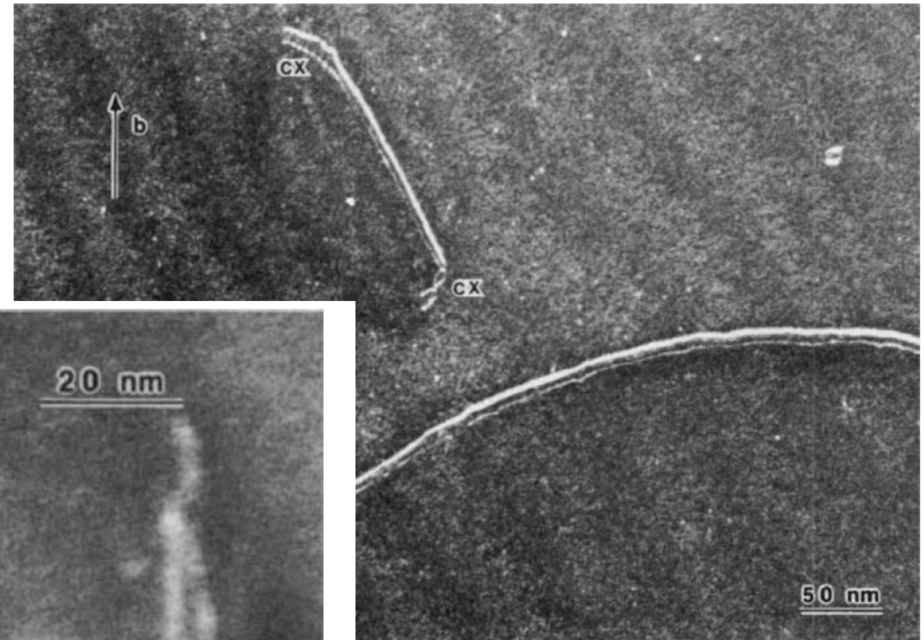


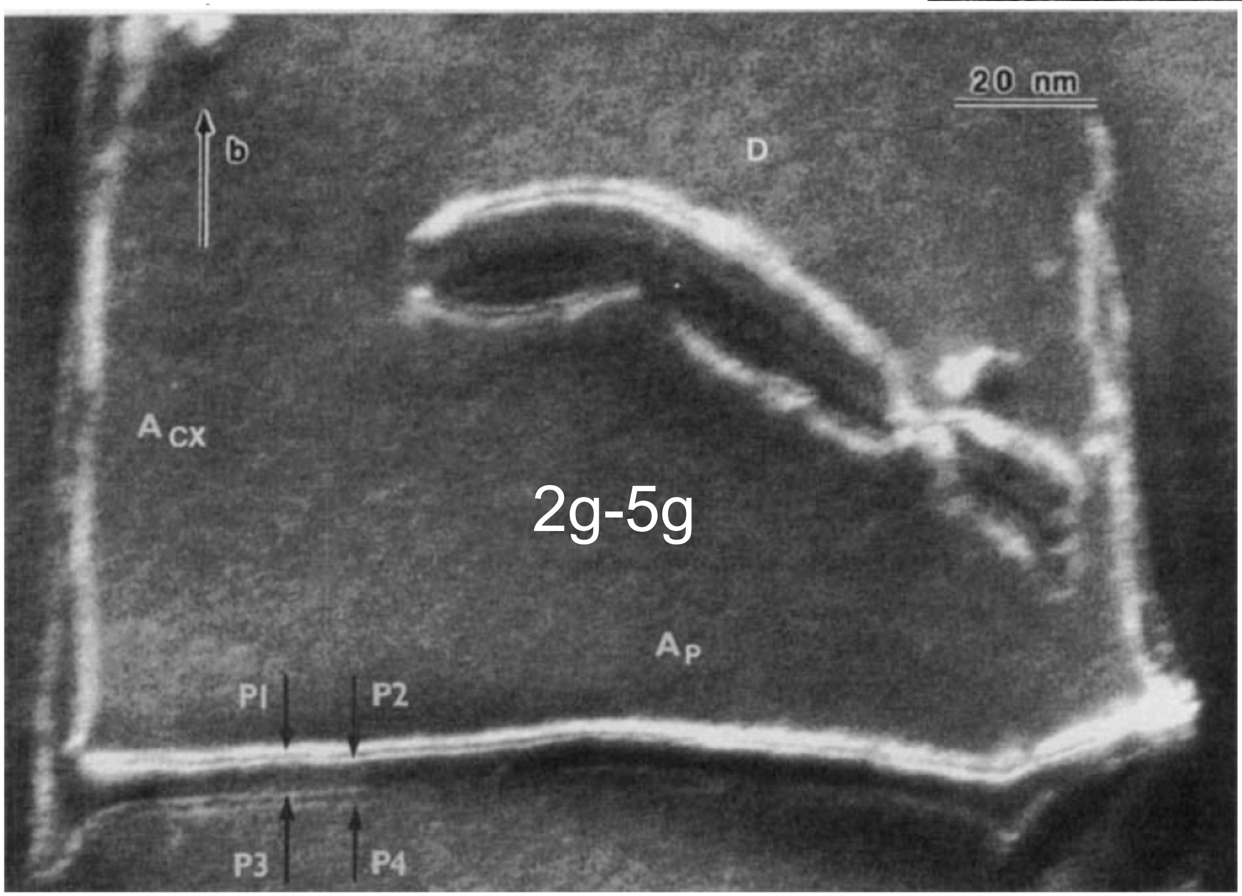


Large deviation parameters enable imaging of fine details associated with defect strain fields

# “Conventional” Diffraction Contrast

- Weak beam imaging
  - APB coupled a<101> dislocations in $Ni_3Al$

*Baluc, et al, Phil Mag 64 (1991)*

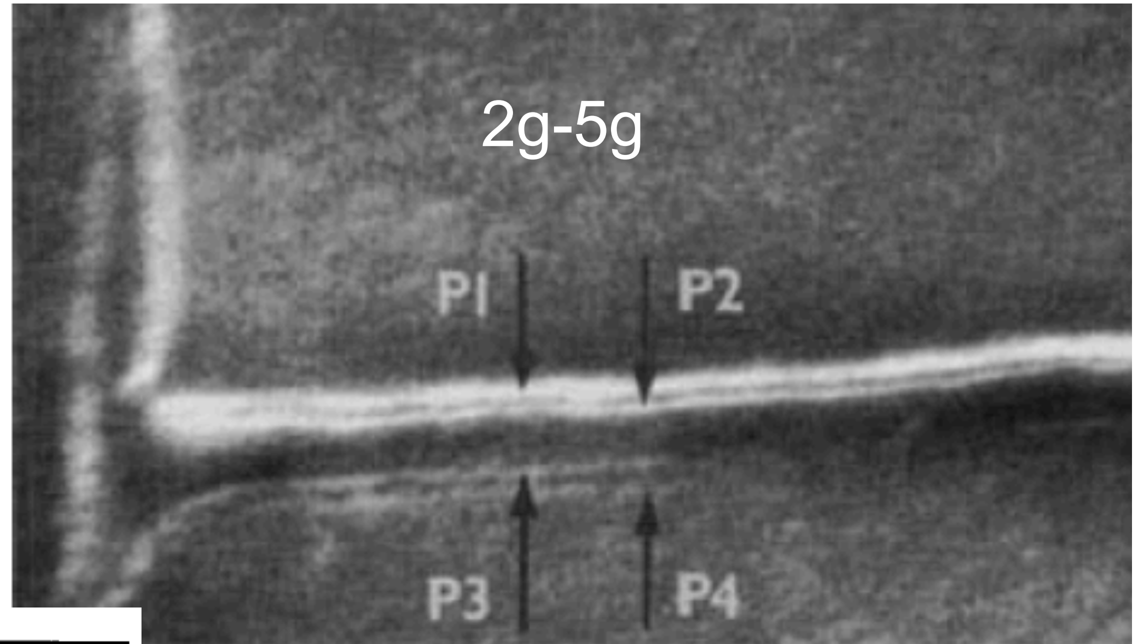


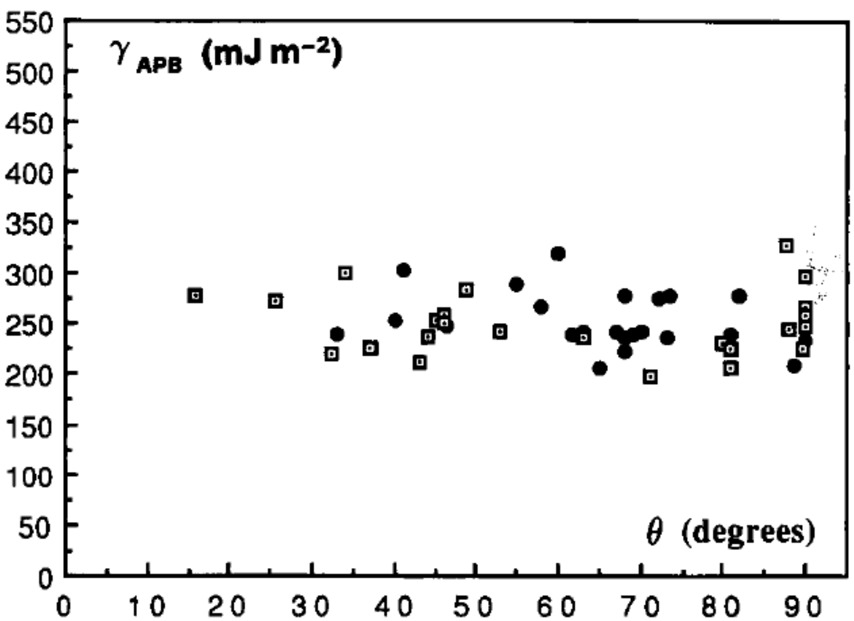



Large deviation parameters enable imaging of fine details associated with defect strain fields

# Conventional Diffraction Contrast – Drawbacks

- Very thin specimens required:
  - Absorption and chromatic aberration of post-specimen lenses
- Very flat foils required to insure precise diffraction conditions
- For fine detail, weak beam conditions:
  - Large contrast but weak intensities
  - Long exposure times = "Shooting in the dark"
  - Drift, sample stability and contamination

*Advances in high brightness sources have not benefitted diffraction contrast defect studies*

# New Generation STEMs *Not* Optimal for CTEM


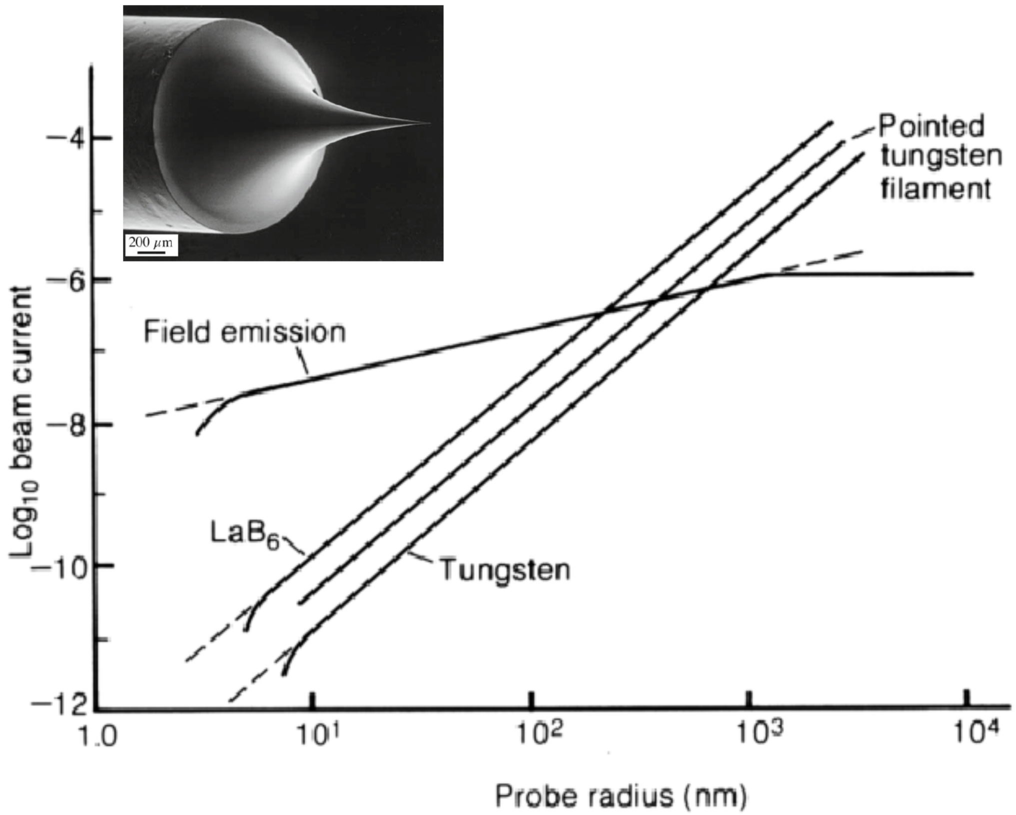


*Figure 1.8. Beam current versus probe radius for various electron sources. Data obtained from Veneklasen (1972) and Joy (1974).*

- Field emission guns far superior to thermionic emitters for fine-probe STEM and chemical analysis

# Conventional Diffraction Contrast – Drawbacks


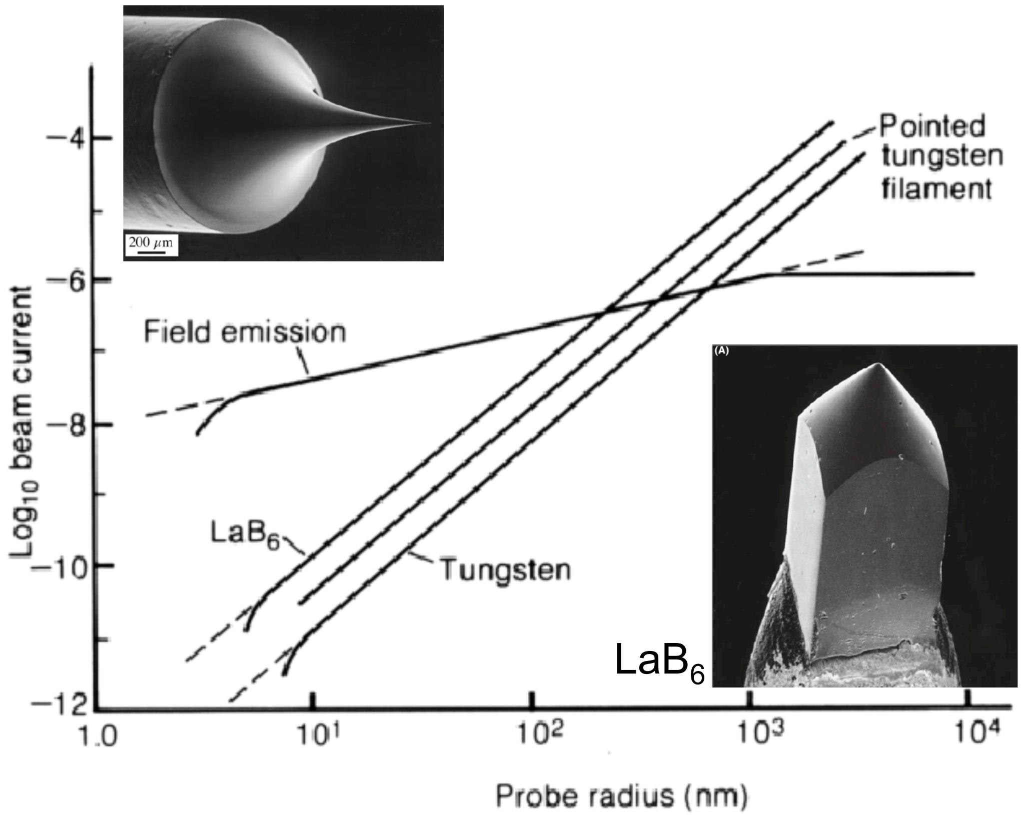


*Figure 1.8. Beam current versus probe radius for various electron sources. Data obtained from Veneklasen (1972) and Joy (1974).*

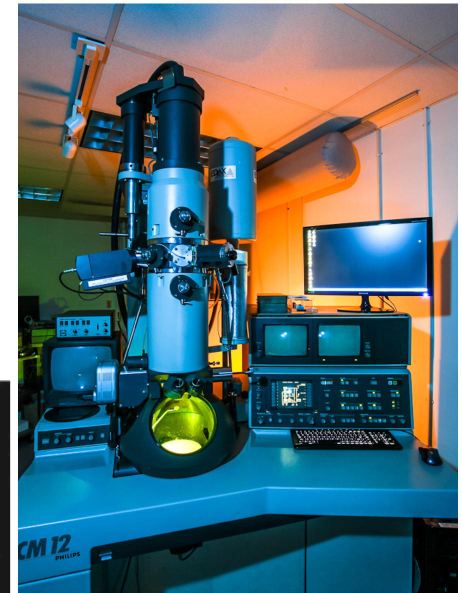


- $LaB_6$ provides better current density for conventional (and weak beam) imaging !!
- Field emission guns far superior to thermionic emitters for fine-probe STEM and chemical analysis

# "Revised" Spiral History of TEM

*A. Howie, M&M Proceedings, 2012*

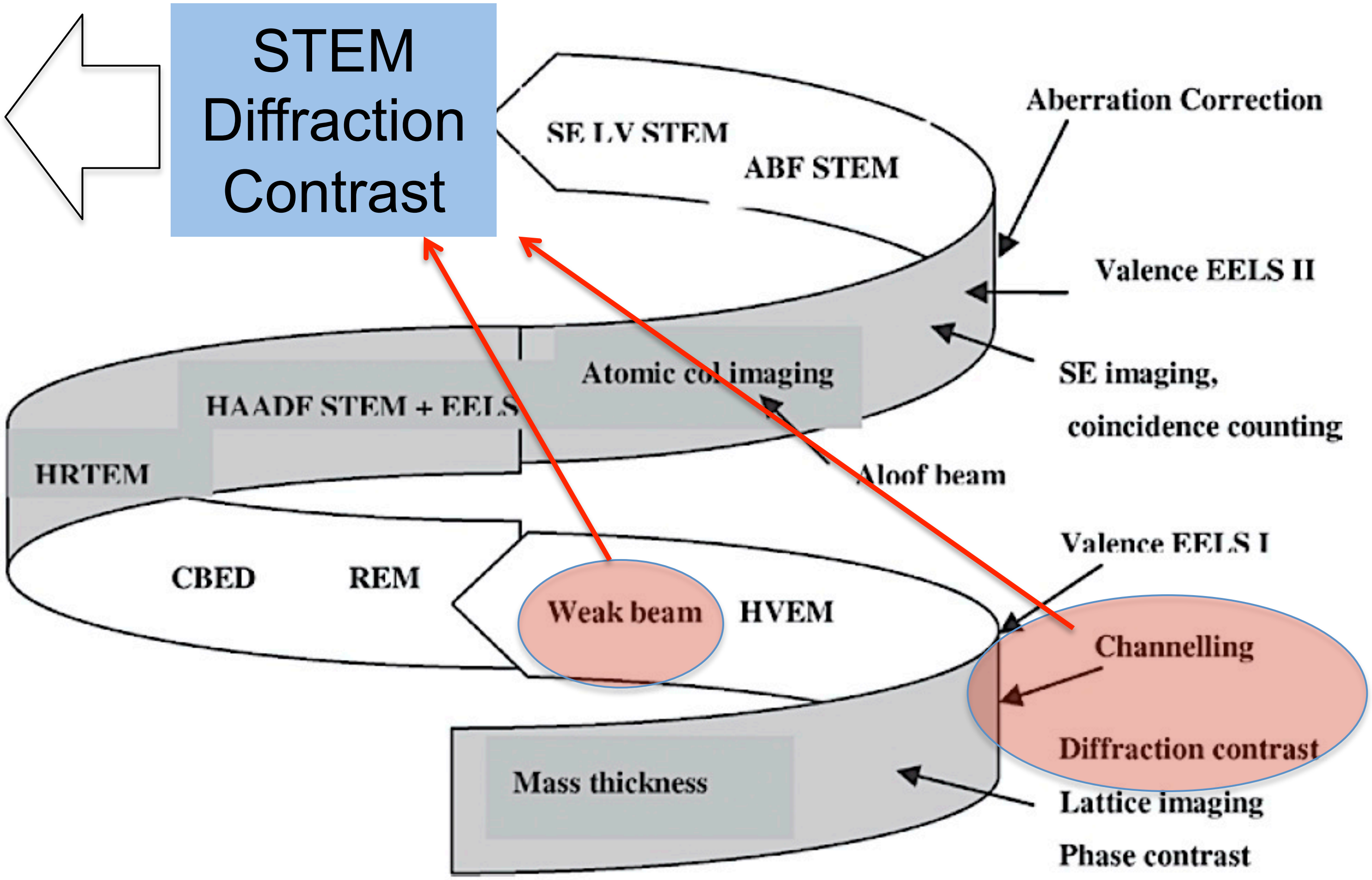


*Advances in high brightness sources can benefit diffraction contrast defect studies*

# "Conventional" vs. STEM Diffraction Contrast

*Williams and Carter*

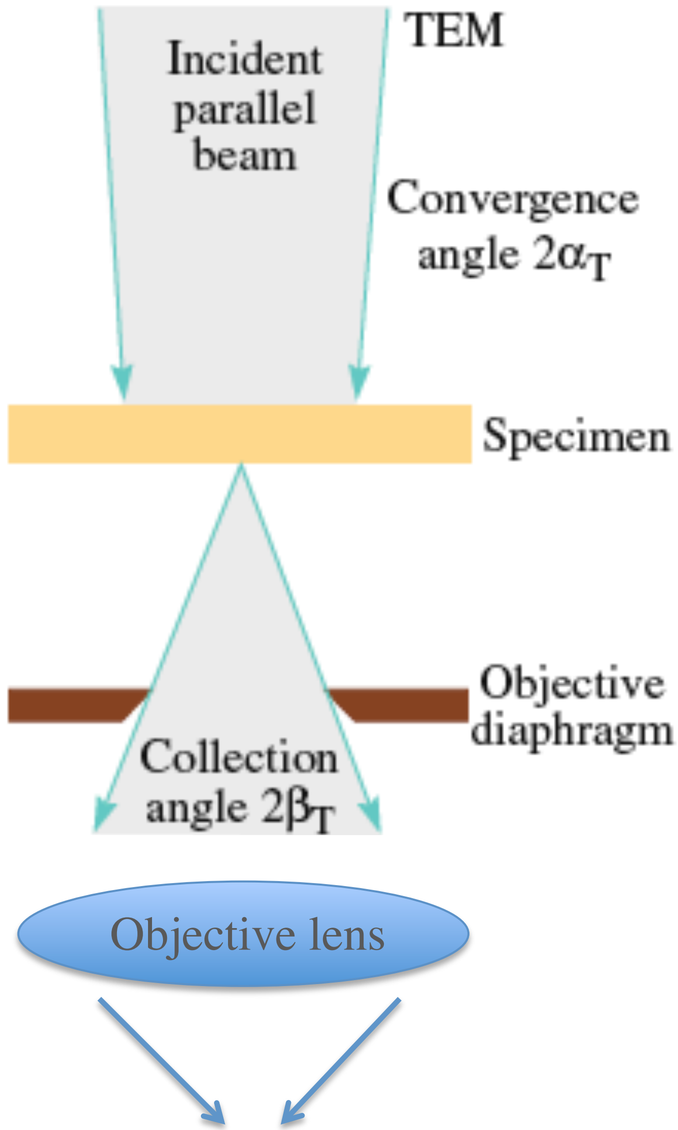


*PJ Phillips, MJ Mills, M De Graef*
*Phil Mag (2011)*

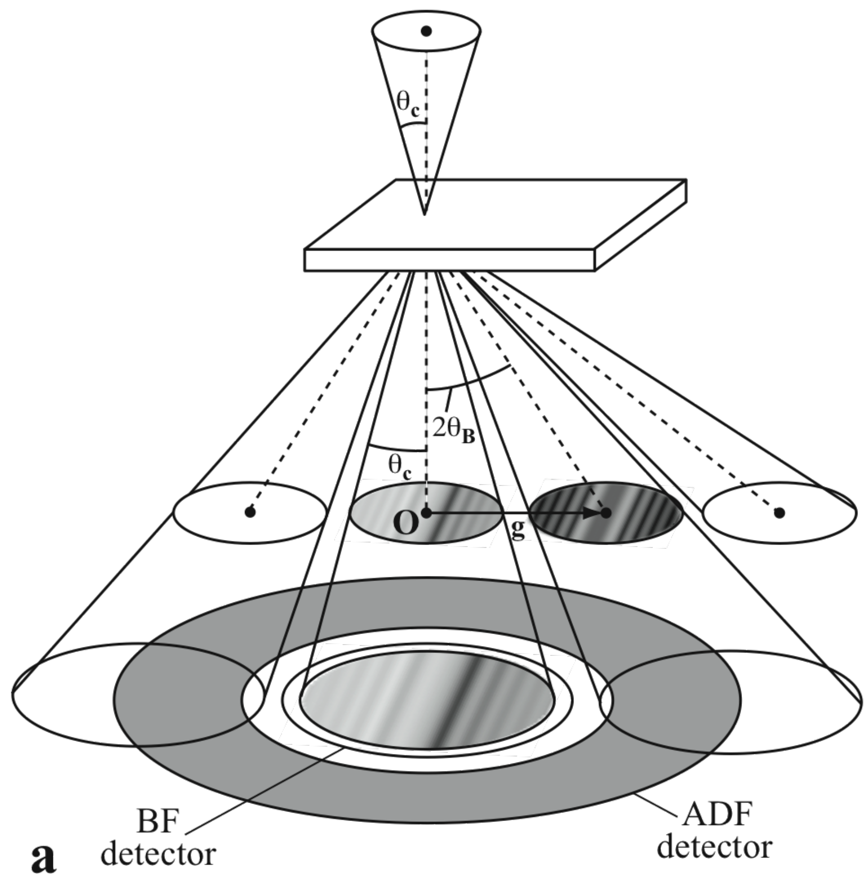


- Underdeveloped technique !
- Significant advantages relative to conventional diffraction contrast

# Early STEM Diffraction Contrast Studies

- CJ Humphreys, et al., Proc. of the 5th SEM Symposium (1972) 205-214.
- GR Booker, et al., Proc. of the 7th SEM Symposium (1974) 225-234.
- DM Maher and DC Joy, *Ultramicroscopy*, **1** (1976) 7-12.
- KE Easterling, *J Mater Sci*, **12** (1977) 857-868.
- HL Fraser, et al., *Phil Mag*, **35** (1977) 159-176.

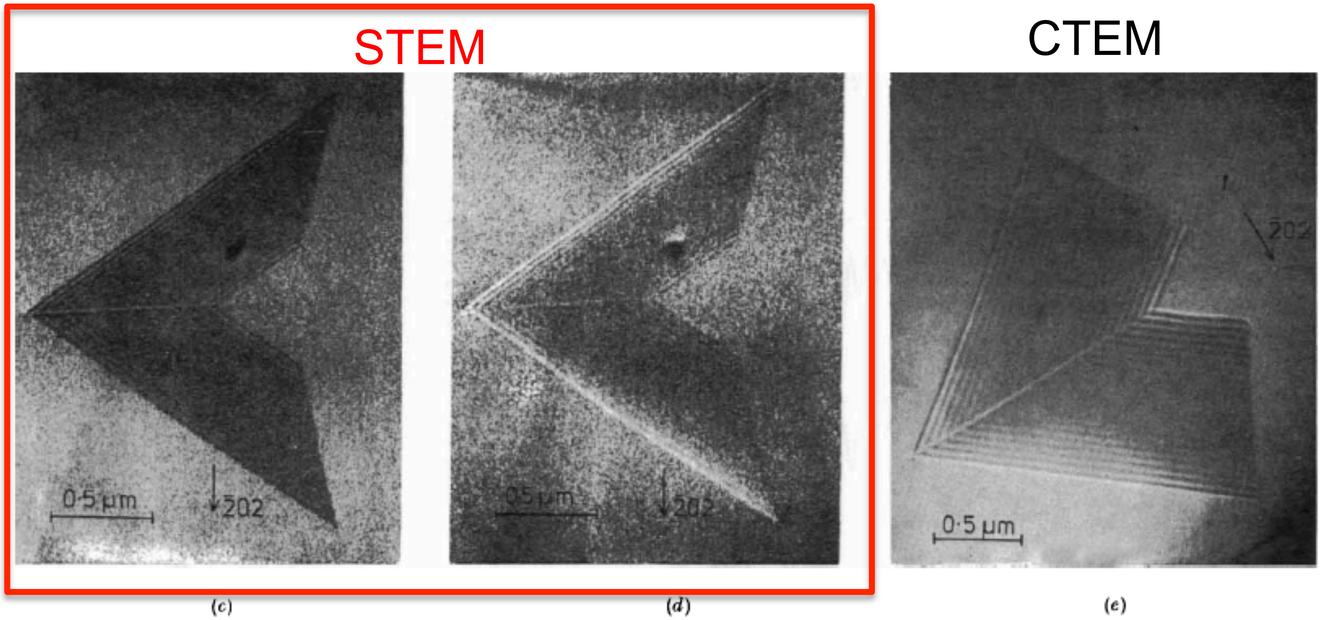


Series of STEM micrographs taken at 200 kV with the $\bar{2}02$ diffracting vector indicated. (*a*) and (*b*) are a bright-field/dark-field pair taken close to the Bragg condition so that $w \simeq 0$. The value of $2\beta_s$ was $1 \times 10^{-2}$ radians and $2\alpha_s$ was about $1{\cdot}0 \times 10^{-2}$ radians. For (*c*) and (*d*) which are also a bright-field/dark-field pair the value of $2\beta_s$ was reduced to $3{\cdot}5 \times 10^{-3}$ radians. For all these micrographs the electron beam direction **B** was close to [111]. A CTEM image of the same fault with **B** close to [141] is shown in (*e*). The top surface (T) and bottom surface (B) of the foil are marked.

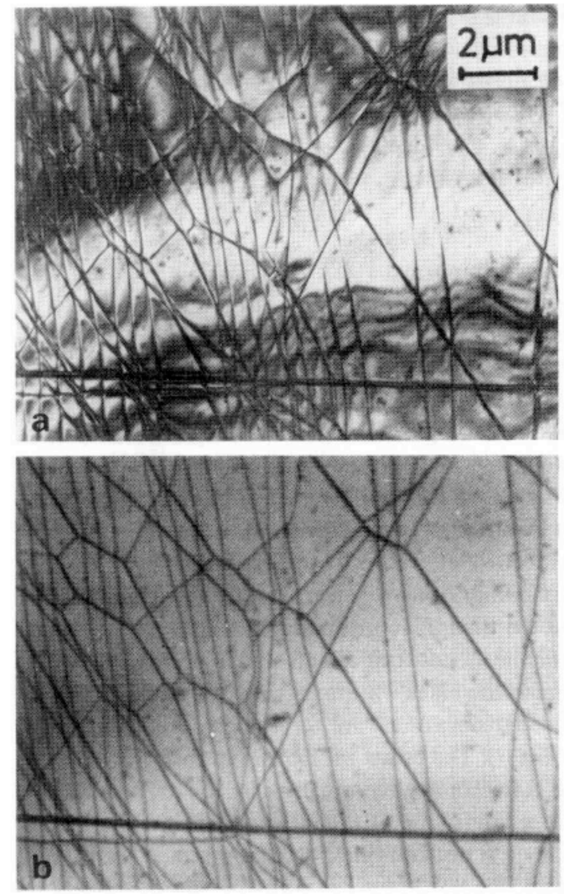


Dislocations in bent $MoS_2$ foil. (a) CTEM, incident beam divergence **0.5 mrad** (b) STEM, detector acceptance angle **5 mrad**. Figure 5 of Humphreys *Ultramicroscopy* **7** (1981) 7-12.

# "Conventional" Diffraction Contrast

- Bend contours limit defect visibility

*Williams and Carter*

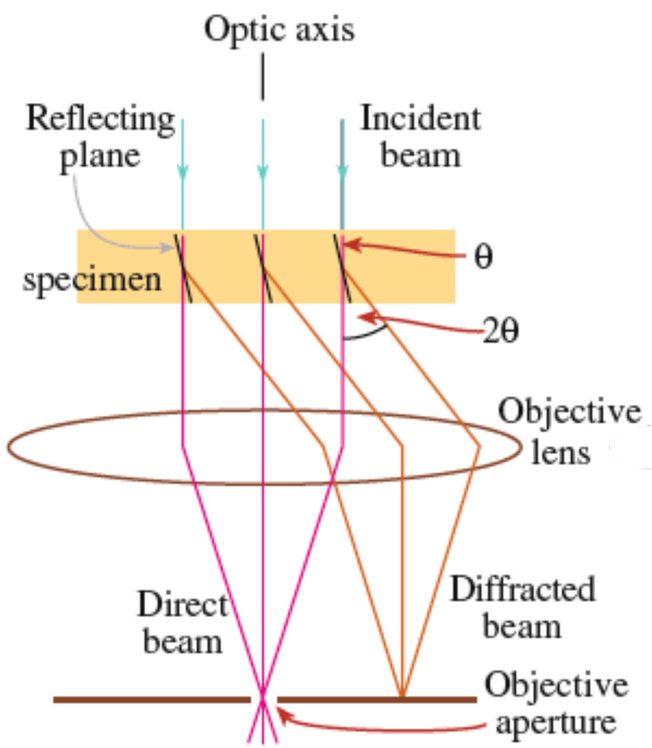


*Image Formation*

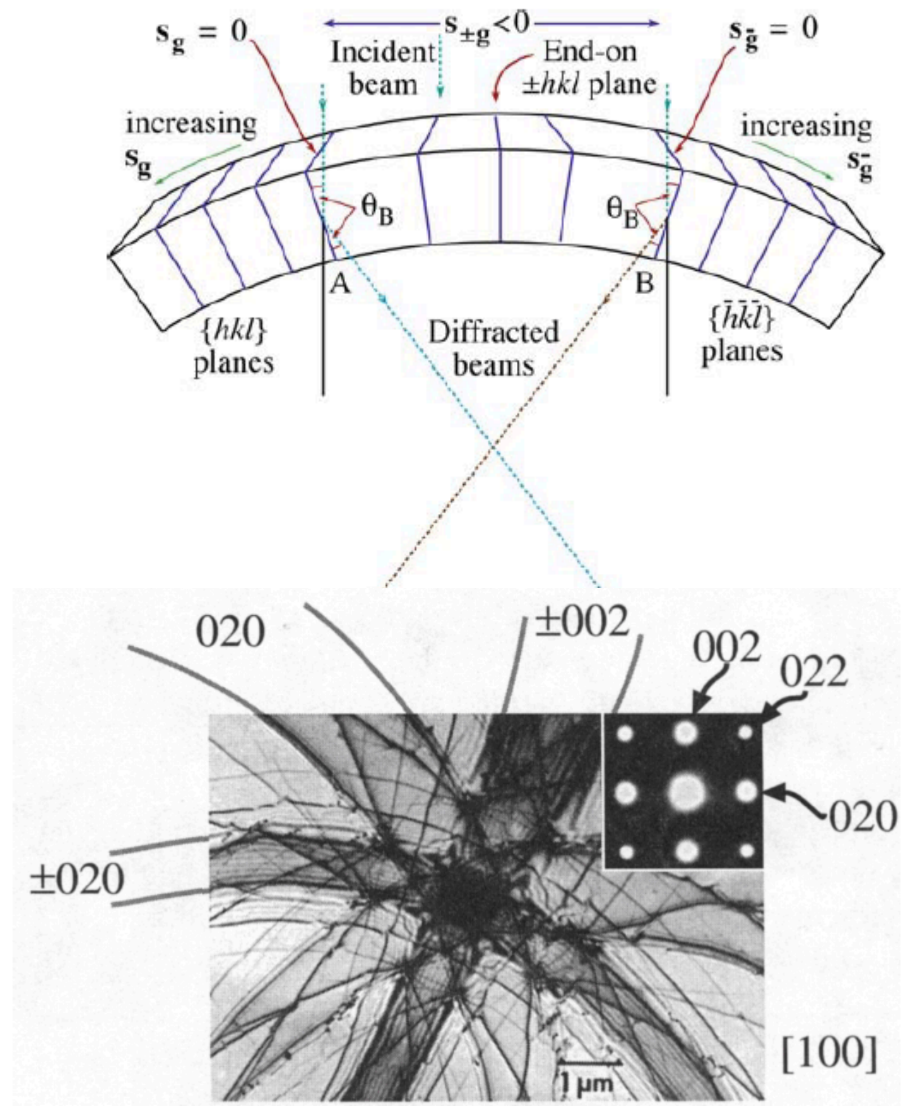

# "Conventional" Diffraction Contrast

- Bend contours limit defect visibility

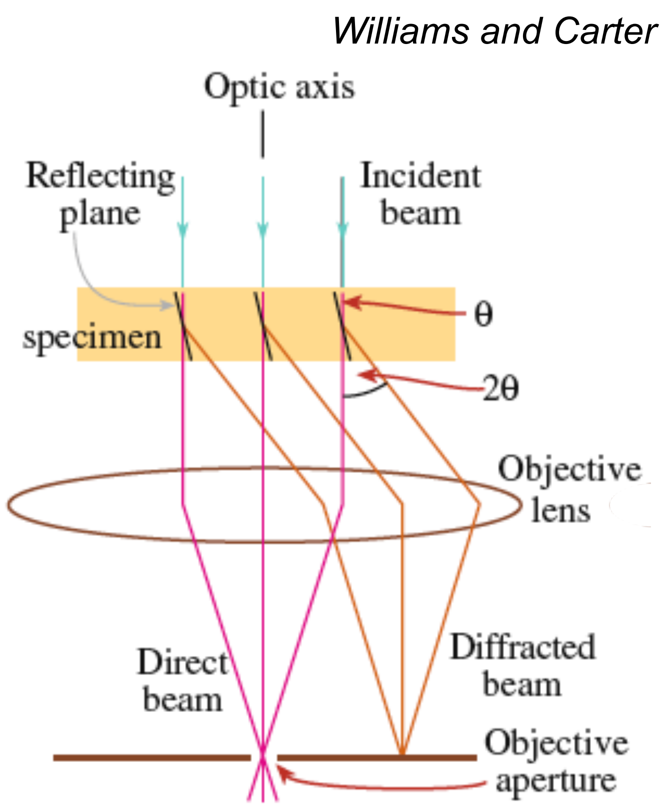


*Image Formation*

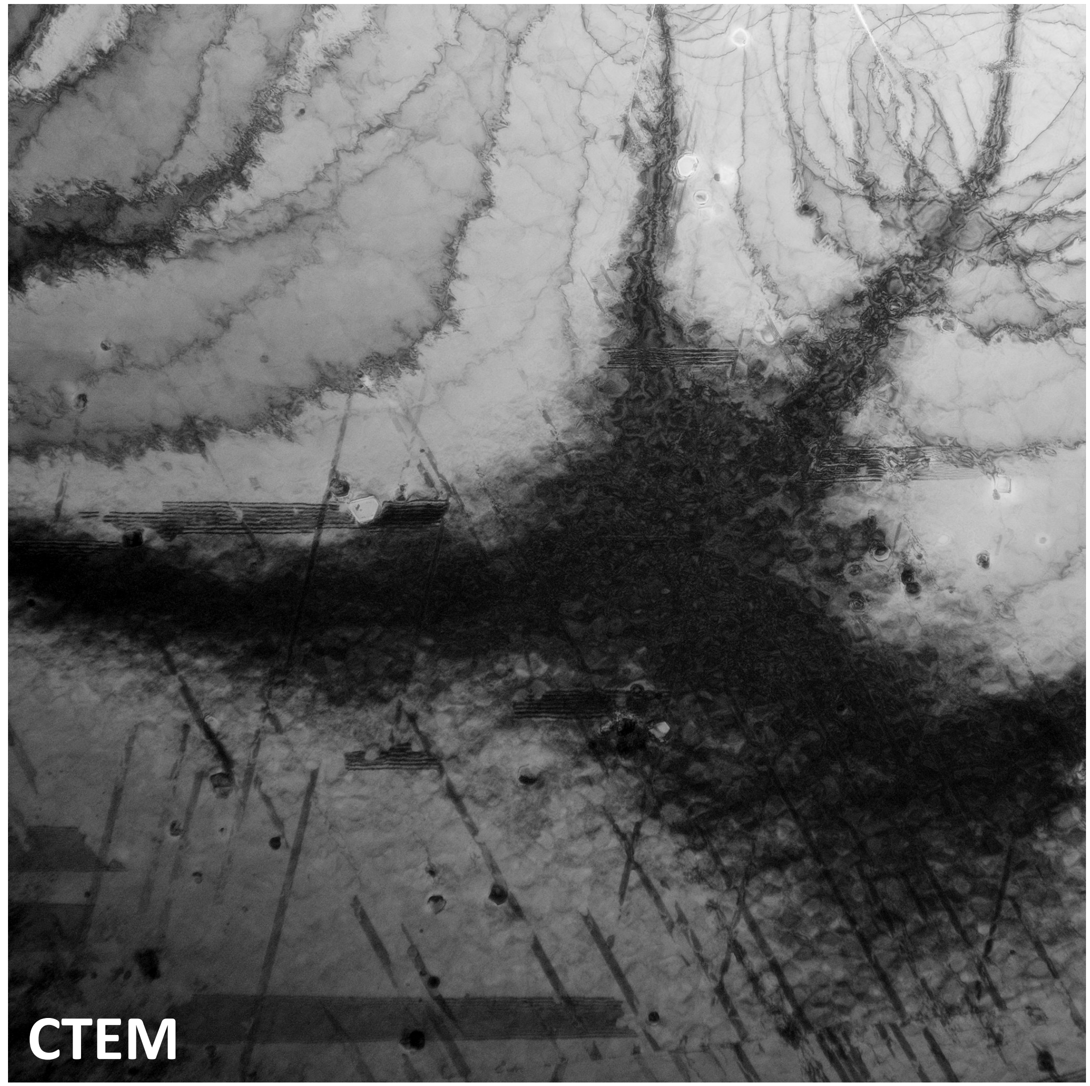

# Advantage 1:  Minimize Bend Contour Effects

- Bend contours and defect visibility

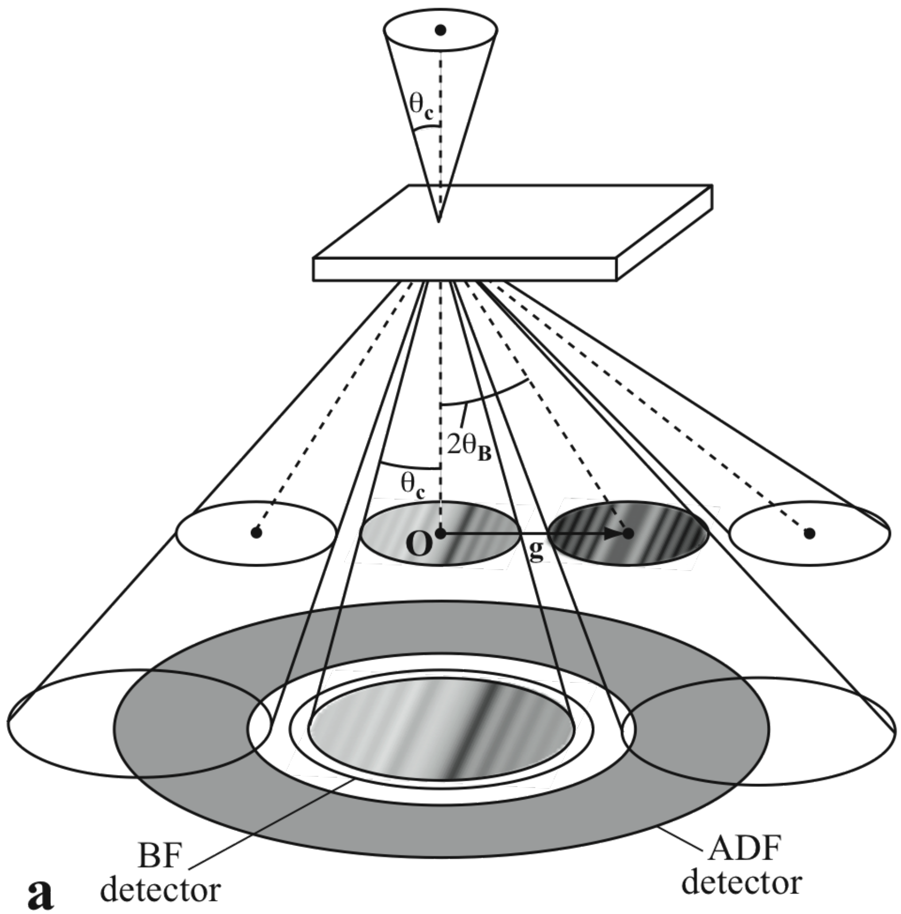


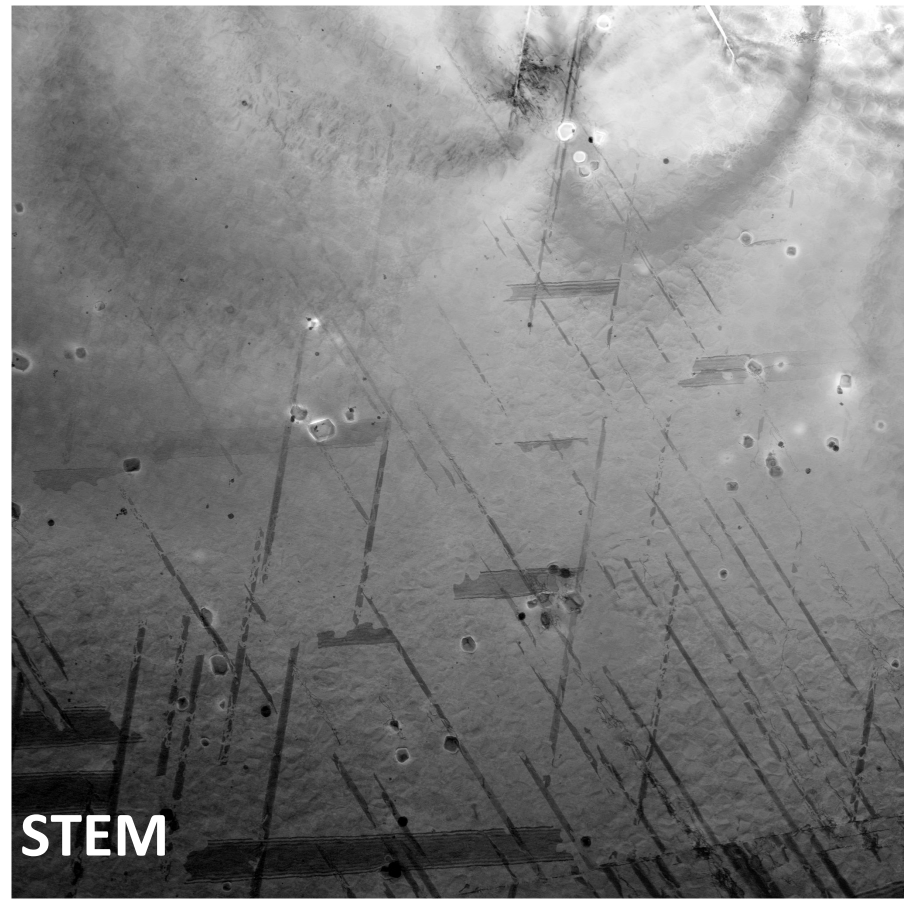


Converged beam "mutes" bend contours but reveals dislocation and stacking fault contrast

*PJ Phillips, MJ Mills, M De Graef, Phil Mag  (2011)*

# "Conventional" vs. STEM Diffraction Contrast

• STEM Images in Al-4Cu alloy as function of collection angle

*Williams and Carter*

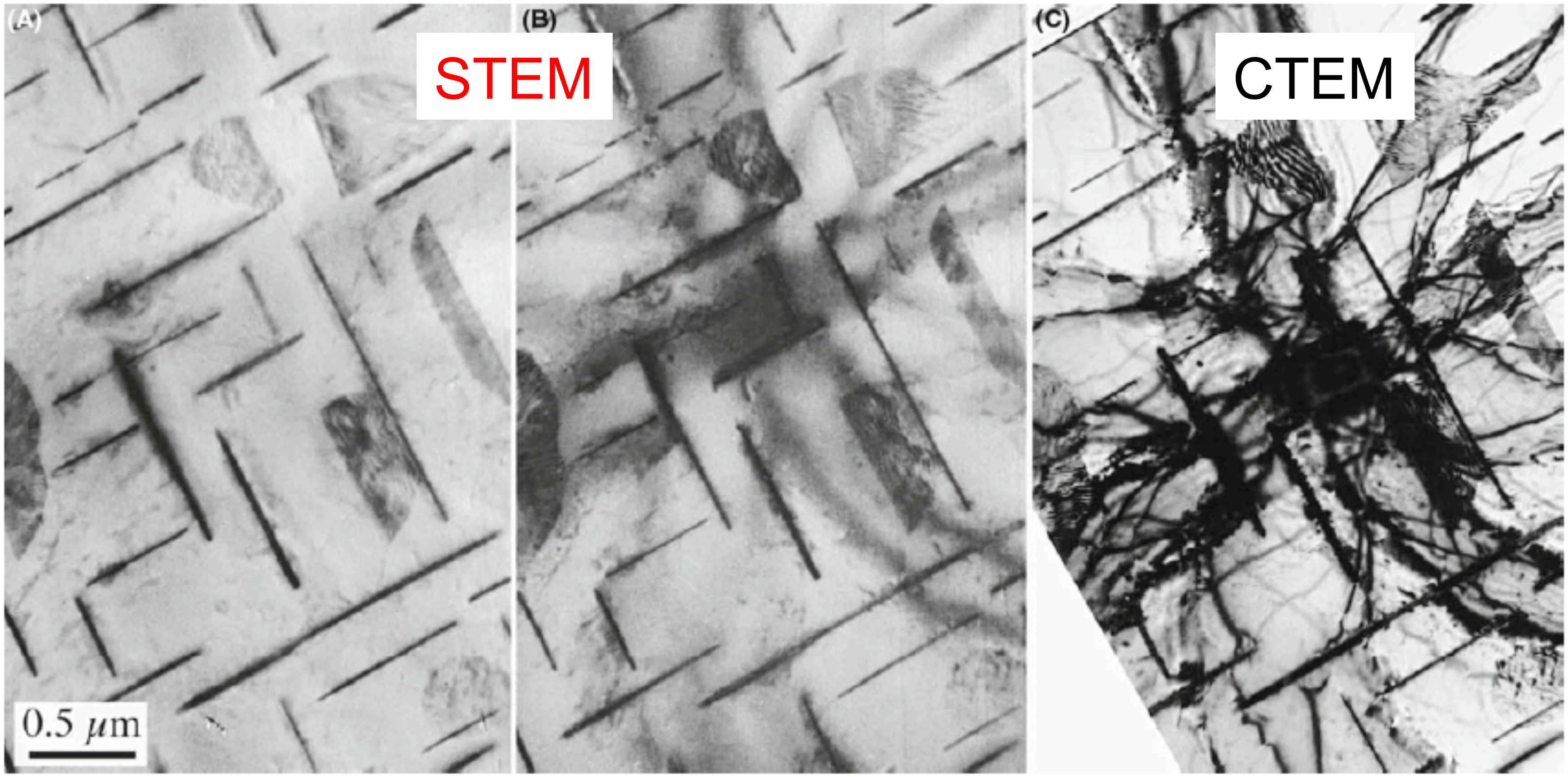


• As collection angle decreases, approach conventional diffraction contrast condition
• "Compares unfavorably to TEM images…"
• "Imaging crystal defects is soley the domain of TEM…"

# Advantage 2: Higher Order g Imaging of Strain Fields

- **Higher Order g** imaging
  - similar image contrast to CTEM **weak-beam dark field**
  - rapid, simultaneous acquisition of bright field/dark field images
  - fewer limitations than WBDF
    - thicker samples
    - practical applications

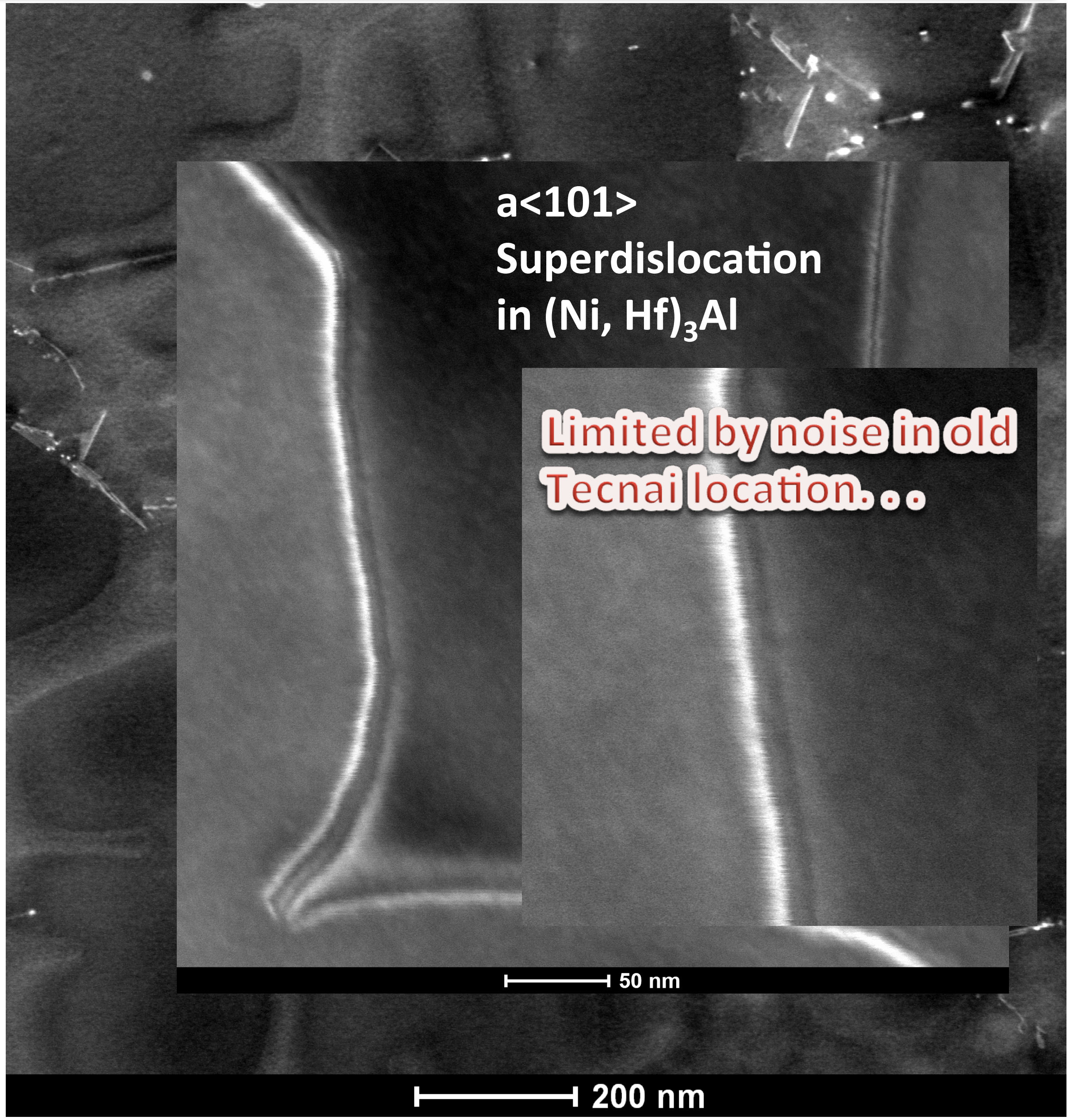

# Advantage 2: Higher Order g Imaging of Strain Fields

**a<101> Superdislocation in $(Ni,Hf)_3Al$**

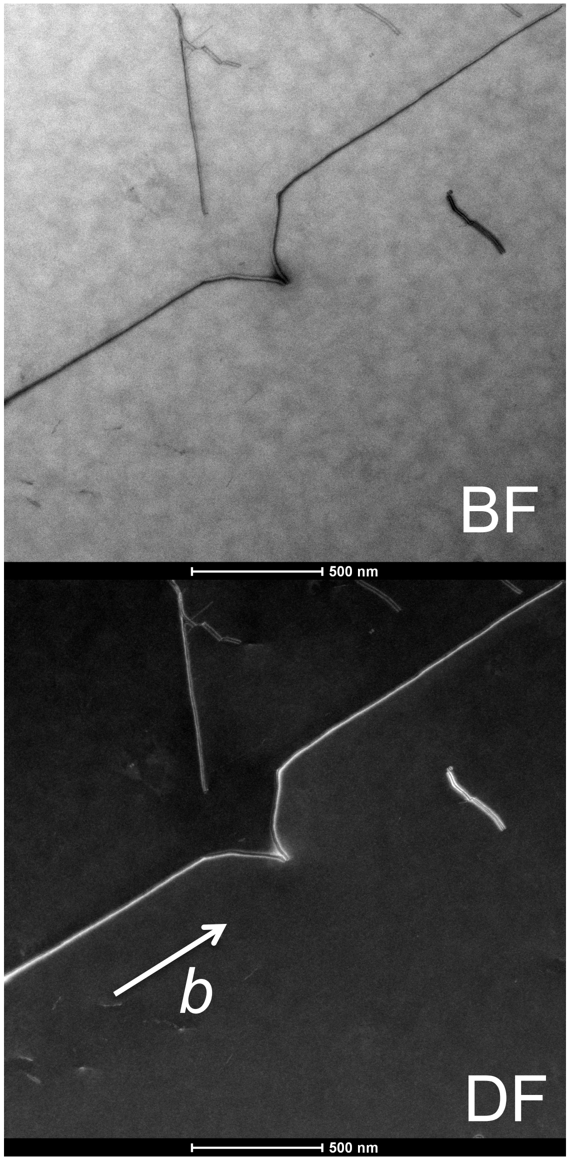


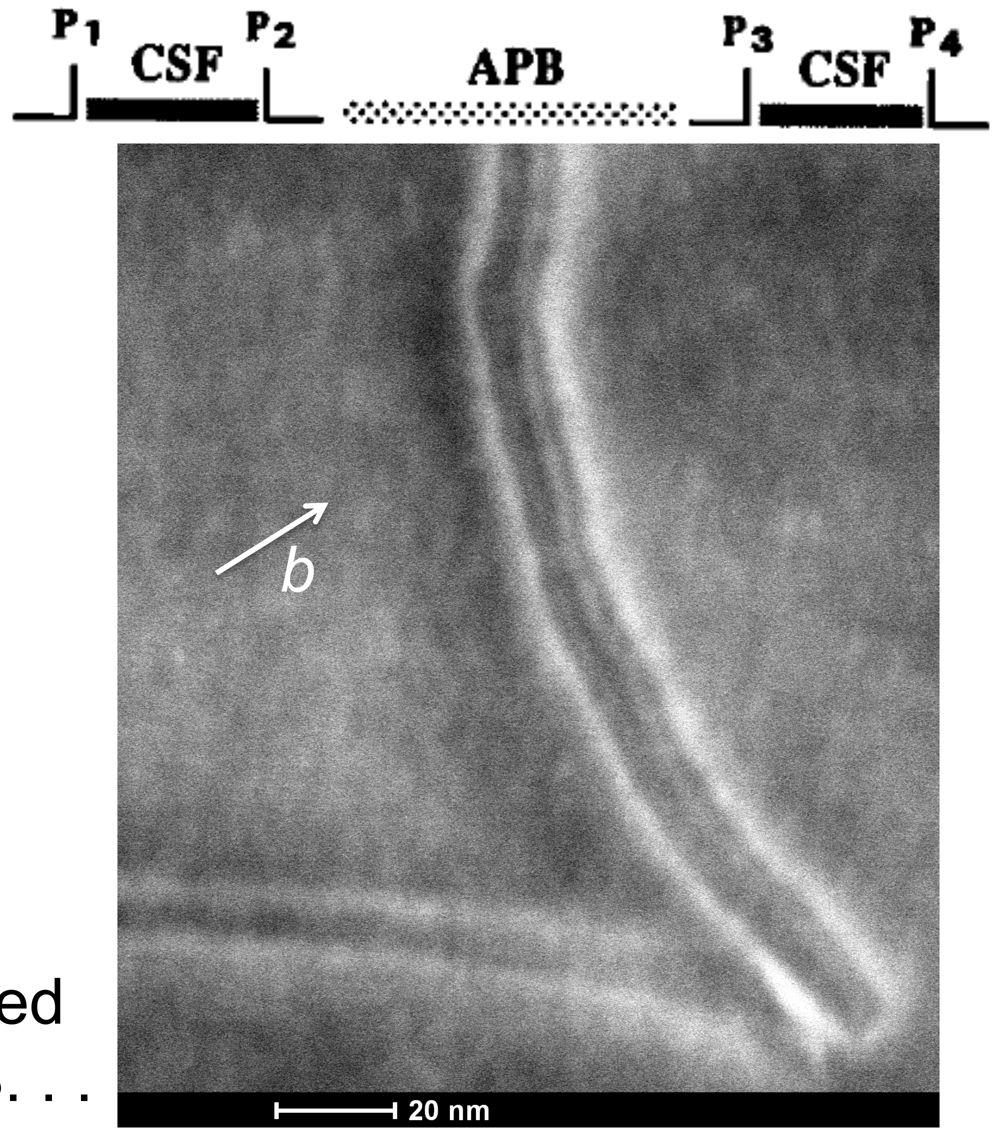


No longer noise limited in CEMAS. . .

# Advantage 3:  Thick Samples Can Be Examined

- In CTEM, ***loss of resolution*** in thicker samples due to chromatic aberration

Williams and Carter

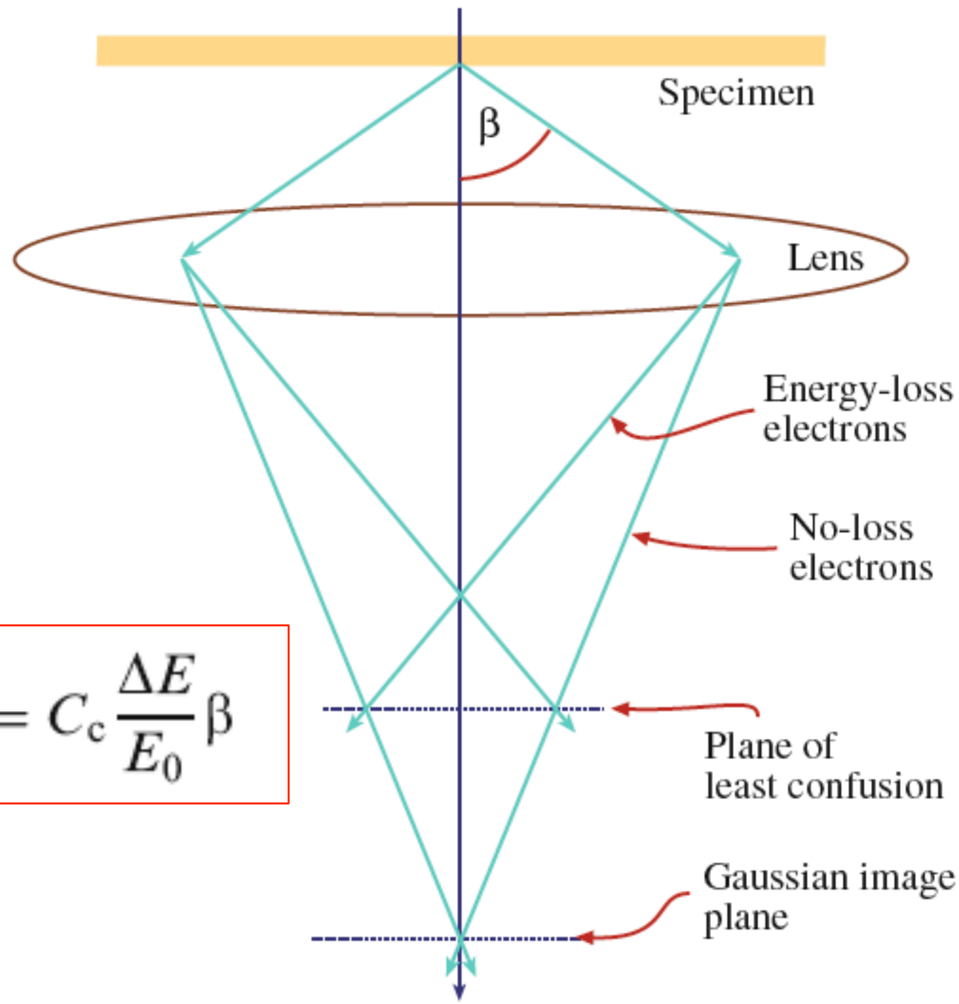


$$r_{chr} = C_c \frac{\Delta E}{E_0} \beta$$

# Advantage 3: Thick Samples Can Be Examined

- In CTEM, ***loss of resolution*** in thicker samples due to chromatic aberration

- In STEM, no post-specimen lenses, thus **chromatic aberrations** normally suffered are non-existent

*Williams and Carter*

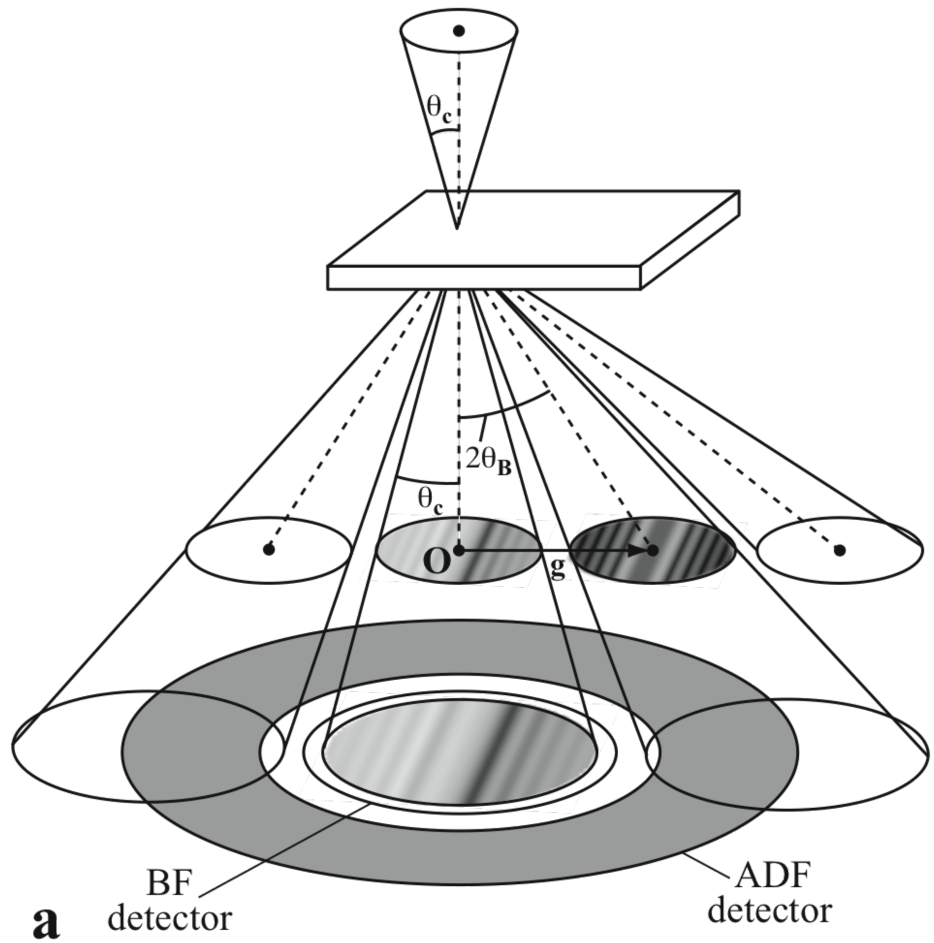

# Advantage 3: Thick Samples Can Be Examined

• In CTEM, ***loss of resolution*** in thicker samples due to chromatic aberration

• In STEM, no post-specimen lenses, thus **chromatic aberrations** normally suffered are non-existent

• High brightness FEG sources enable shorter exposure times (less drift)

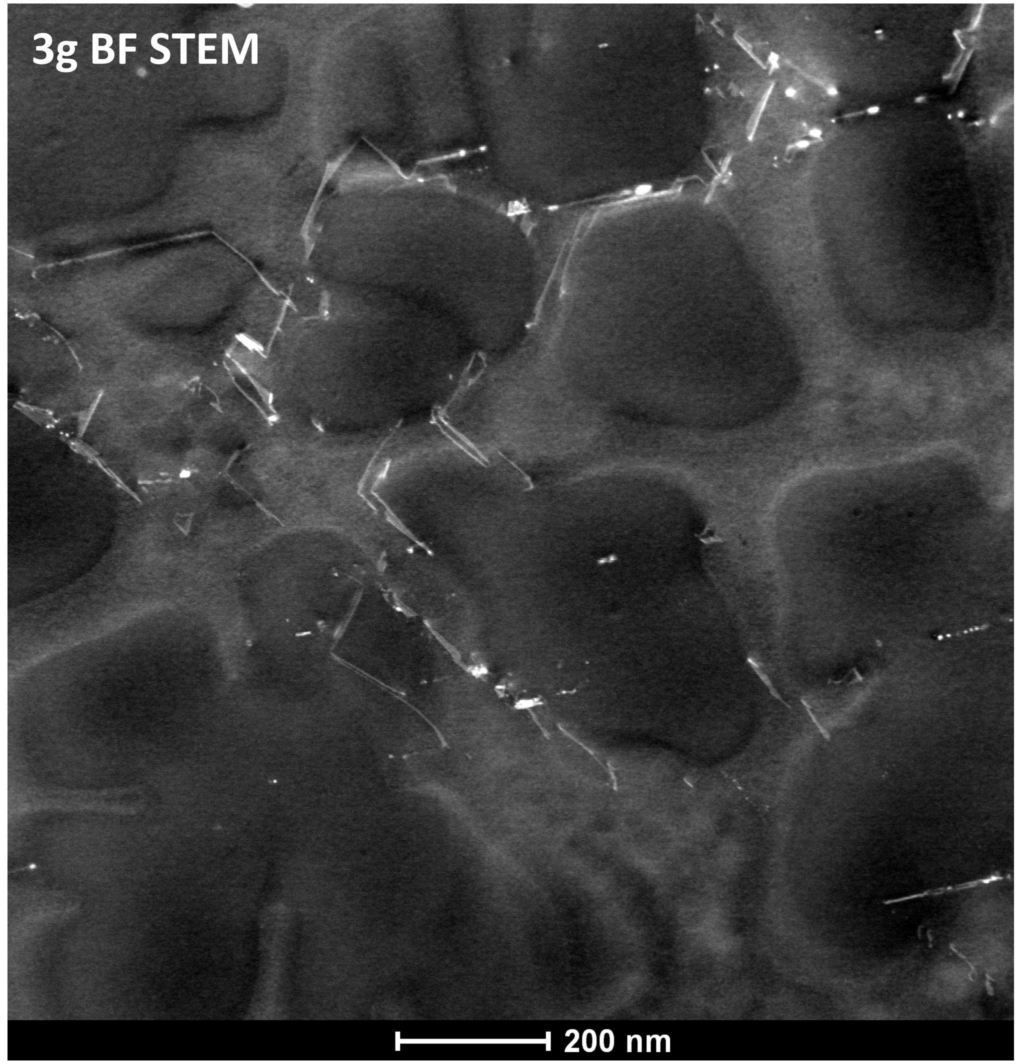


*370 nm thick specimen of Ni-superalloy*

*CTEM WBDF also attempted but low intensity and long exposure times introduced sample drift*

# Assessment of Deformation Mechanisms in Commercial Alloys

- Grain-to-grain variation in deformation modes
- Correlate orientation information from specific grains to deformation activity
- Many grains need to be assessed
- STEM diffraction contrast has been crucial due to ability to probe thicker regions

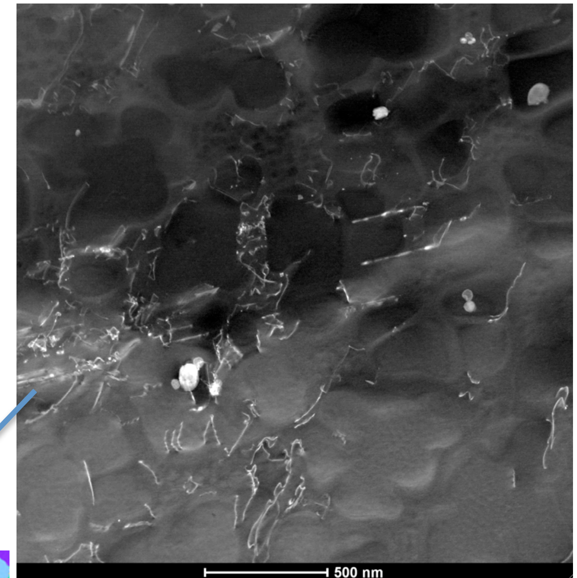


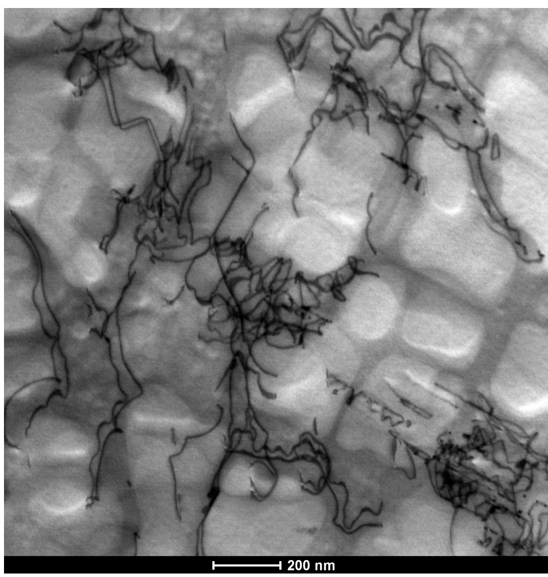


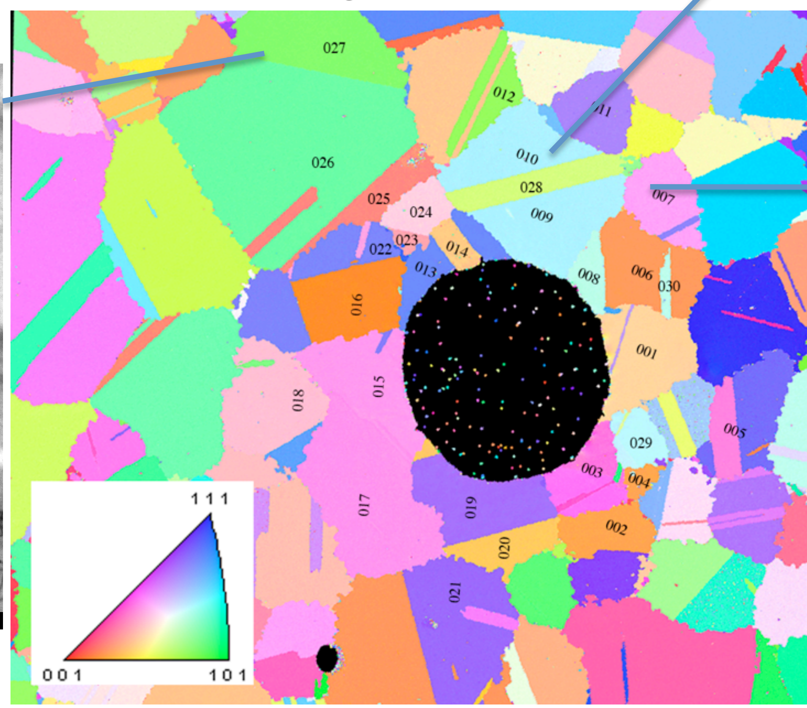


# Dislocation Substructure within Ultra-fine Grains

STEM images obtained at four different "tilts" of the sample for dislocation density measurements

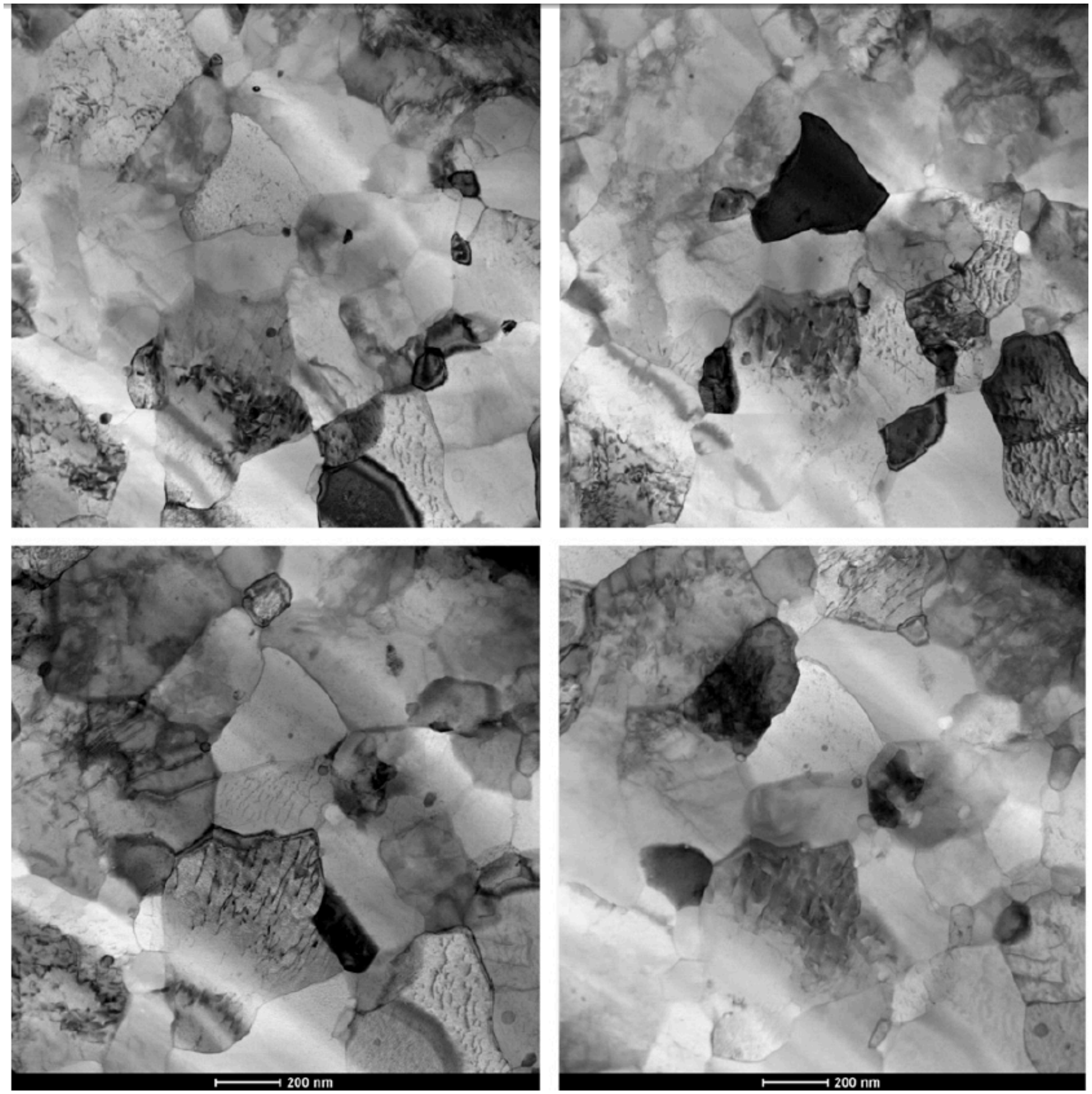


*M. C. Brandes, et al, Acta Materialia 60 (2011) 1827–1839.*

# Defect Analysis with STEM Diffraction Contrast

- Systematic studies in STEM on variety of materials in Tecnai TF20

- Variations in:
  - camera length (CL)
  - convergence angle ($\theta_c$)
  - diffraction aperture placement

- Imaging:
  - two-beam diffraction
  - **3g**
  - zone axis orientation

- Promising but need simulations to support apparent capabilities / advantages

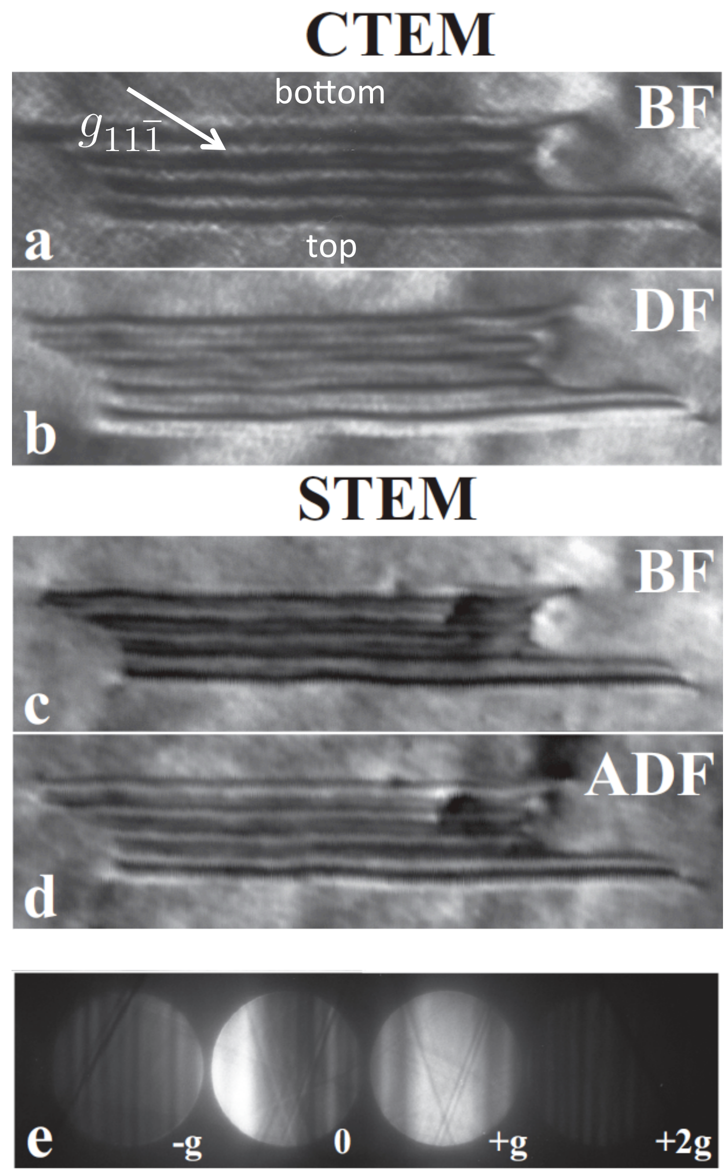

# CTEM vs. STEM Diffraction Contrast

- Previously instrumentation made STEM an inefficient and impractical tool for defect analysis
  - Tungsten or $LaB_6$ source
  - Low intensities, long exposures
  - Now, FEG sources readily available
  - Digital imaging capabilities
- Reciprocity:

$$\alpha_s = \beta_c$$

$$\beta_s = \alpha_c$$

not generally applicable to STEM image interpretation

- Simulation capability required to support promising results

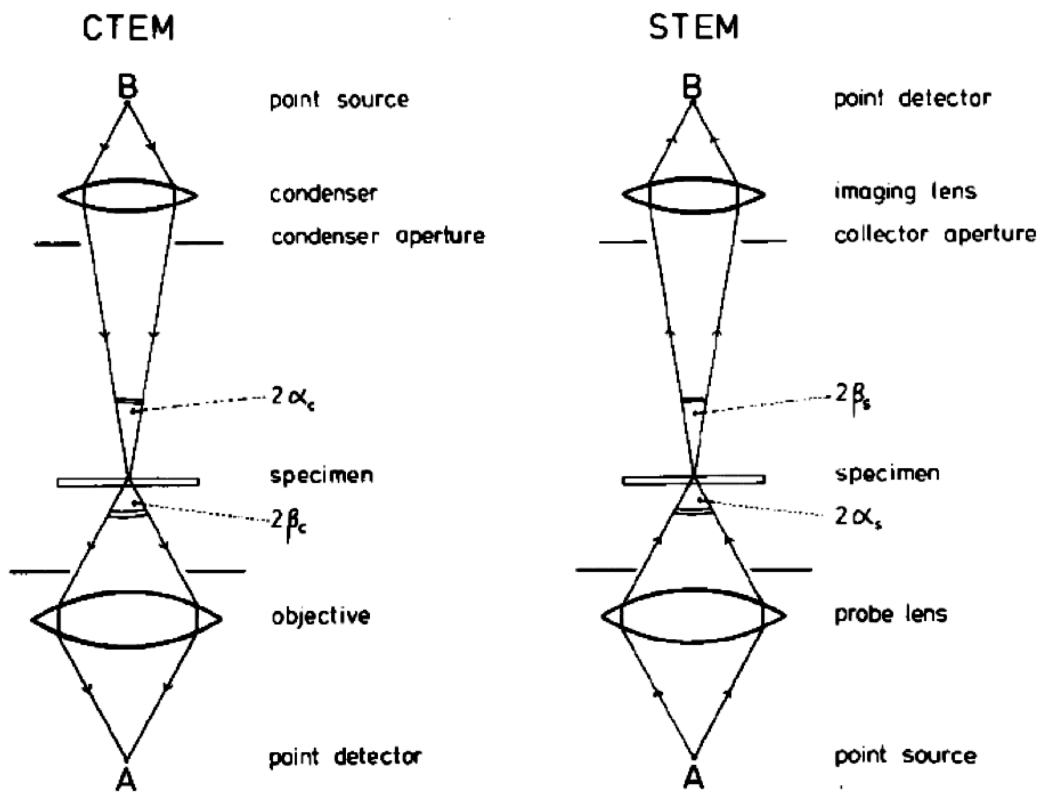


$$\beta_s \approx 10\alpha_c$$

Maher and Joy *Ultramicroscopy* 1 (1976) 231-253
Humphreys *Ultramicroscopy* 7 (1981) 7-12

# Simulation of STEM Diffraction Contrast

- Depending on imaging conditions, reciprocity may not hold

- Need ***computational*** validation of contrast rules for interpreting defect images:
    - Diffraction condition changes across disks (transmitted/diffracted)
    - Each incident beam orientation averaged according to appropriate weight factor
    - Length of chord perpendicular to systematic row
    - Scattering matrix approach utilized (much faster than conventional solution of DHW)

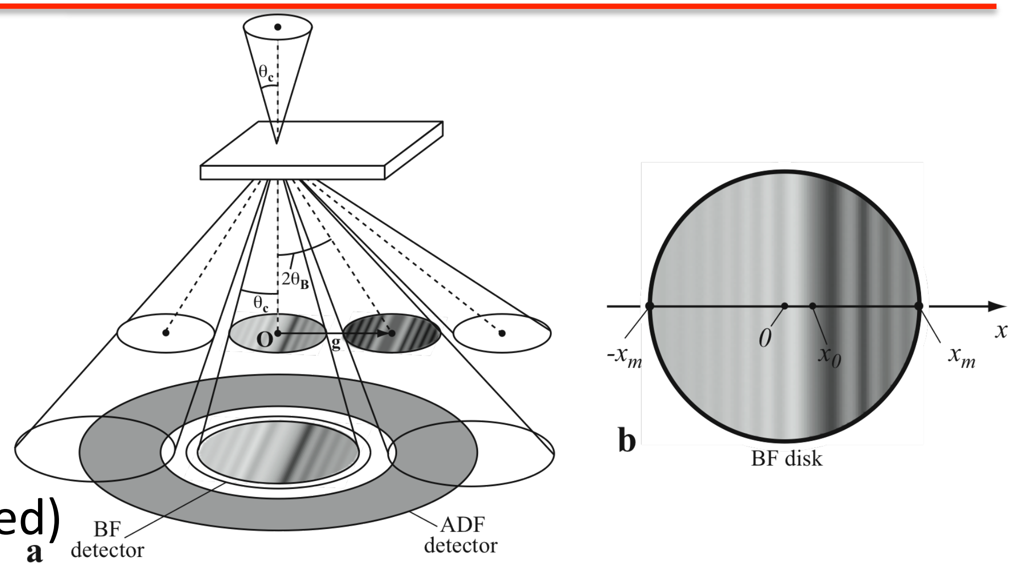


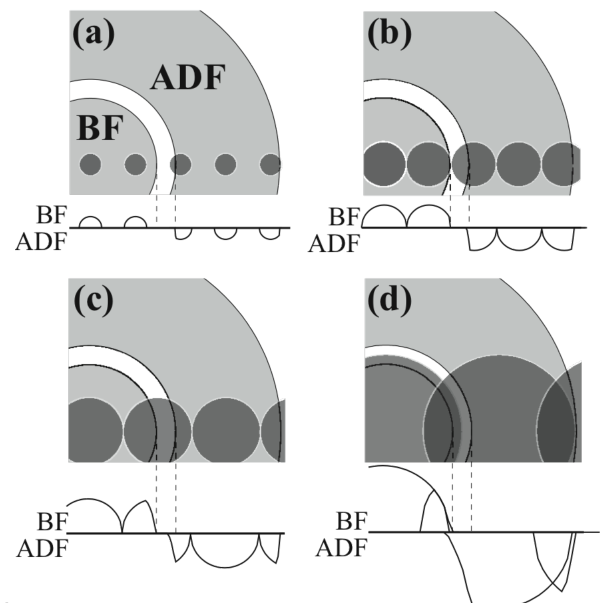


*PJ Phillips, MJ Mills, M De Graef, Phil. Mag.* ***91*** *2081-2101 (2011)*
*PJ Phillips, MC Brandes, MJ Mills, M De Graef, Ultramicroscopy* ***111*** *1483-1487 (2011)*

# Background on Scattering Matrix Approach

- Darwin-Howie-Whelan multibeam equations
  - describe how the amplitude of a diffracted beam changes with depth in the crystal
  - changes depend on Bragg condition and strengths of interactions with other beams

$$\frac{\mathrm{d}S_{\mathbf{g}}(z)}{\mathrm{d}z} = 2\pi \mathrm{i} s_{\mathbf{g}} S_{\mathbf{g}}(z) + \mathrm{i}\pi \sum_{\mathbf{g}'}{}' \frac{e^{-\mathrm{i}\alpha_{\mathbf{g}-\mathbf{g}'}(\mathbf{r})}}{q_{\mathbf{g}-\mathbf{g}'}} S_{\mathbf{g}'}(z).$$

- With defects:

$$\alpha_{\mathbf{g}}(\mathbf{r}) \equiv 2\pi \mathbf{g} \cdot \sum_{i=1}^{N_d} \mathbf{R}_i(\mathbf{r}) = 2\pi \mathbf{g} \cdot \mathbf{R}_t(\mathbf{r}).$$

- Writing the diffracted amplitudes $S_n$ as column vector gives:

$$\frac{\mathrm{d}\mathbf{S}(z)}{\mathrm{d}z} = \mathrm{i}\mathcal{A}(\mathbf{r})\mathbf{S}(z)$$

→ *Scattering matrix*

↓ *Crystal transfer or structure matrix*

which separates the diffraction geometry and the coupling of diffracted beams

- Matrix diagonal contains excitation errors of all scattering beams while off-diagonal components describe interactions between all the beam through the $q$ parameter, which are *phase-shifted* in the presence of defects

# Observed and Simulations for Stacking Faults

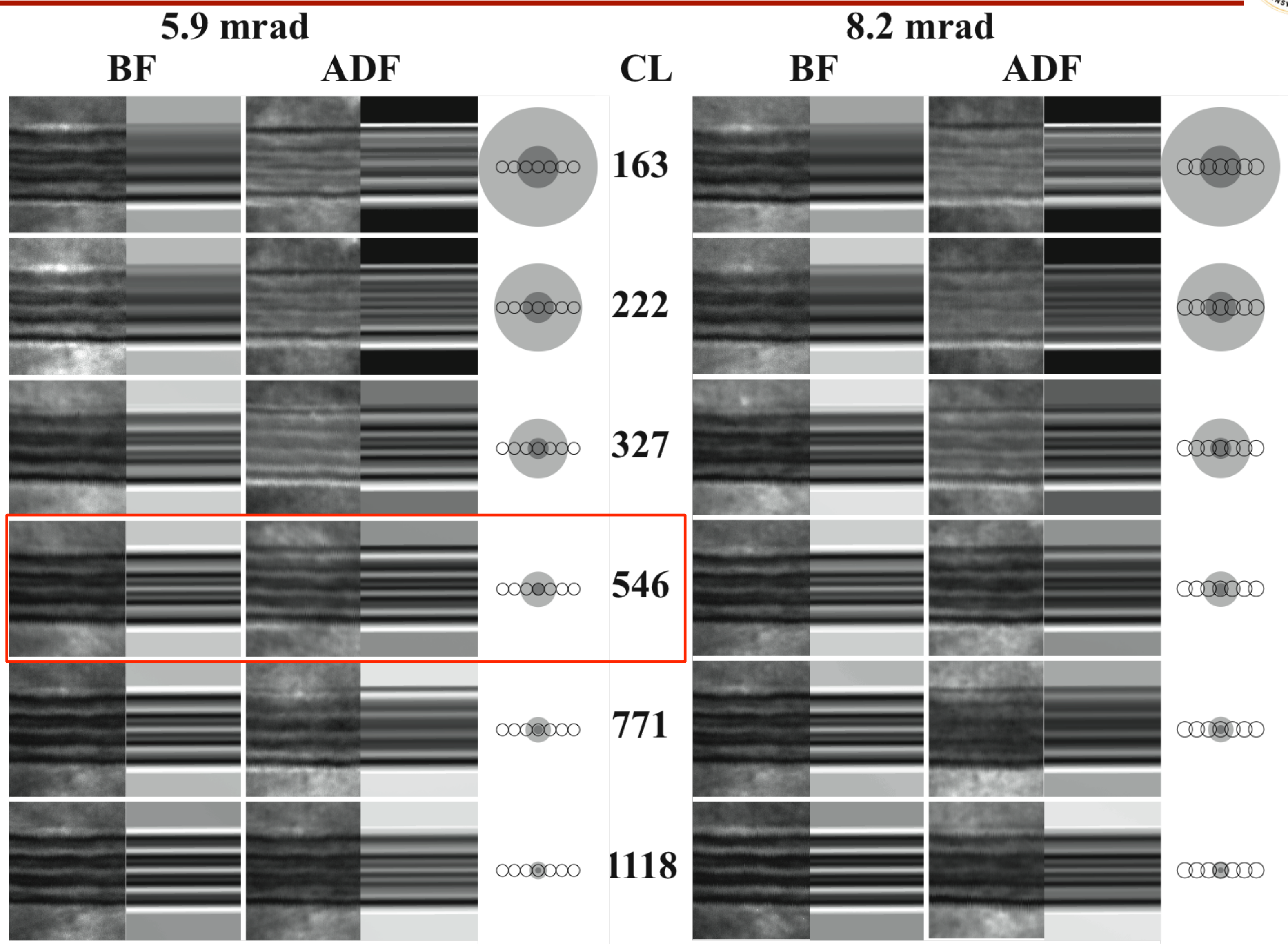


- General fringe pattern consistent in nearly all cases; this is critical for SF analysis
- At "optimal" CL, fault is symmetric/asymmetric in BF/ADF (as in CTEM)

# Dislocations in Ti ($\mathbf{g}_{10\text{-}11}$)

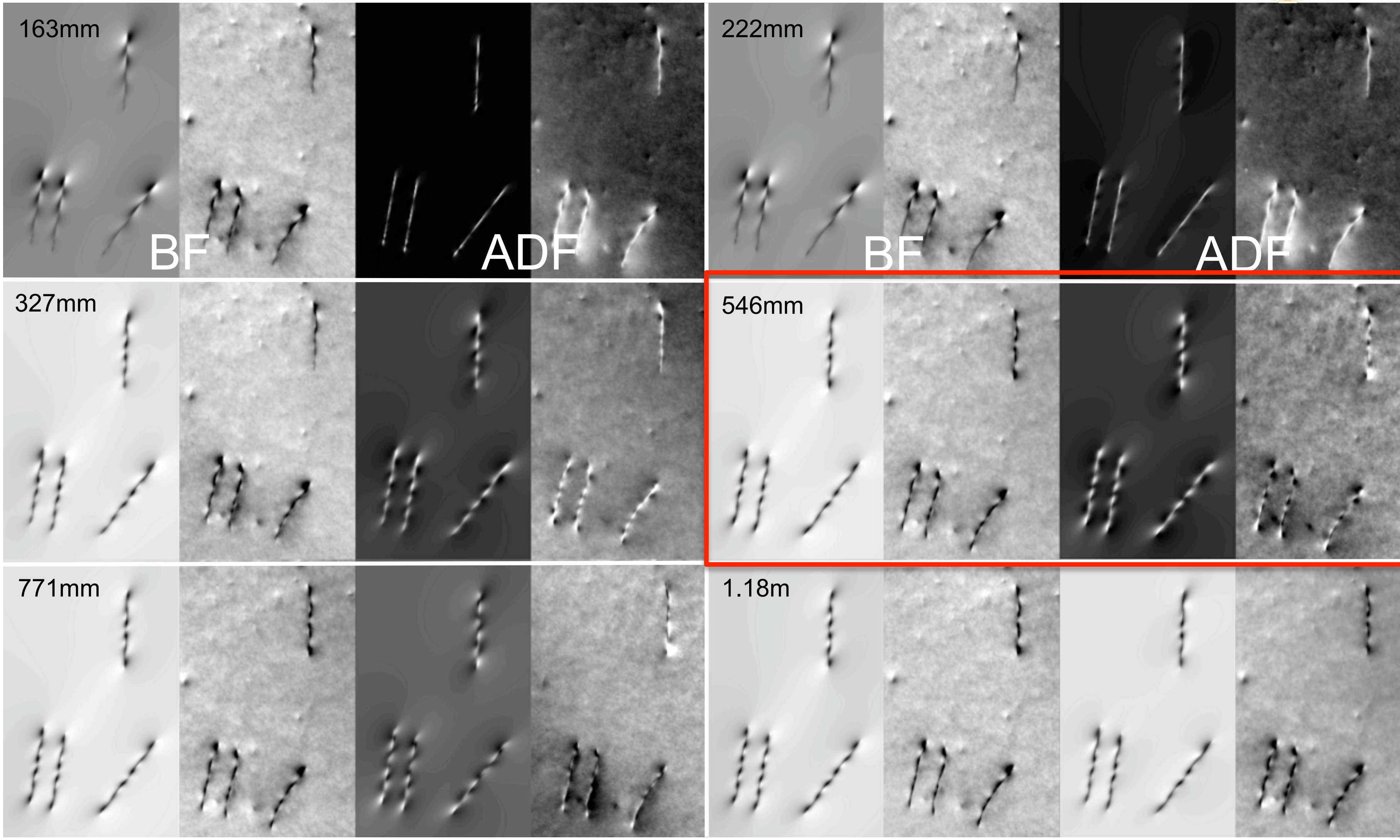


- Fringe blurring toward bottom of foil at low CL
- BF symmetric about foil center, ADF asymmetric (for optimal CL)

# Diffraction Contrast STEM Simulation

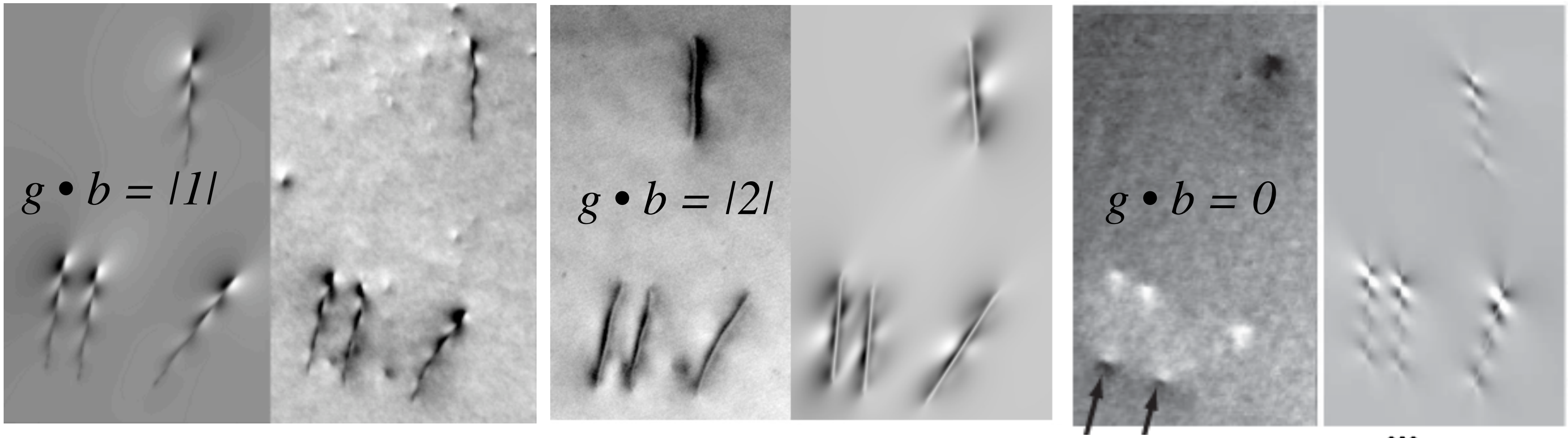


- Can apply "standard" *g • b* imaging criteria
- Higher order reflections (e.g. **3g**) produce very fine detail similar to weak beam

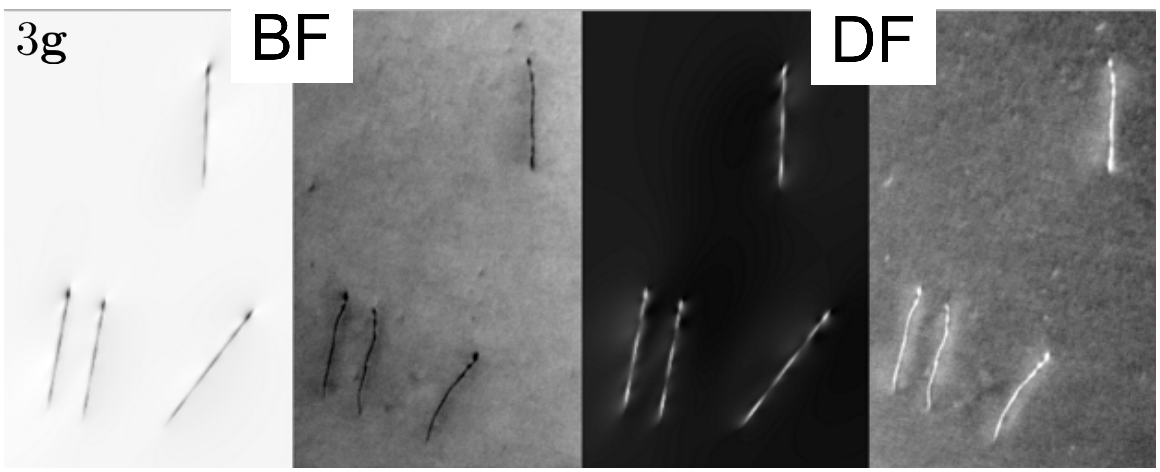


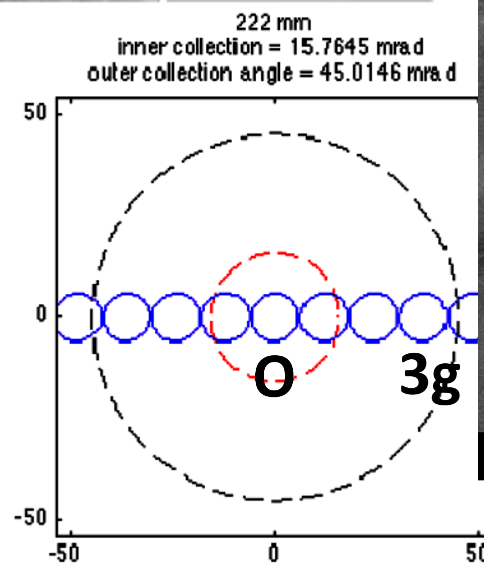


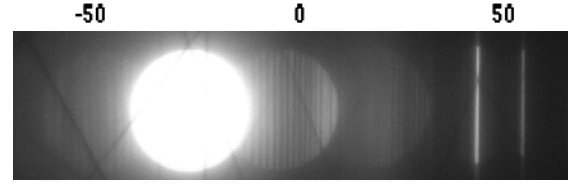

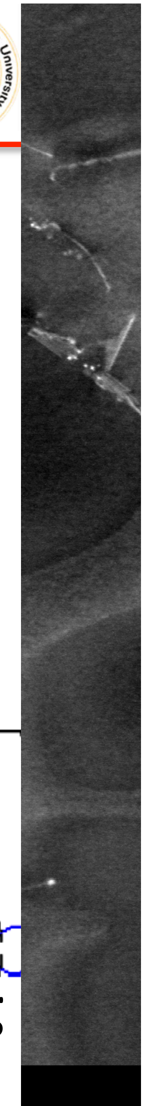

*PJ Phillips, MC Brandes, MJ Mills, M De Graef, Ultramicroscopy **111** (9-10) (2011) 1483-1487*

# Summary of Advantages of STEM-DC

- Obscuring effect of bend contours muted

- High order g imaging enables fine detail (similar to weak beam) but with much faster image acquisition

- Much thicker samples can be examined (> 1 micron)

- “Conventional” defect visibility rules hold for optimal conditions (beam convergence and camera length)

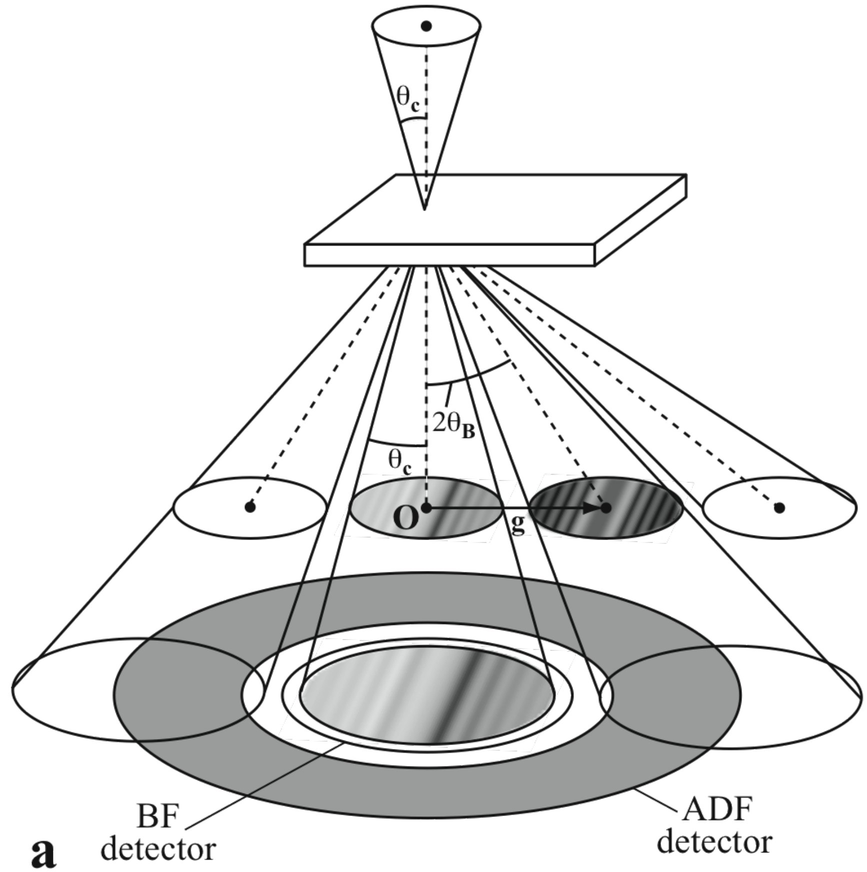


*Useful for 3D defect analysis ?*

# Pillar Testing of Ni-49.3at.%Ti

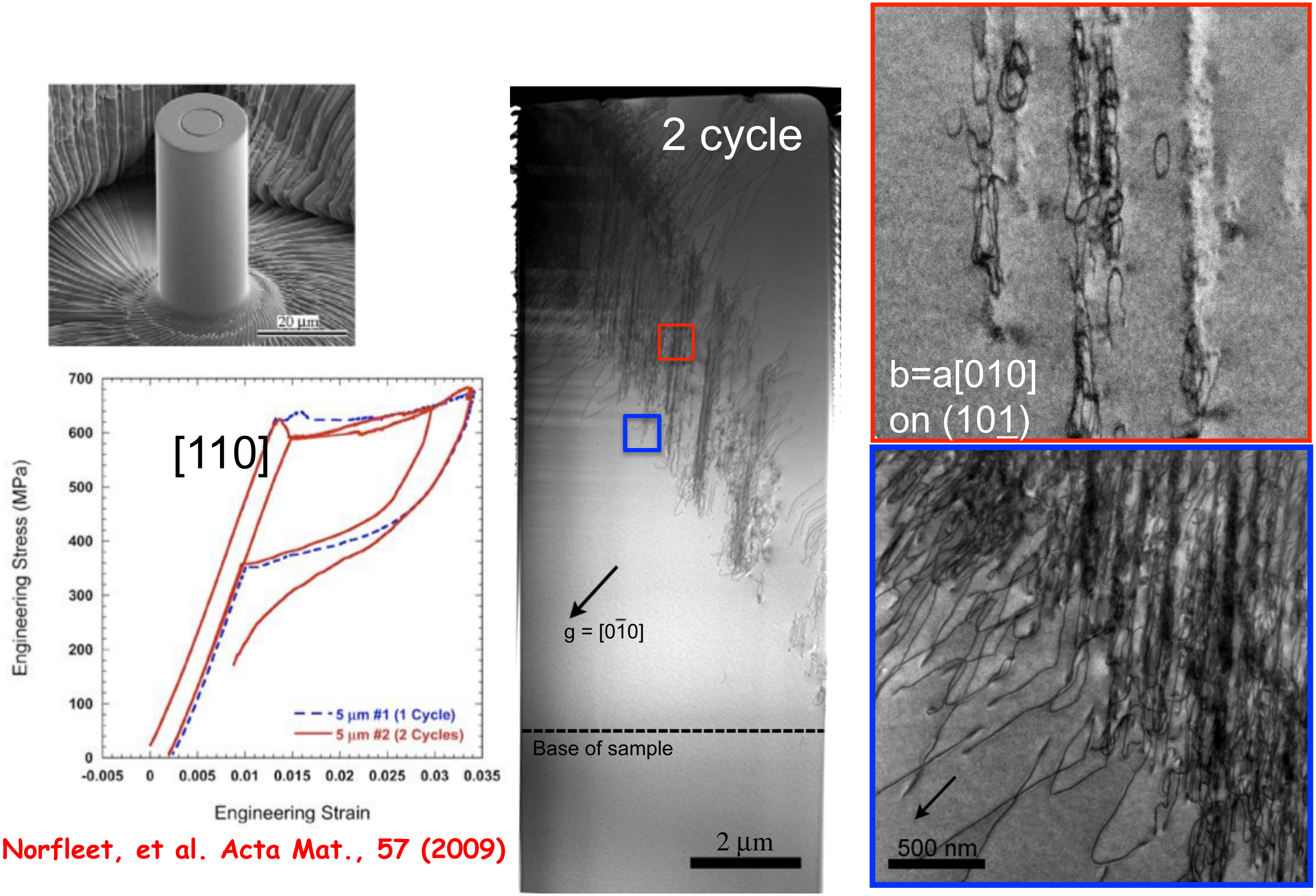


Norfleet, et al. Acta Mat., 57 (2009)

# 3D Geometry of Dislocations in NiTi

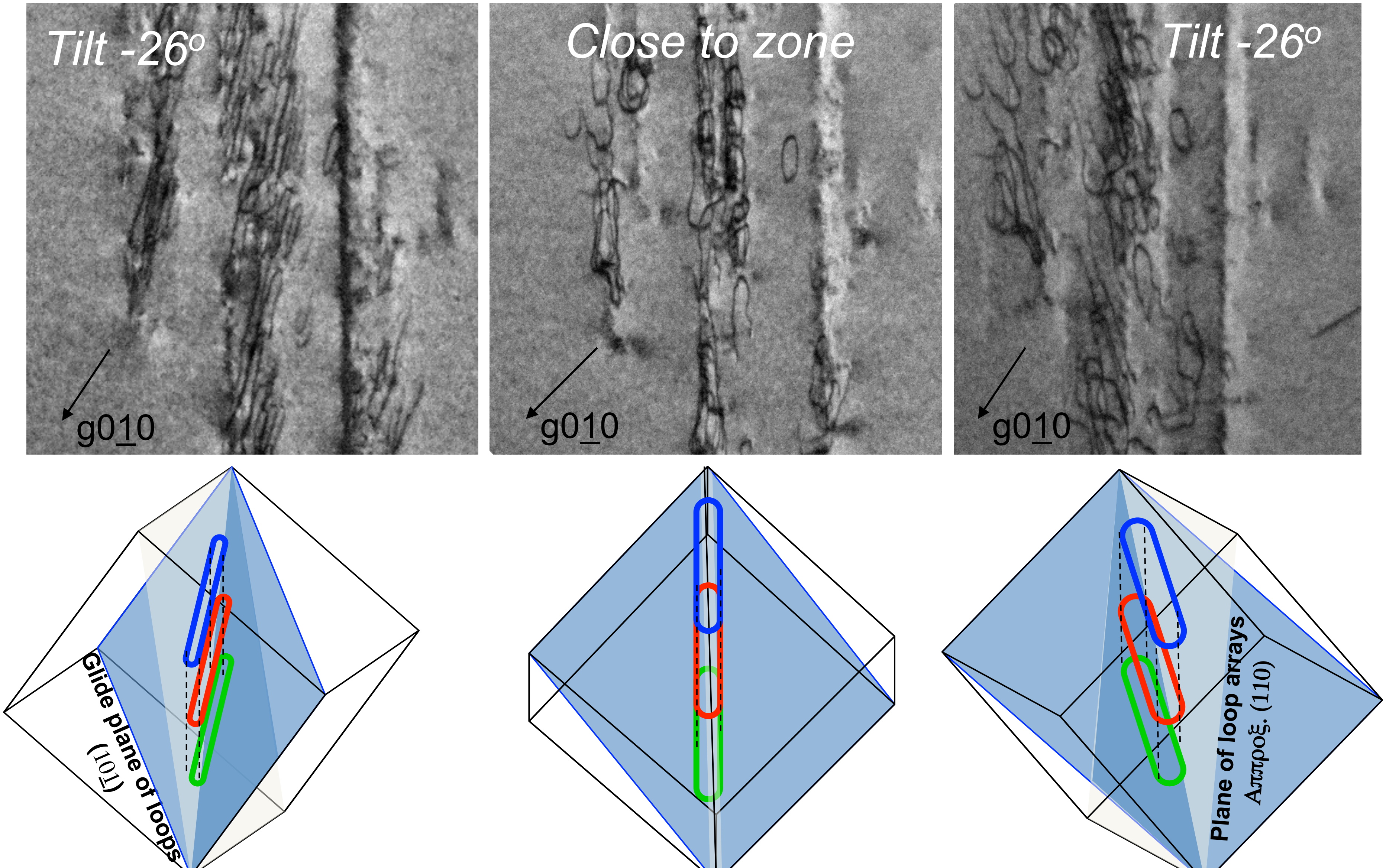


Individual a[0$\underline{1}$0] loops also on (10$\underline{1}$) planes

# Transformation-Induced Dislocation Related to Twin Interfaces of Martensite

For T4 class type II twinning mode after Bhattacharya (2003)

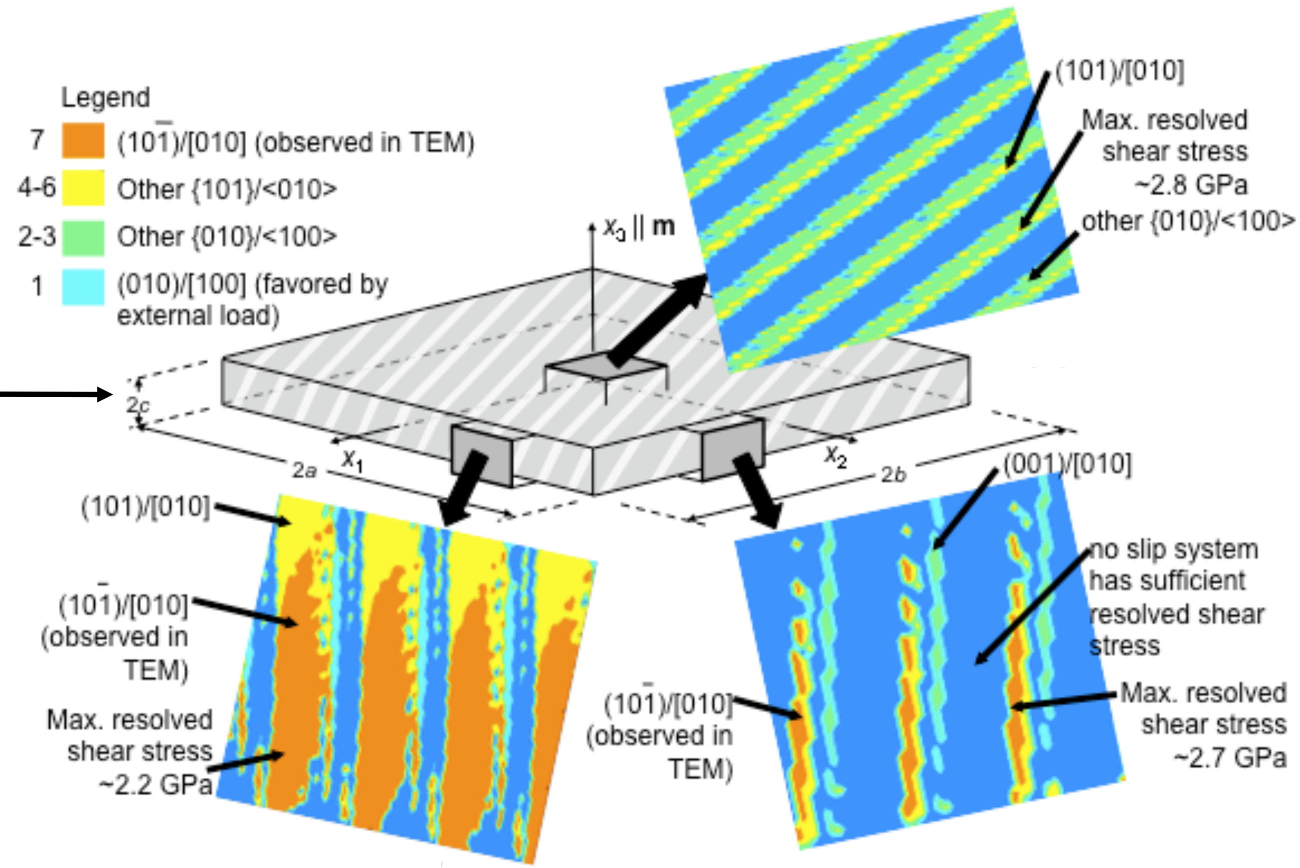


- Supports hypothesis that dislocation loop arrays driven into austenite by local stress field of transforming martensite variants

- Nucleation of loop arrays not presently understood

Norfleet, et al. Acta Mat., 57 (2009)

# Diffraction Contrast STEM Example

Structures in Superalloy ME3 after LCF at 700°C:

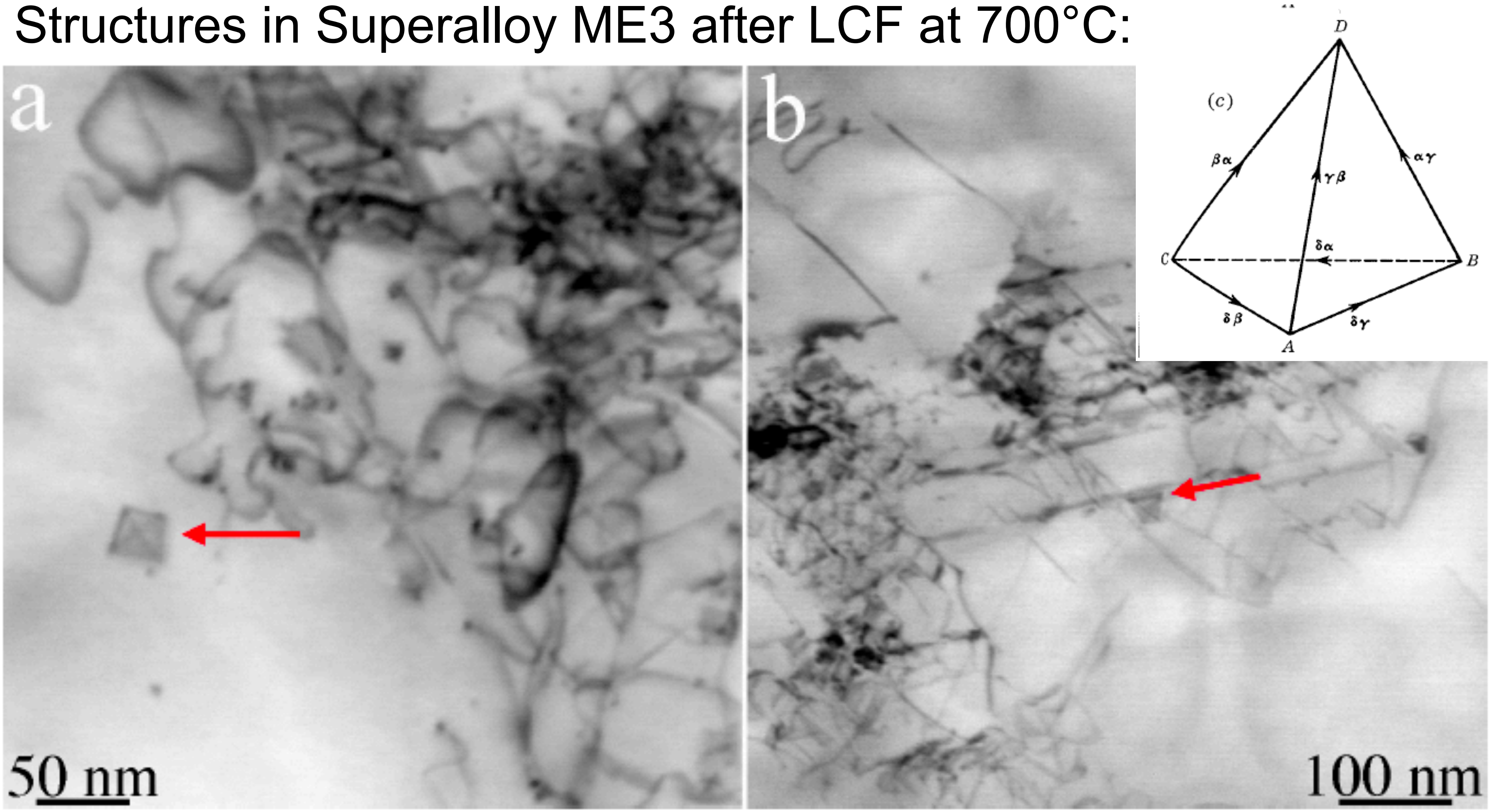


Figure 4.14: Stacking fault tetrahedra; a) specimen 704/0.80/1295, $\vec{B} \approx [001]$; b) specimen 427/0.75/21, $\vec{B} \approx [013]$. Images acquired on TF20.

*Phillips (2011)*

# Planar and Wavy Slip after High Temperature LCF – Superalloy ME3

Edge-on View

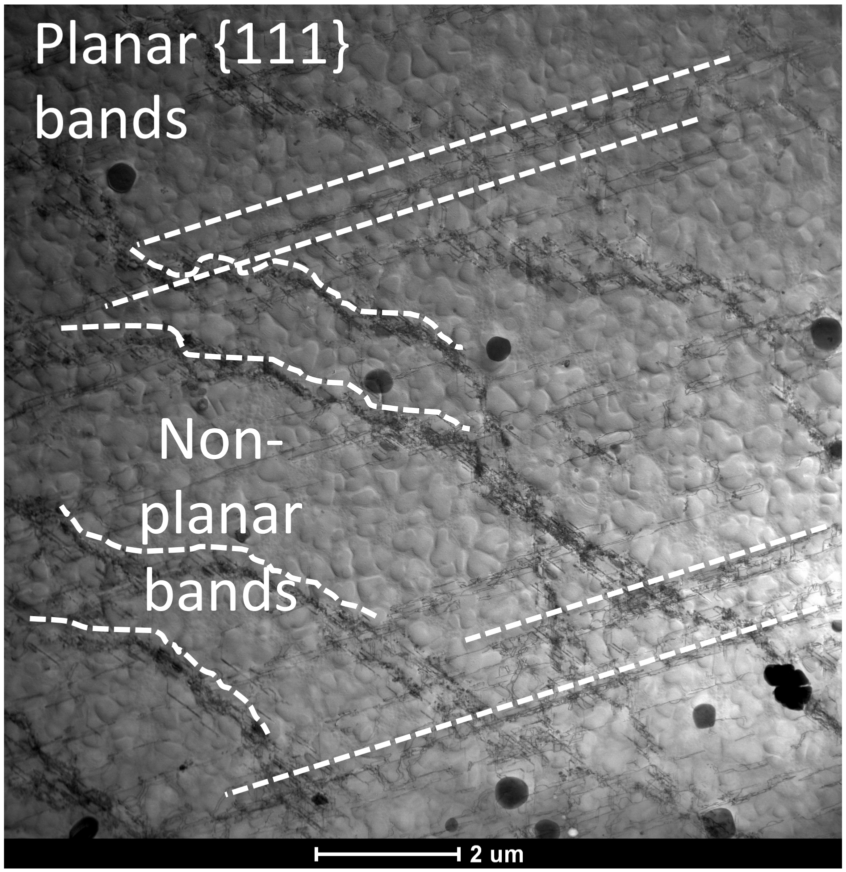


***1295 cycles***

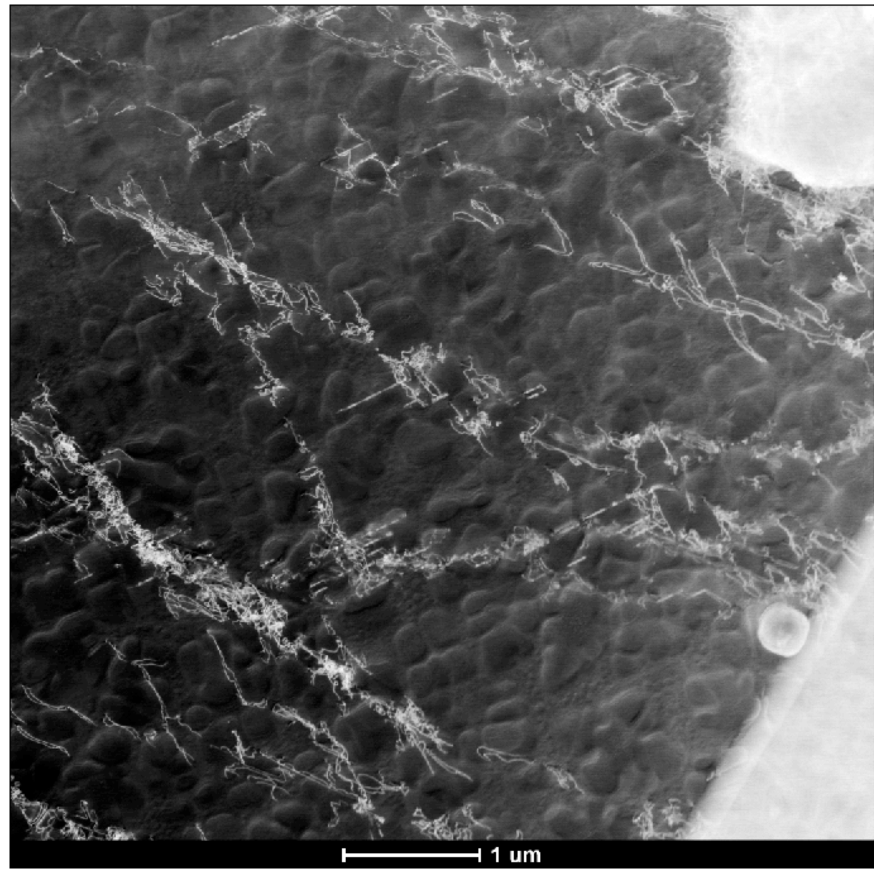


***395 cycles***

*Wavy slip between {111} and {010} planes*

# *Tilting for 3D Information*

## *"Cube Slip" in Superalloy ME3*

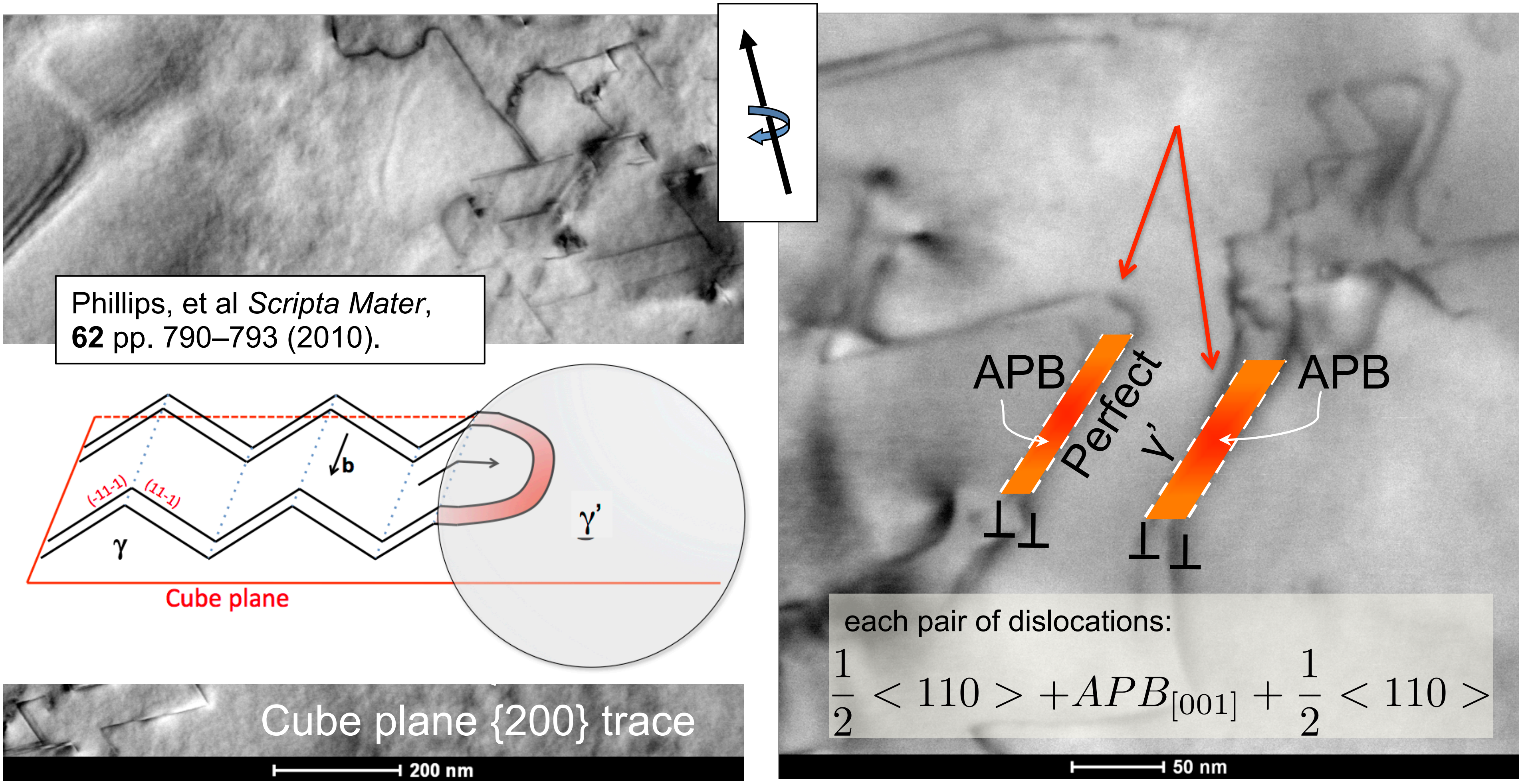


- Coupled dislocations resolved on both {111} and {001} planes

# Diffraction Contrast STEM Stereo-pairs

*L. Agudo Jácome et al / Acta Materialia xxx (2013) xxx–xxx*

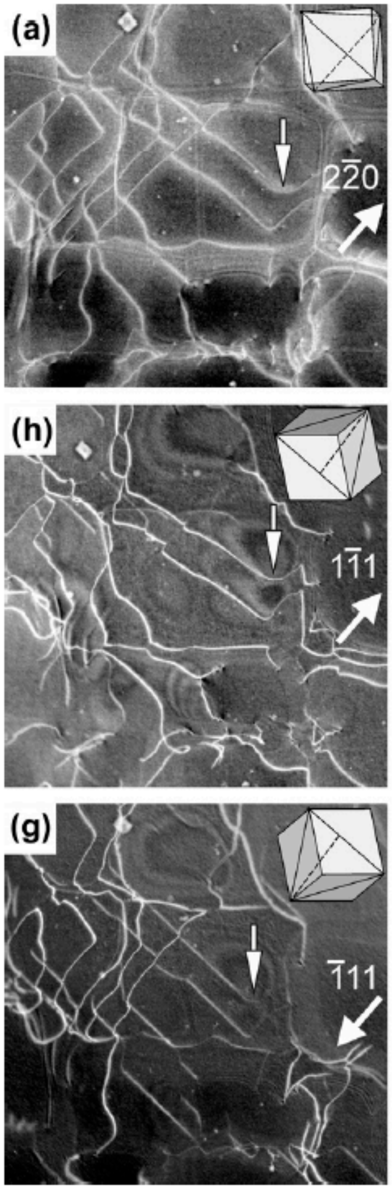


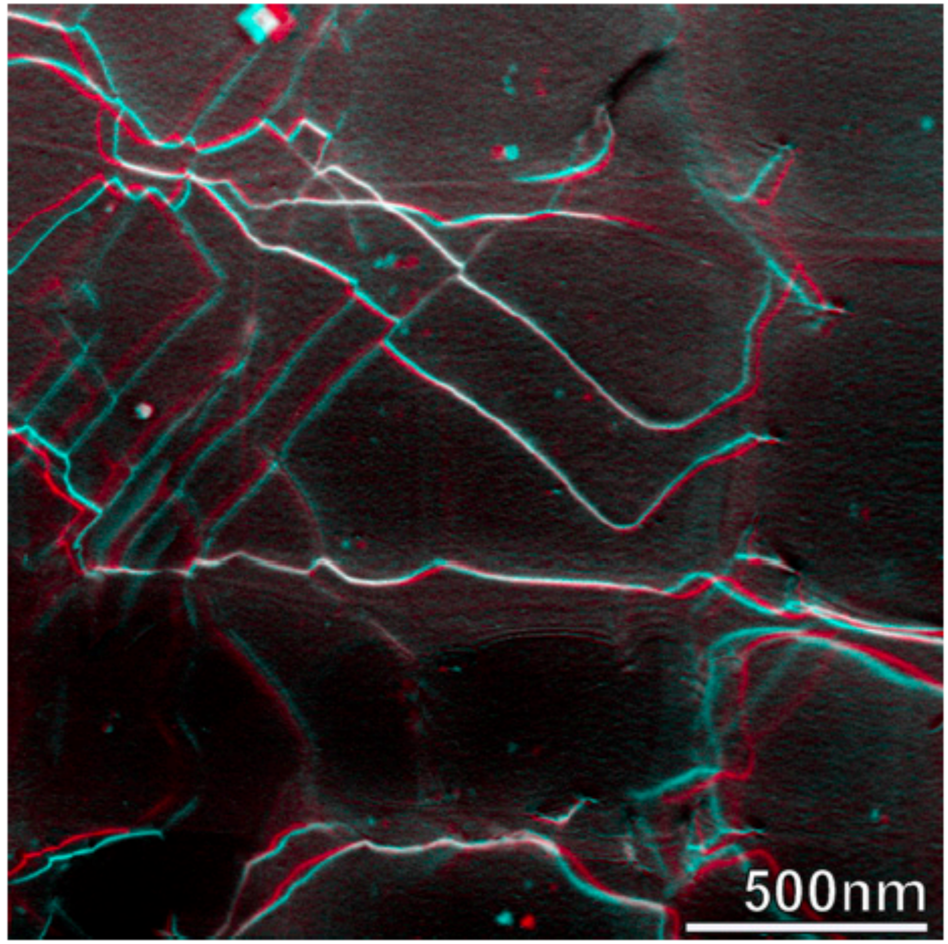


Fig. 6. Three-dimensional anaglyph of the pair of dislocations highlighted in the micrographs in Fig. 5 obtained applying the stereo STEM procedure of Agudo et al. [60]. For a realistic 3D impression, the anaglyph must be viewed with a special pair of colored glasses ( , [60]).

# Diffraction Contrast STEM Tilt Series

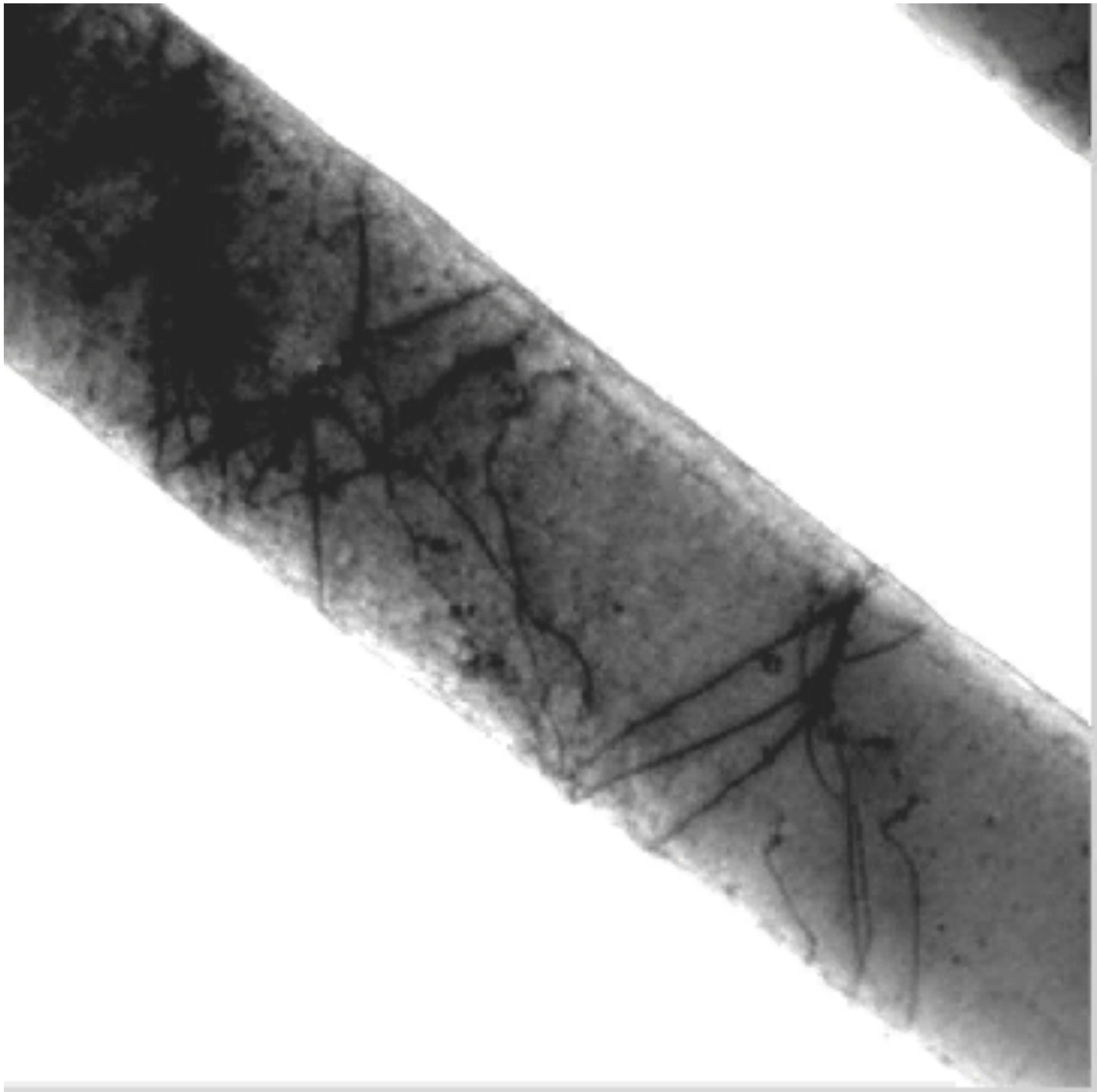

0.6 µm Thick Molybdenum (Z=42) Fiber

BF tilt series using g200

Images obtained every 1.5°

Tilt range: -30 to +30°

*J. Kwon (OSU)*
*EFRC Center for Defect Physics (DOE-BES)*

# STEM Tomography

## Practical considerations for tilt series acquisition:

- Align sample so single tilt axis (alpha) is diffraction vector
  - Same diffraction condition (systematic row) must be maintained throughout tilt series
  - Multiple tilt axes makes tilting and subsequent image alignment difficult
  - Depending on sample and image quality, automated tilt series acquisition routines may be used (FEI Inspect3D)

- Uniform intensity is vital for quality reconstructions!
  - ADF-STEM offers many advantages over conventional weak beam dark field:

1. Fewer dynamical effects (bend contours, thickness fringes, oscillatory dislocation contrast due to inclination)

2. Less sensitive to small misalignments, such as from regions of large strain

3. Capable of resolving details from much thicker specimens (up to ~1µm) than CTEM

# Options for alignment and reconstruction

- **IMOD**
  - Created by Boulder Laboratory
  - Image segmentation, cross-correlation and manual alignment, tomographic reconstruction
  - Capable of handling dual axis tilt series
- **TomoJ (ImageJ, FIJI)**
  - ImageJ plugin developed at Curie Institute
  - Automated and manual alignment with landmark detection, tomographic reconstruction (back projection, SIRT, ART, etc) for single tilt axis
  - Allows preprocessing of raw images (hot spot removal, background subtraction, etc.)
- **EM3D**
  - Developed at Stanford (no longer in development)
  - Created for segmentation, alignment, and reconstruction of electron tomography
  - Capable of handling dual axis tilt series
- **FEI Xplore3D**
  - Microscope-integrated software package
  - Automated electron tomography tilt-series acquisition (including drift correction), alignment and reconstruction

# Visualization of tomographic data:

- **Chimera: 3D molecular visualization software**
  - Developed at UCSF
  - Refinement and processing of 3D data sets
  - Thresholding and segmentation of tomograms
  - Many visualization options: solid, mesh, surface, etc.
  - Movie creation

# Diffraction Contrast STEM Tilt Series

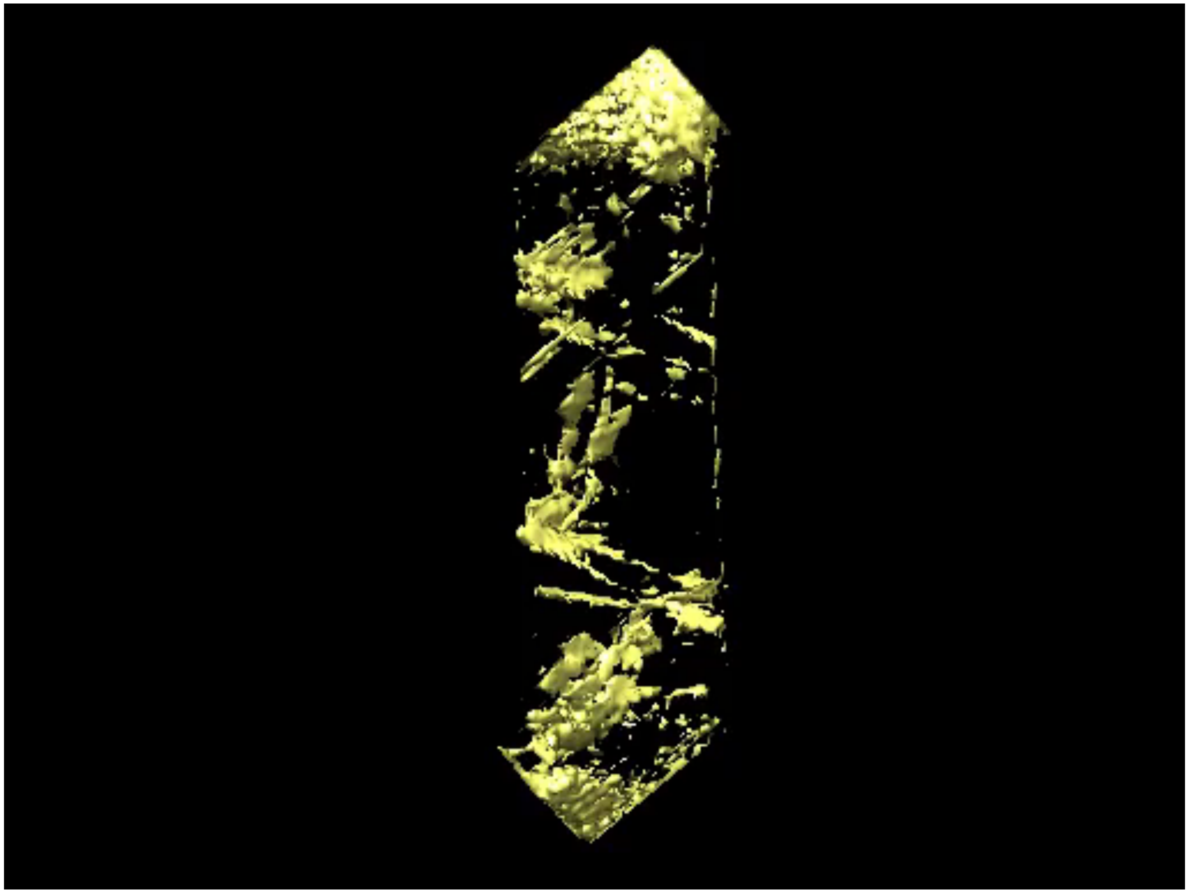

0.6 μm Thick Molybdenum (Z=42) Fiber (8% prestrain)

BF tilt series using g200

Images obtained every 1.5°

Tilt range: -30 to +30°

*J. Kwon and Matt Bowers (OSU)*
*EFRC Center for Defect Physics (DOE-BES)*

# Diffraction Contrast TEM Tomogram

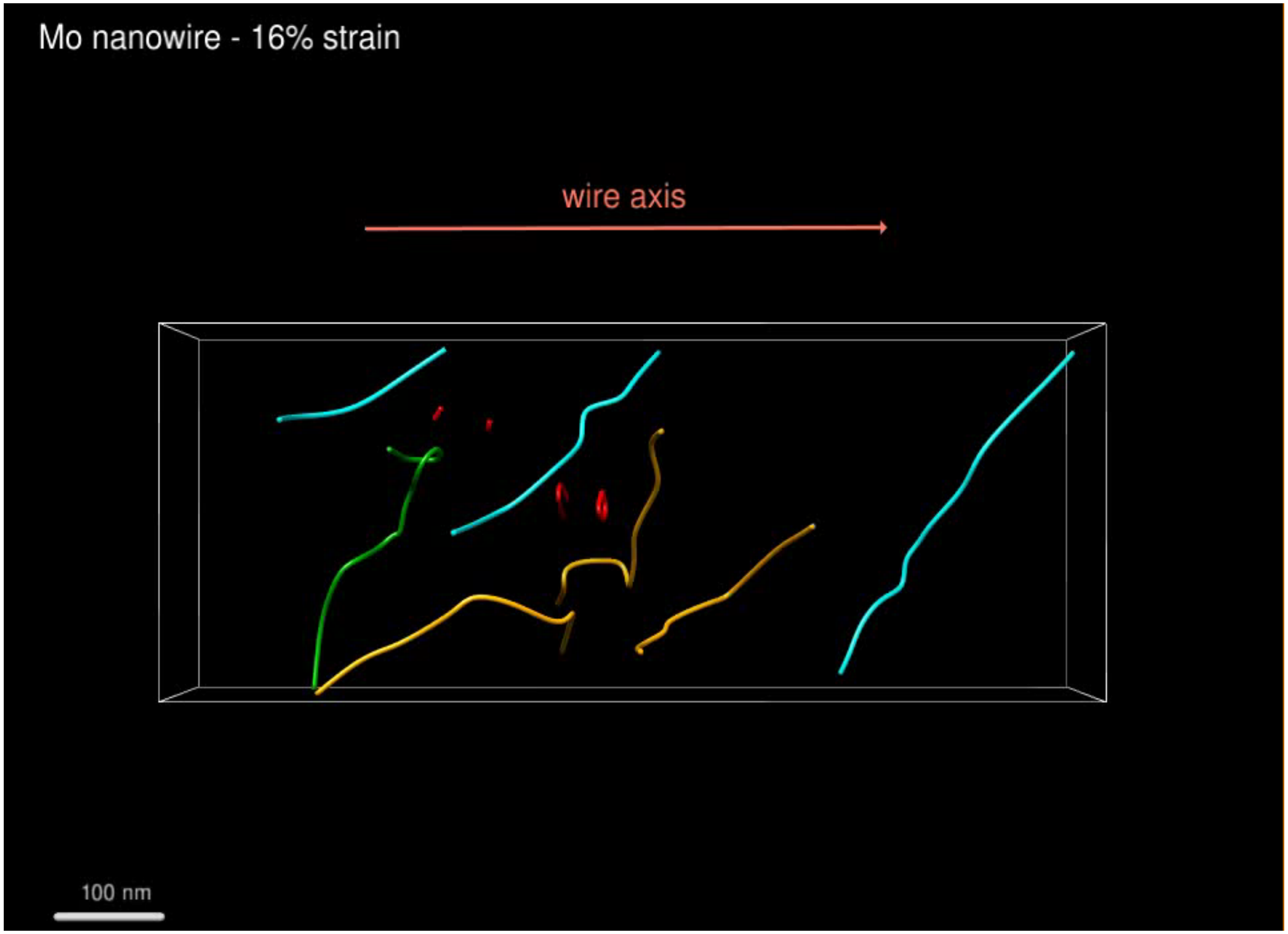


0.6 μm Thick Mo fiber

- "Tracing" of lines in 3D tomogram
- Use prior knowledge of end-points at surfaces/ interfaces

Virginia McCreary (UIUC)

# Ideal Strength of Perfect Mo Fibers

Bei, et al (2008)

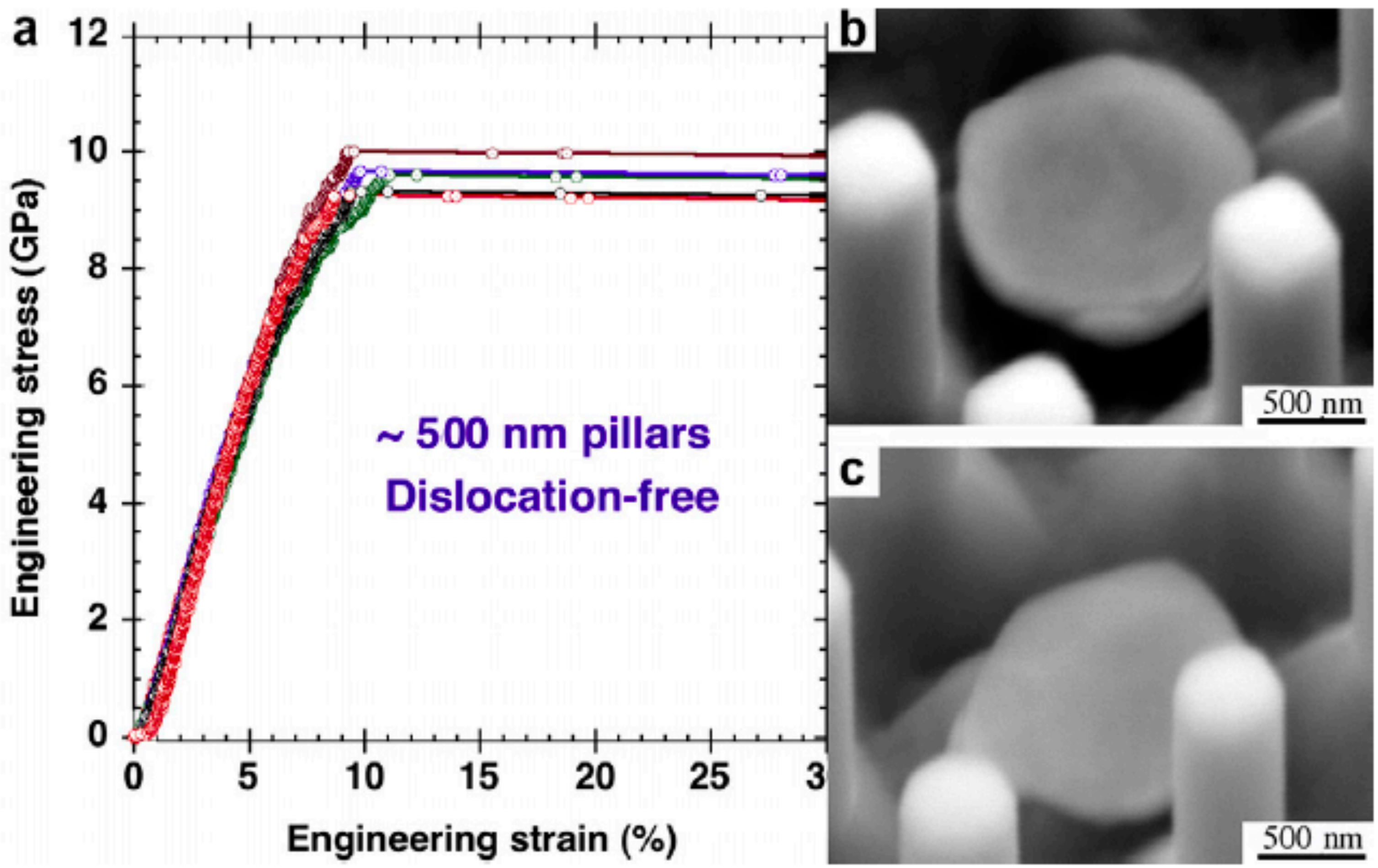

# Stochastic Behavior at Intermediate Pre-strain

Bei, et al (2008)

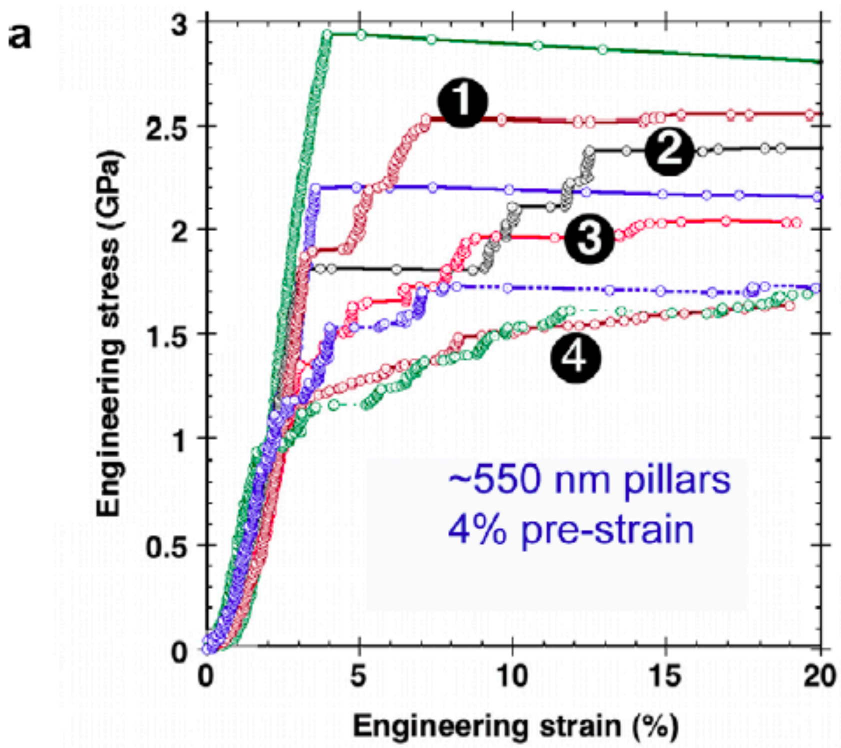


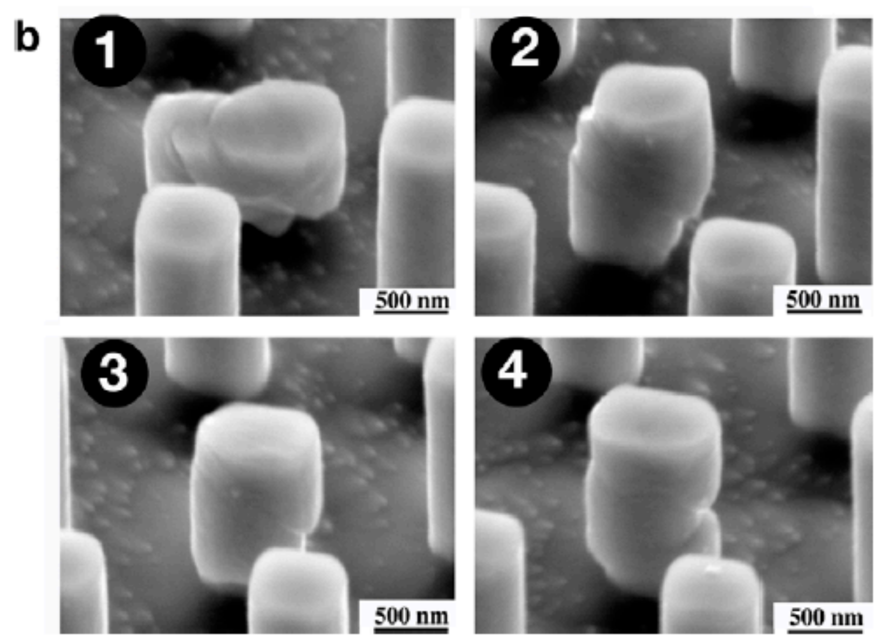


- Stochastic behavior – not predictable!
- Hypothesis: depends on details of dislocation sources prior to deformation

# “Bulk-like” Behavior at Larger Pre-strain

Bei, et al (2008)

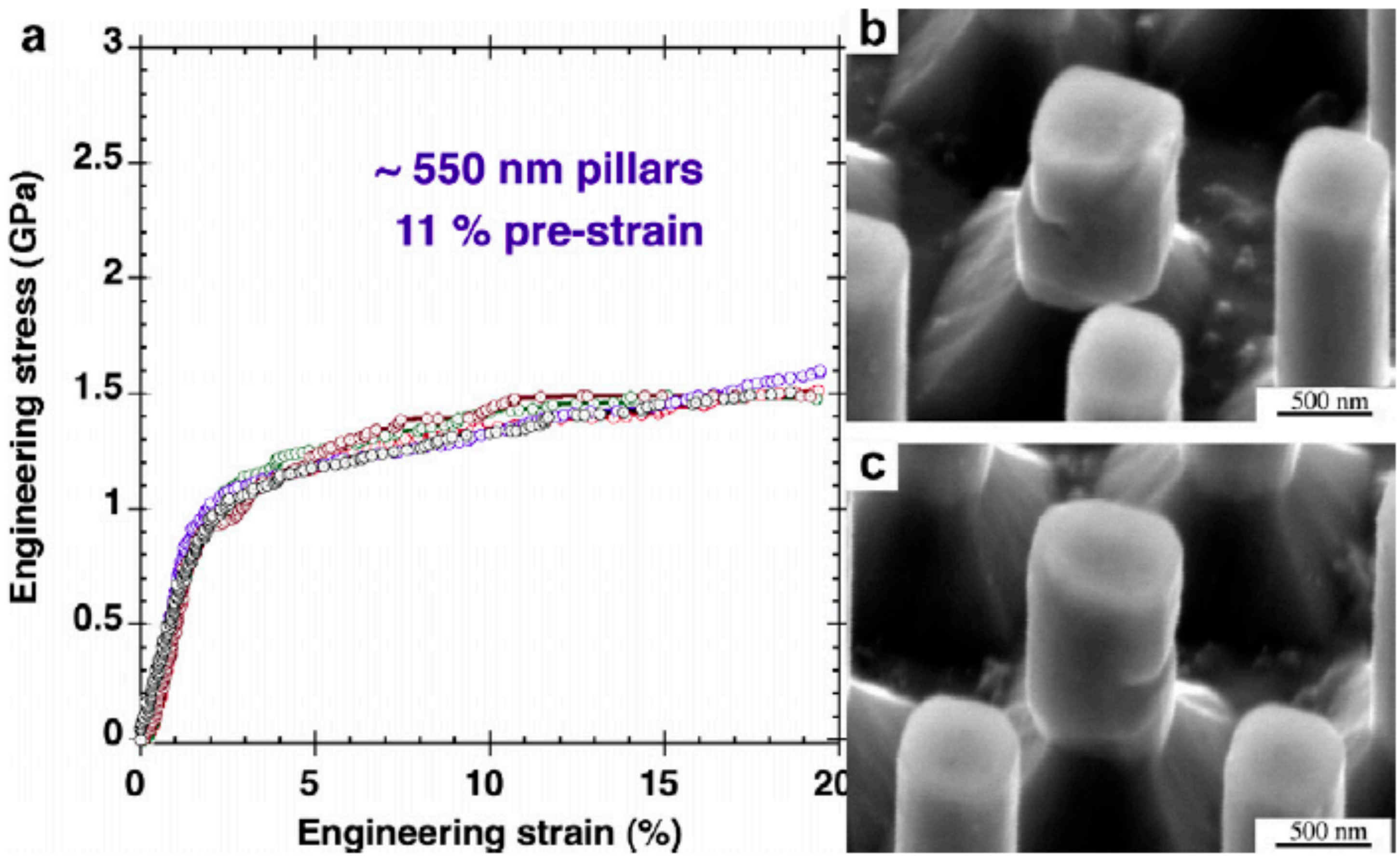

# Dislocation Configurations at Larger Pre-strain

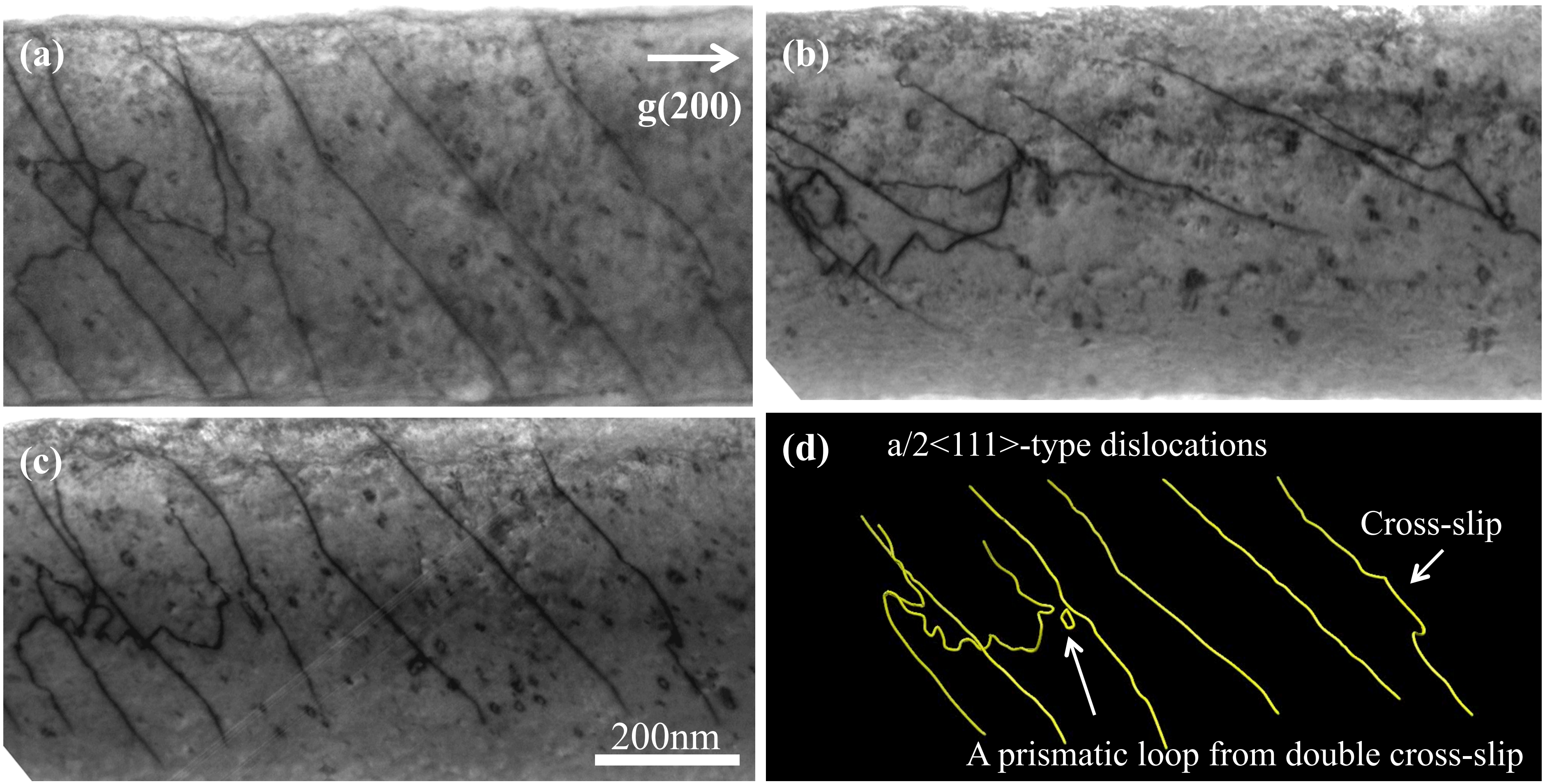

# Dislocation Configurations at Larger Pre-strain

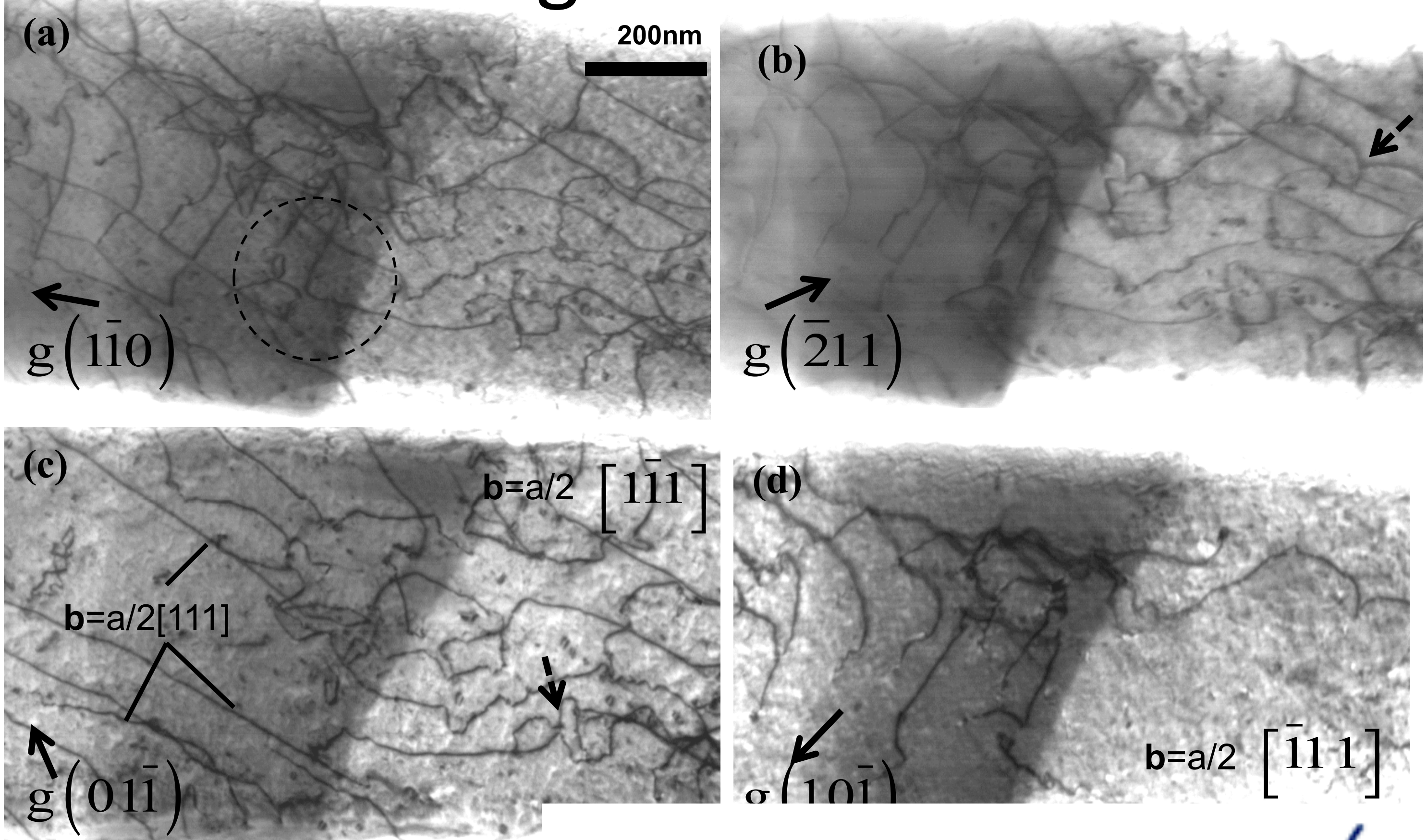


- Multi-junction observed
- Favorable as a persistent dislocation source

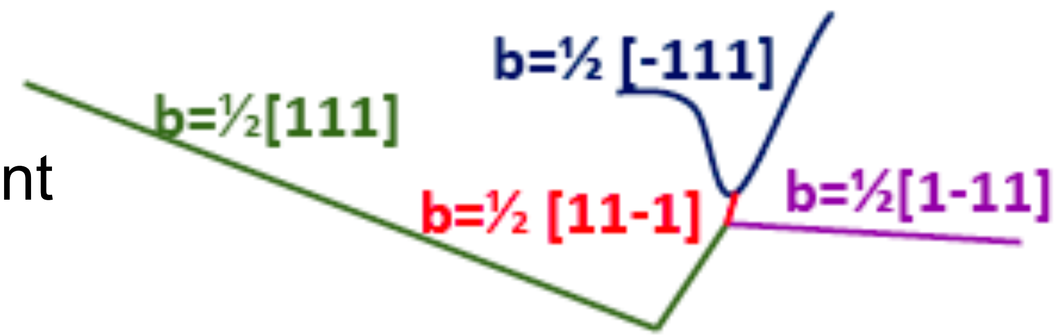

# Zone Axis MAADF and HAADF Imaging

*FEI Titan[3] 80-300 Probe Aberration Corrected*


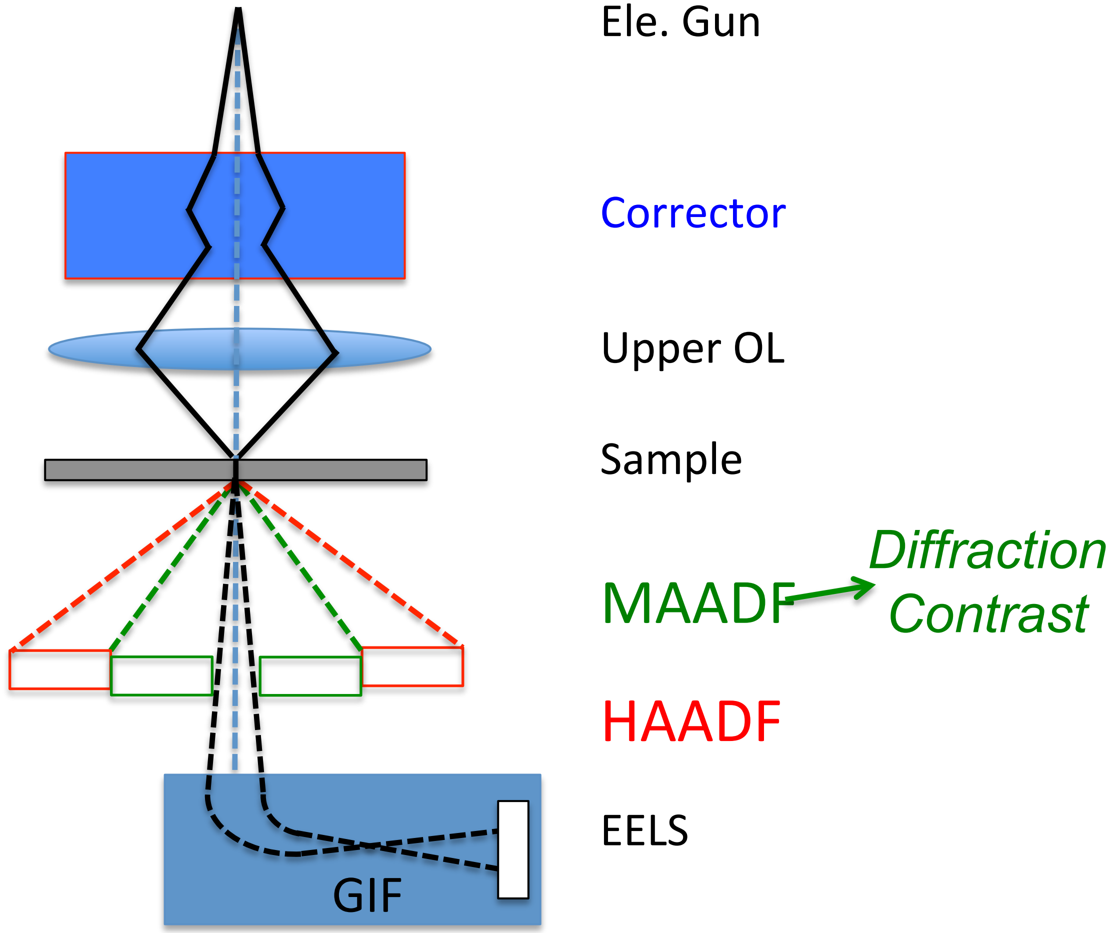


Both diffraction contrast and atomic number (Z) contrast can be accessed in zone axis orientations

# Zone Axis STEM Defect Imaging

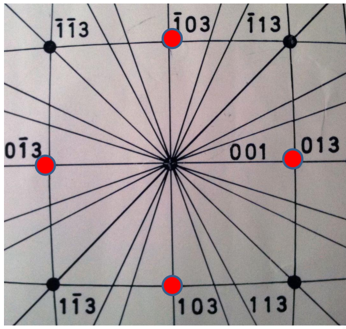


0.6 µm Mo fibers

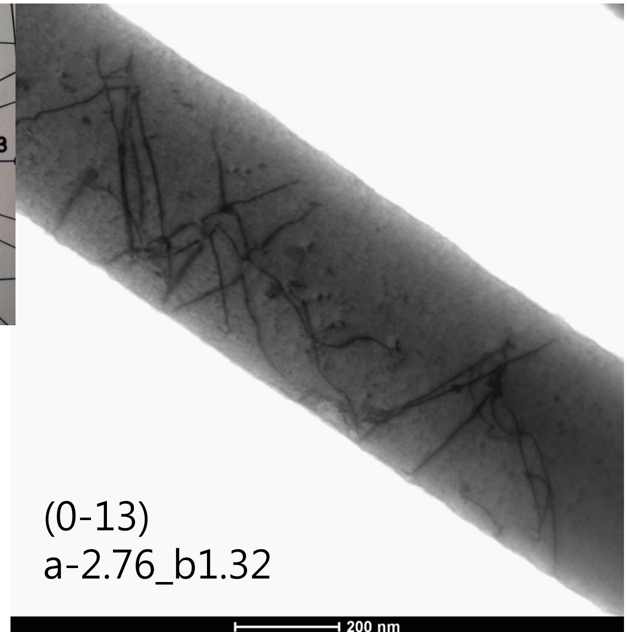


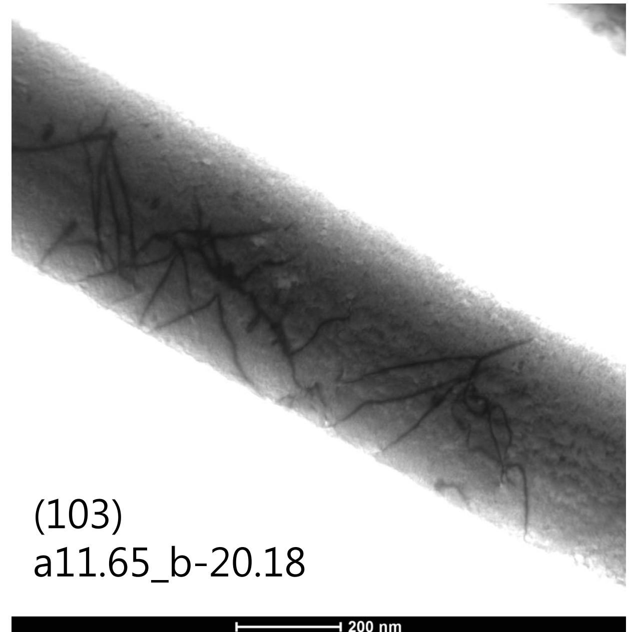


Interesting possibilities for 3D tomography !

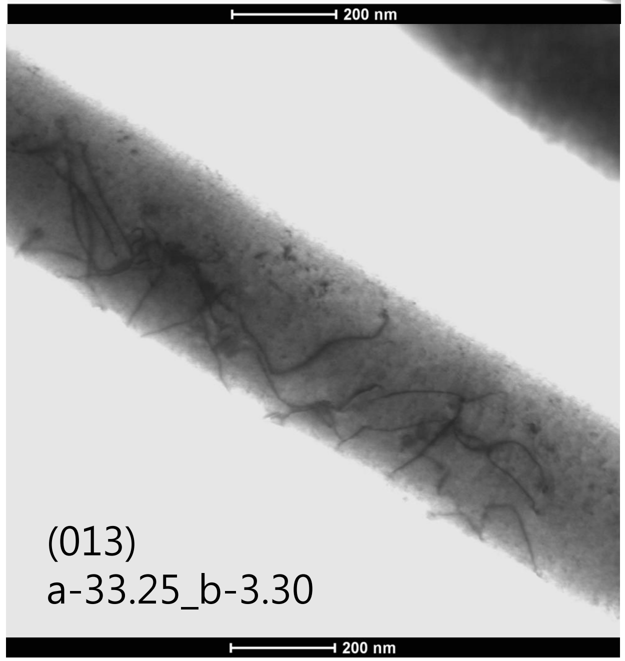


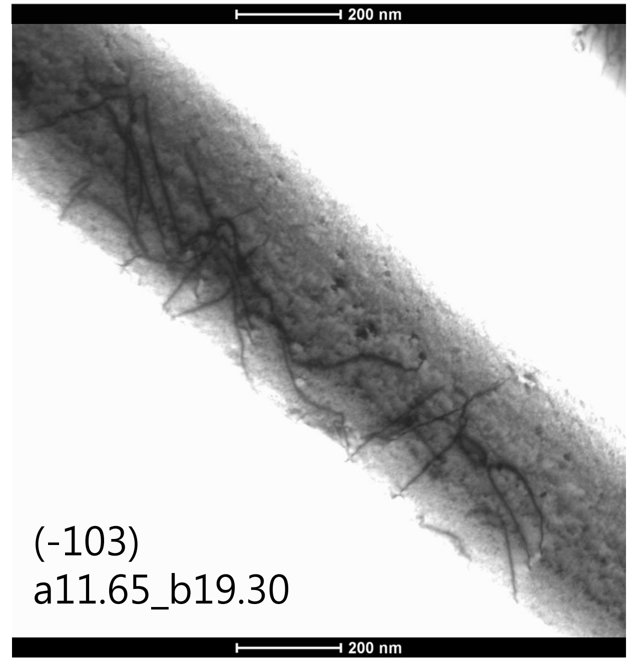

# Spiral History of TEM

*A. Howie, M&M Proceedings, 2012*

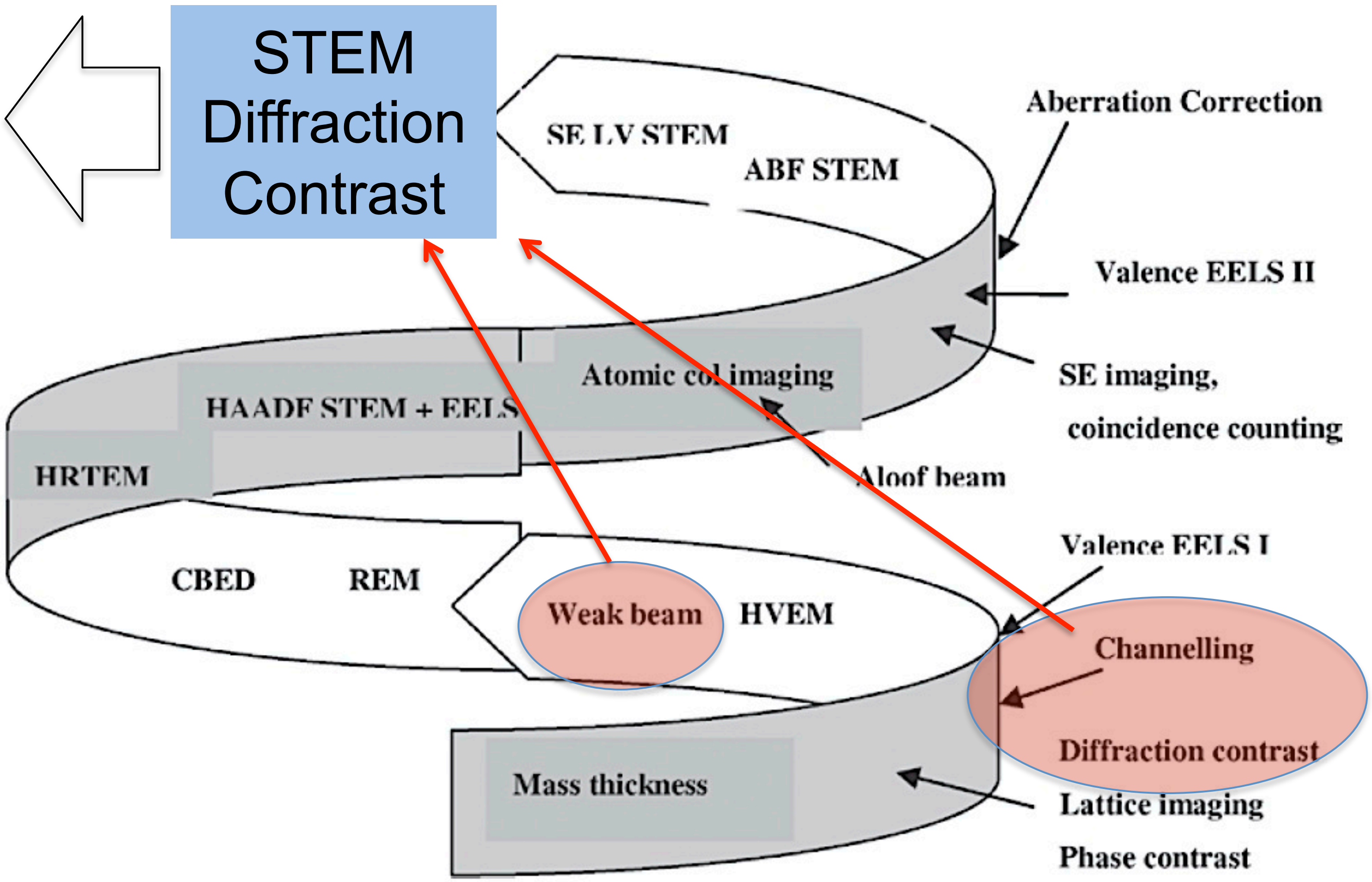


*Advances in high brightness sources **can** benefit diffraction contrast defect studies*

# Possibilities

- Automated specimen stages for computer-controlled tilting:
  - Tilt series acquisition
  - Zone axis image acquisition
  - 3D Reconstruction software

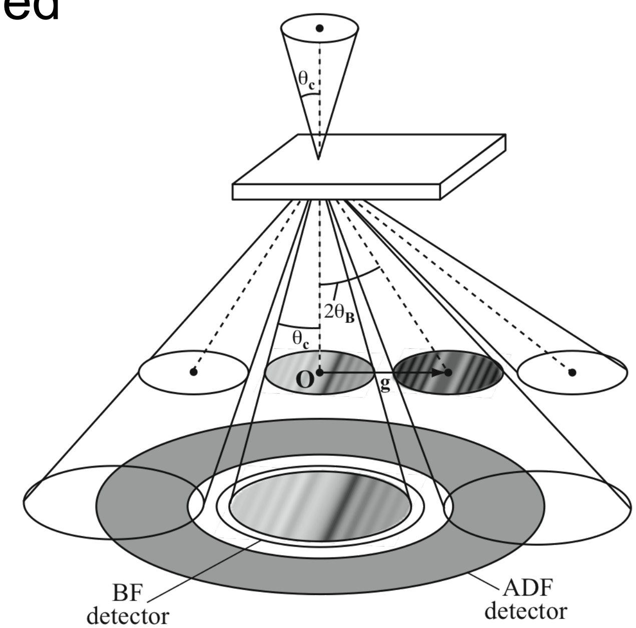


- Sector (or CCD array) detectors for:
  - Accurate selection of diffraction conditions
  - Post-processing "g•b" experiments with zone axis images

- In situ deformation experiments taking advantage of enhanced thickness capabilities of STEM diffraction contrast

- Rapid STEM acquisition for in situ observations